T-2993

GEOCHEMICAL DETECTION OF SULFIDE-BEARING VEIN STRUCTURES IN A DISTURBED SURFICIAL ENVIRONMENT, CENTRAL CITY DISTRICT, COLORADO

by

Lee J. Pivonka

T-2993

A thesis submitted to the Faculty and the Board of Trustees of the Colorado School of Mines in partial fulfillment of the requirements for the degree of Master of Science (Geology)

Golden, Colorado

Date 8/19/85

Signed: Lee J. Pivonka

Lee J. Pivonka

Approved: L. Graham Closs

Dr. L. Graham Closs,
Thesis Advisor

Golden, Colorado

Date August 19, 1985

Dr. Joseph J. Finney,
Head, Department of
Geology

Abstract

Soil disturbance in well-prospected mining districts reduces the applicability of traditional surficial geochemical exploration techniques. The Central City district is a classic example of a well-prospected base and precious metal mining district. A surficial geochemical study over mineralization was carried out with the objective of characterizing the trace element dispersion haloes around base and precious metal vein structures in this area. The purpose was to develop a geochemical exploration tool to detect vein structures in contaminated mining districts.

Free sulfides are present in abundance in the soils near areas where the ground was disturbed by mining activity. To reduce the effects of this contamination, a 30 minute cold HCl digestion was integrated with the MAGIC extraction system. This method selectively dissolves Fe-Mn oxyhydroxides in the soil, but dissolution of sulfides is minimal. The concentrations of Ag, As, Au, Cd, Cu, Fe, In, Mn, Mo, Pb, and Zn were determined using this method.

Even though numerous interrelated factors affect the dispersion of elements in the surficial environment, a simple and significant geochemical exploration tool was identified. Soil pH is the most important variable controlling the mobility of Fe-Mn oxyhydroxides in the

surficial environment. Soil pH can be lowered significantly by the oxidation of subcropping sulfide-bearing veins. Ratioing of statistically standardized Fe and Mn concentrations of the oxyhydroxide soil component accentuates this predictable chemical condition. This potential exploration tool is applicable in contaminated districts even where steep slopes prevail and soil profile development is poor. The locations of some potentially mineralized and unexploited structures were identified.

Results obtained from this study have established a basis for the direction and utility of future detailed surficial geochemical exploration studies in this and other similar mining districts. The methodology developed in this study can be used to locate veins which have been projected into an area, but which are not visible at the surface.

Table of Contents

List of Figures

List of Tables

List of Plates

Acknowledgements

This study was financially supported predominantly by loans from my parents, Arnold and Maxine Pivonka; their continuous support is gratefully acknowledged. The Colorado School of Mines Geology Department allowed access to analytical equipment and financial support for supplies was acquired from the Harold Bloom Geochemistry Fund. Thanks for financial support goes to the Lincoln Gem and Mineral Club, Inc. of Lincoln, Nebraska. Chevron Minerals, Inc. also deserves thanks for a field work-related scholarship.

I acknowledge the help supplied by committee members, Dr. Samuel B. Romberger and Dr. Fred E. Moore during the course of this research. I appreciate the help and encouragement supplied by my Thesis Advisor, Dr. L. Graham Closs, throughout all stages of this study. Many strategic modifications were necessary during its progress. Graham's continuous interest in the problems encountered and his guidance allowed for the satisfactory resolution of answers to questions addressed in this thesis.

I thank Mr. William C. Russell, Jr., Bonanza Property Owner, for allowing access to the study area. I acknowledge the help supplied by committee member, Mr. Van Cullar of Western Mining Consultants, Inc. Constructive discussions with Van contributed greatly to the progress of this study.

Technical instruction and advice pertaining to the establishment of field survey control for geochemical sampling were provided by Mr. Gaby Nuenzert. I acknowledge John Farrell for his valuable assistance during surveying and sampling. A resounding thank you goes to Dr. John Robert Clark of the U.S. Geological Survey for his patience and help during the analytical stage of this research. Thanks to Peggy O'Mara, Mike Ripp, Ron Keil, and Dr. John Viets for their technical advice pertaining to analytical techniques. I thank Dr. Keith Turner for his assistance in the statisical analysis of the research data. During the interpretative stages of this research, I had many helpful discussions with Mike Allen, Pete Herrera, Jim Shannon, and Steve Zuker.

Introduction

Objective

The objective of this study was to characterize the surficial geochemical expression of mineralized structures in the Central City district. Once this has been accomplished, surficial geochemical exploration models for the base and precious metal veins in this area can be developed.

Little developmental work in the district has included geochemical exploration methods. Primary alteration about veins in this district is typically very restricted in its extent away from mineralization. The detection of these structures using lithogeochemical techniques requires sample spacing which is very close and prohibitively expensive for the purposes of exploration. In general, when outcrops exist, the location of alteration and/or mineralization can be defined more efficiently by visual inspection rather than by analyzing the samples chemically.

Most ore in the Central City district was discovered as a result of visual inspection of exposed rocks and by the application of basic prospecting principles which were often intuitive. Even though soil cover is poorly developed on the steep slopes in this area, it is often deep enough to conceal outcrop in many places. Where outcrops were not

well-exposed, trenching by prospectors was extensive. Even though this method was often effective, it was (and is) far from efficient. Many trenches were dug (by hand) which did not reveal mineralization. Furthermore, the nature of mineralization is somewhat sporadic. A mineralized structure, several feet in thickness, can close to an unnoticable hair-line fracture or be displaced by faulting within a distance of a few tens of feet along strike.

The district is mature in terms of ore discovery and development at or near the surface. It is perhaps because of this fact that surface geochemical exploration techniques have not been employed in this area. Disturbance of the surface resulting from mining activity contamination and problems with steep slope geochemical dispersion, have undoubtedly reduced the appeal of surficial geochemical exploration methods. It seems likely, however, that some mineralized dilational zones which are not exposed as outcrop may not have been uncovered by the trenching of prospectors.

A surficial geochemical orientation survey was carried out in order to address and alleviate some of these exploration problems. Such an orientation survey would provide an indication of the utility of surficial geochemical exploration methods in a contaminated

mineralized area, i.e., the Central City district. If a useful surficial geochemical exploration tool could be defined for this area, then such a tool might certainly be applicable and quite useful in many districts in the world which are similar in overall character to the Central City district.

Location and Access

The Central City mining district is located in the Front Range portion of the Colorado mineral belt. The Colorado mineral belt has an irregular outline and trends northeast-southwest across the generally north-south trending Southern Rocky Mountain Range (Figure 1). The Central City district is arbitrarily bound by latitudes 39° 46′ 25" and 39° 49′ 25" and longitudes 105° 28′ 25" and 105° 32′ 00", directly north of the city and district of Idaho Springs.

The study area includes the area outlined on Figure 2 on the south side of Maryland Mountain, located in Gilpin County about 0.5 mile northeast of Central City and about 0.5 mile northwest of Black Hawk, Colorado (SE 1/4, Sec. 1 and NE 1/4 Sec. 12 T3S, R73W). Black Hawk is accessible by State Highway 119 and is connected to Central City by State Highway 279 0.5 mile to the west (Figure 2). Maryland Mountain is positioned between Chase Gulch on the south and

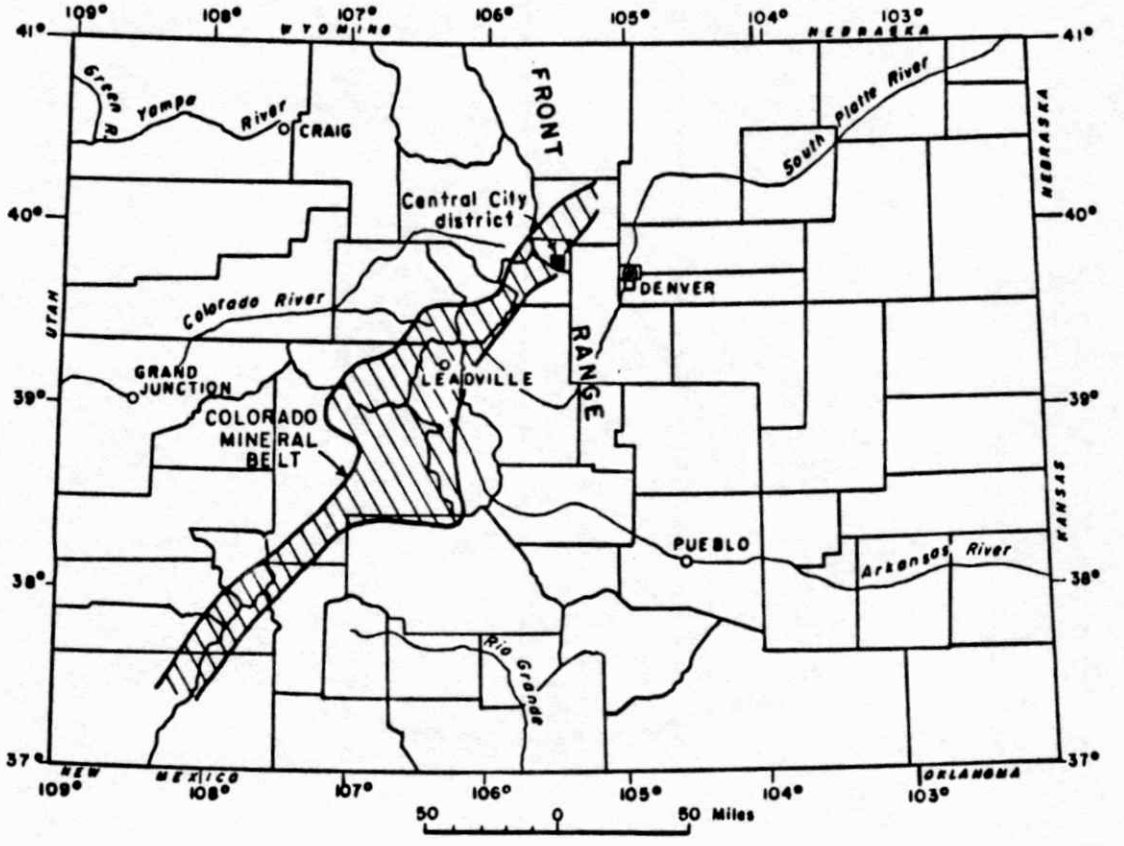

Figure 1. Location map of Central City district and the Colorado mineral belt (from Sims and Barton, 1962)

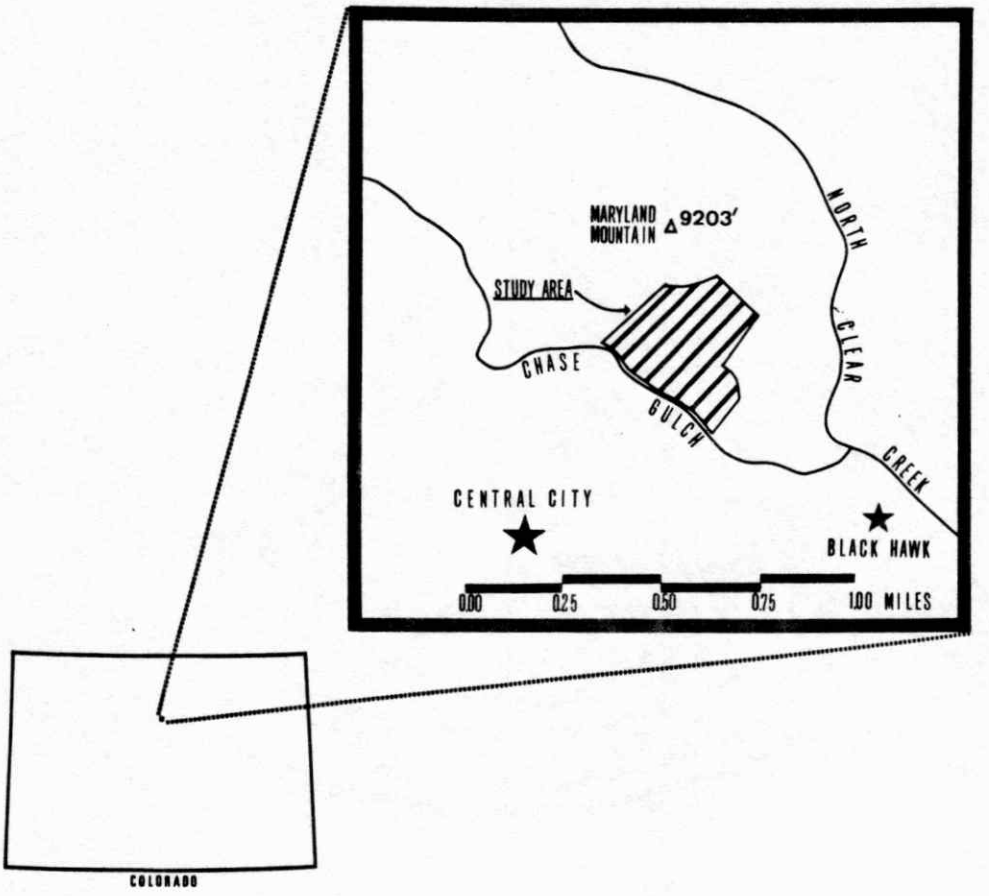

Figure 2. Location map of the study area (modified from United States Department of Interior Geological Survey Black Hawk and Central City 7.5 Minute Topographic Quadrangles, 1972)

North Clear Creek on the north. The middle of the southwest boundary of the study area is located 0.5 mile from State Highway 119 on Chase Gulch road. The Sans Souci Mine and Bonanza Adit are located on the south side of Maryland Mountain. The portal of the Sans Souci Mine is at 8600 feet of elevation. The Bonanza Adit has been driven northeastward into Maryland Mountain and its portal is at 8290 feet of elevation.

Topography and Physiography

The Central City district is on the east side of the Front Range with elevations ranging from 8,000 feet in the east to about 9,750 feet in the west. The elevation of the Maryland Mountain peak is 9,203 feet (Figure 2). North Clear Creek, flowing south of east against the northern boundary of Maryland Mountain, forms the main drainage in the district. Relief in the district generally does not exceed 1,000 feet and it more commonly consists of high gently rolling hills (Sims, and others, 1963b). Most streams in the district are intermittent, which made the earliest placer-type gold production in the district difficult.

Previous Work

Geology

The earliest reports on Gilpin County and the Central City district were published by Rogers (1883), Rickard (1898), and Collins (1910). Bastin and Hill (1917) published the first comprehensive U.S. Geological Survey Professional Paper describing the economic geology of Gilpin County and surrounding area. Lovering and others (1929; 1930; 1935; 1938; 1950; and 1953) have published reports on the Colorado Front Range. The U.S. Geological Survey geologic map of the Central City quadrangle was published by Sims, and others in 1964.

Geochemistry

Lovering and Goddard (1938) published chemical analyses of the igneous rocks in the Front Range in order to better understand their genetic development. Sims and others (1961; 1962; 1963a; 1963b; and 1982) published some of the best known and most recent research results on the Central City district. Sims and Barton (1961) have studied the geochemistry and fluid inclusions of sphalerite in the Central City district in order to determine hypogene temperature zonation relationships.

Tooker (1963) studied the chemistry and mineralogy of hypogene and supergene altered rocks in the district. Rice,

and others (1982b) determined the timing of precious and base metal mineralization in the Central City district by direct and indirect methods.

Budge (1982) studied trace element dispersion in wallrocks around base and precious metal veins in the Idaho Springs district, directly south of the Central City district. The most recent known work at Maryland Mountain is a Master's thesis by Ann Kramer (1984), covering ore controls in the Smith Gold Mine located on the southeast side of Maryland Mountain. Little known surficial geochemical work has been used to address the exploration problems related to surficial cultural contamination existing in the vein-type base and precious metal mining districts of the Front Range.

Investigation Approach and Methodology

Dispersion of trace elements in soils on the southern portion of Maryland Mountain is controlled by climatologic, botanical, topographic, geomorphic, chemical, pedological, biochemical, mineralogical, and cultural processes. It is understood that the quantity of data considered in this study is only a very small proportion of that which would be necessary to adequately define all processes acting upon this system. This is not to say, however, that the proper selection and analysis of a small portion of data can not be

used to resolve a problem such as the one addressed in this thesis.

Certain minerals and trace element-bearing compounds which are distinctly anomalous, relative to those in the wallrocks, exist in the soils over and proximal to mineralized structures. These phases are dispersed by processes which include those in the partial list above. Mineral phases and elemental species are segregated and redistributed as the rock and soil moves downslope. The following pages describe the methodology which was necessary in order to define the geochemical dispersive process, related to mineralization, which is presently occurring at the surface of Maryland Mountain.

Surveying methods were used to accurately locate all surface pits and alteration structures in the area at a scale of 1 inch equals 100 feet in order to provide detailed sampling control (Plate I). Surface geochemical soil sample stations were accurately located in three detailed sampling traverses oriented perpendicular to the vein structure traces. Details of the surveying procedure are presented in Appendix I. A sample interval of 10 feet was used where the sampling line crossed the traces of observed surface vein structures, and 25 feet where vein structures were not observed (Plate I). Details of the soil sampling procedure

are presented in Appendix II.

Representative mineralized rock samples were collected underground from stopes in drifts off of the Bonanza Adit. Pulps of these samples were prepared by crushing, splitting, and sieving to U.S. Series -60 and -200 mesh. The heavy mineral fraction was separated from the -60 mesh fraction using a Wilfley Table. A sulfide selective hot sulfuric acid-bromate digestion and organic extraction method (MAGIC) developed by Clark and Viets (1981) was applied to the -60 mesh concentrate and -200 mesh pulps to separate trace elements from interferring matrices. These data were used to establish relative abundances of various elements in the known mineralized structures. Representative analytical data for these mineralized samples are presented in Appendix VIa.

The 208 soil samples collected were prepared for analysis by separating them into U.S. Series -10 to +60, -80, and -230 mesh size fractions. The -10 to +60 soil fraction was prepared in order to evaluate the effects of clastic trace element dispersion. The -80 mesh soil fraction was chosen for analysis because it is a standard used by industry. The -230 mesh soil fraction was chosen in order to evaluate the effects of hydromorphic trace element dispersion.

Four digestion/extraction methods were applied to the three soil fractions during preliminary analysis before one fraction and one method were determined to be the best. The four methods tested included a hot nitric acid digestion, a hot sulfuric acid-bromate digestion/MAGIC extraction (Clark and Viets, 1981), a 24 hour cold HCl digestion/MAGIC extraction (Clark, personal communication, 1985), and a 30 minute cold HCl digestion/MAGIC extraction (Clark, personal communication, 1985). The hot nitric acid digestion method was used to analyze all soil samples (-80 mesh) for Cu, Pb, Zn, Cd, Fe, and Mn. The 30 minute cold hydrochloric acid leach was deemed most significant of the four methods, however, and was employed with the -230 mesh soil fraction. This method is selective in that it dissolves a substantial proportion of Fe-Mn oxyhydroxides in the soil, but dissolution of base metal sulfides is minimal and the dissolution of pyrite is virtually nil. The 30 minute cold HCl digestion was integrated with the MAGIC extraction system (Clark, personal communication, 1985) and the concentrations of Ag, As, Au, Cd, Cu, Fe, In, Mn, Mo, Pb, and Zn were determined in all samples. Flame and graphite furnace atomic absorption spectrophotometric methods were used to analyze the extracted trace elements in aqueous and organic solutions. The -230 mesh soil fraction was the most

appropriate choice for this analytical step because this fraction possesses the highest relative total grain surface area and it logically contains the highest concentration of Fe-Mn oxyhydroxide coatings. In summary, the sampling design and the analytical methods used were selected for the purpose of detecting pre-mining geochemical dispersion and not the effects of mining activity contamination.

Geology of Central City District

General Geology

The Central City district is located within the Colorado mineral belt. The trend of the Colorado mineral belt appears relatively independent of the structural grain in the Southern Rocky Mountain Range. However, it does trend roughly parallel to the regional grain of the Precambrian basement rocks (Figure 1).

The Precambrian rocks in the district consist of interlayered gneisses, granites, and pegmatitic units. Microcline-bearing gneisses with some interlayered biotite gneiss and pegmatites are the common hosts to ore veins. Wallrocks of felsic and intermediate compositions host ore locally.

Precambrian rocks of the Front Range are overlain nearly everywhere by Paleozoic rocks which dip steeply away from the uplift. Mesozoic rocks are found directly upon basement rocks near Breckenridge. Tertiary sedimentary rocks are found locally in the Front Range on the upturned ends of Paleozoic and Mesozoic rocks and on some basement rocks. Sedimentary Tertiary rocks in the northern Colorado Front Range are primarily clastic in nature, while those in the south include interbedded shale, algal limestone, tuffs and lavas (Lovering and Goddard, 1950).

During late Cretaceous and early Tertiary time, the Laramide Orogeny produced uplift and folding of the present Rocky Mountains. Intrusive activity during the Laramide Orogeny was common in the central portions of the Rocky Mountain Range and less pronounced elsewhere. Relatively older Laramide intrusions are generally small irregular stocks while the relatively younger intrusions form long thin dikes in the Central City district. The intrusive rocks are porphyritic and include granodiorites, quartz monzonites, bostonites, and quartz bostonites.

Rock Units

Precambrian

Precambrian gneisses in the Front Range have been grouped by Spurr, and others (1908) into an older Precambrian Idaho Springs formation and a younger relatively thinner Swandyke Hornblende Gneiss unit. Generally, later workers (e.g., Sims and others, 1963a) do not retain this nomenclature (for these rocks) but rather describe them compositionally (Table 1).

Interlayered Gneisses

Most of the Precambrian gneisses in the Central City district are microcline-quartz-plagioclase gneisses and sillimanite-biotite-quartz gneisses. These are often

Table 1. Principal Precambrian rock units in the Central City district (from Sims, and others 1963b)

Rock units	Comments
Granitic rocks:	
Biotite-muscovite granite	Equivalent to Silver Plume granite at Silver Plume, Colo.
Quartz diorite and associated hornblendite.	
Granodiorite	Probably equivalent to Boulder Creek granite. Lovering and Goddard (1950).
Pegmatite (includes minor granite gneiss)	Also constitutes felsic layers in migmatites. Unit is correlative with granite gneiss and pegmatite unit of Freeland-Lamartine district (Harrison and Wells, 1956). Some pegmatite is younger than biotite-muscovite granite.
Gneissic rocks:	
Microcline-bearing gneiss	Age relations among these rock units are unknown. Most of the rocks previously were grouped in the Idaho Springs formation. The microcline-bearing gneiss is the granite gneiss of Bastin and Hill (1917); it was referred to as quartz monzonite gneiss in a previous report (Sims, 1956).
Cordierite-amphibole gneiss	
Biotite-quartz-plagioclase gneiss	
Sillimanitic biotite-quartz gneiss	
Lime-silicate gneiss	
Skarn and related rocks	
Amphibolite	
Quartz gneiss	

[1] Rocks are listed from youngest to oldest.

interlayered with other gneisses including lime-silicate, cordierite-amphibole, and amphibolite types (Table 1).

The microcline-bearing gneiss is typically gray in color, medium-grained and generally well foliated. In hand specimen it may appear massive. Weathered surfaces are commonly light brown and pegmatites are often randomly distributed throughout this common gneiss.

The biotite-quartz-plagioclase gneiss and the sillimanite-biotite-quartz gneiss are most often found interlayered with each other. These two gneisses have variable compositions and are usually distinguished from one another by their color. Local accessories in the biotite gneisses include garnets.

Veins in the Central City district are commonly found in the microcline-quartz-plagioclase-biotite gneiss. Veins are also localized in discrete layers of amphibolite, lime silicate gneiss, skarn, and cordierite-amphibole gneiss (Sims, and others 1963b).

Taylor (1976) suggests that interlayered tuffaceous sedimentary units, rhyodacitic and dacitic tuffs were metamorphosed to produce the feldspar-rich gneisses. Calc-silicate gneiss and amphibolites are thought to be metamorphic derivations of graywackes, impure carbonates, and basaltic flows. It is thought that a relatively short

time elapsed between sedimentation and the initiation of metamorphic activity. Metamorphic grades reached the upper amphibolite facies as evidenced by the presence of sillimanite and cordierite in some gneisses.

Granitic Rocks

Colorado, in the Precambrian, was characterized by three major plutonic events. The Boulder Creek granite was the first batholithic granite to be intruded in the central Front Range during the Boulder Creek Orogeny 1750-1690 m.y. (Hutchinson and Hedge, 1967). The Silver Plume Disturbance Thermal Event took place 1470-1390 m.y. ago and was responsible for emplacement of the Silver Plume granite and its equivalents (Hutchinson and Hedge, 1967). The Silver Plume granitic bodies are dispersed throughout the Front Range and are given different local names (Lovering and Goddard, 1950). The third Precambrian, Pikes Peak Plutonic Event, was responsible for the relatively restricted emplacement of the Pikes Peak granite 1027 to 1053 m.y. ago (Hutchinson, 1959; Hedge, 1967; Hutchinson and Hedge, 1967 and 1976; and Hedge, 1970).

Very few granitic rocks are exposed at the surface in the Central City district (Figure 3). The nearest surface exposure of the Boulder Creek granite to the Central City district is in the Georgetown quadrangle south of Idaho

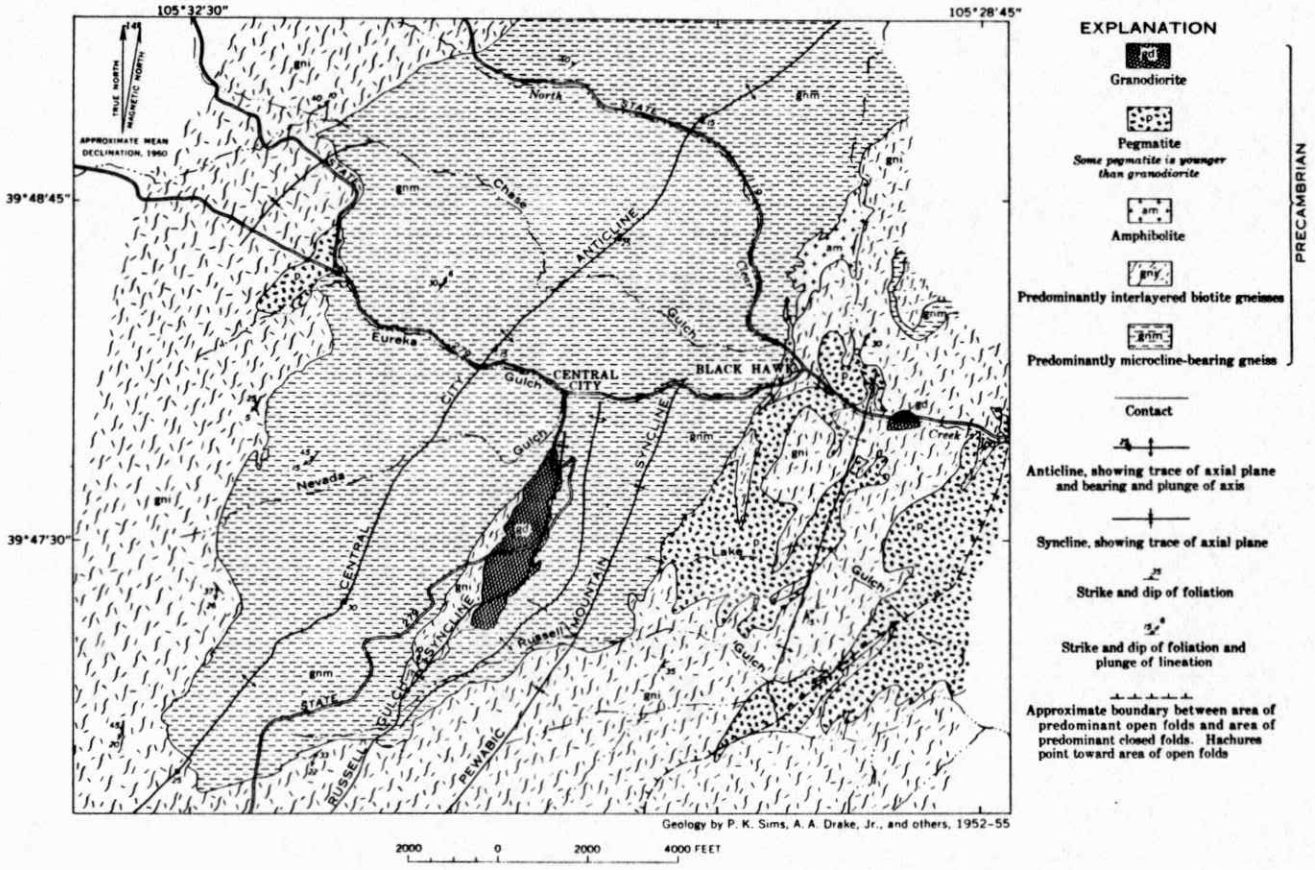

Figure 3. Generalized geologic map of the Central City district, showing the major Precambrian rock units and structures (from Sims, and others 1963b)

Springs. A biotite-muscovite Silver Plume granite is present in the Central City district.

Pegmatites

Four types of pegmatites, distinguished on the basis of mineralogy, texture, and structure are found in the Central City district (Sims, and others 1963b). The most common type is a white to tan coarse-grained, weakly foliated generally conformable rock. Its minerals include quartz and feldspar with some biotite and magnetite. Locally, pods of coarsely-crystalline quartz less than 1 foot thick are present within the study area.

Paleozoic and Mesozoic

There are no Paleozoic or Mesozoic rocks in the Central City district. Paleozoic and/or Mesozoic rocks may have been deposited in the Central City district but would have been stripped away following deposition because of uplift during the Laramide Orogeny.

Cenozoic

Tertiary Igneous Rocks

The following list gives the six Tertiary intrusive porphyry types which are present in the Central City district, from oldest to youngest, as named by Sims, and others (1963b).

(1) leucocratic granodiorite porphyry
(2) alkalic syenite porphyry
(3) quartz monzonite porphyry
(4) bostonite porphyry
(5) trachytic granite porphyry
(6) quartz bostonite porphyry

Younger, small quartz bostonite porphyry rocks (6) are found at Maryland Mountain but outside of the study area (Sims, 1964).

Breccia

Breccia structures occur underground within the Bonanza Adit as well as on the surface within the study area. On the surface, the breccia has a distinct melanocratic appearance relative to the adjacent gneiss. The breccia fragments are both angular and rounded and include quartzite, schist, and the predominant gneiss. Individual breccia fragments generally range from 0.5 inches to 6 inches in longest dimension, though some fragments are significantly larger than this. The matrix consists of a quartz monzonitic(?) material. Visible sulfides (i.e., pyrite) are present in the breccia. Magnetite concentrations in the breccia are high, sometimes reaching as much as 5%.

The form of the breccia units on the surface is very irregular and, occasionally, apparently discontinuous. The number and distribution of breccia structures in the

subsurface is very difficult to correlate with those on the surface.

Where the dilational hydrothermal vein structures intersect breccia structures (in the Bonanza Adit), the precious metal grades (especially gold) increase significantly relative to the adjacent ore (Cullar, personal communication, 1985). The breccia structures appear to have been intruded prior to or perhaps during the initiation of displacement along these fault structures. Some breccia structures are intersected by fault structures, but the distribution of breccia structures in the study area is not limited to the known fault structures.

Structure/Tectonics

Precambrian deformational development occurred during two separate tectonic events in the Central City district (Moench, and others, 1962). The earliest stage produced a major fold system with axes bearing north-northeast. Disharmonic folds and abnormal anticlinoria-synclinoria were produced as the rocks responded plastically. Recrystallization of the rocks facilitated the development of gneissic texture.

A notable structural feature in the Central City district, which formed during the earliest stage of Precambrian folding, is the northeast-southwest doubly

plunging Central City Anticline (Figure 3). The crest of the northeast plunging portion of the anticline passes through the peak of Maryland Mountain. Strata generally dip northwest and southeast, symmetrically, away from the crest of this anticline, though some locally overturned units are found.

Granodiorite and biotite-muscovite phacoliths were intruded near the end of the earliest Precambrian folding phase. These intrusions are equivalents of the Silver Plume granites emplaced 1470-1390 m.y. (Hutchinson and Hedge, 1967).

The later less extensive stage of Precambrian folding was accompanied by intense cataclasis with fold system axes bearing approximately north 55 degrees east superimposed upon the earlier structural features. The Idaho Springs-Ralston shear zone is the principal Precambrian shear zone in this area and it averages about 2 miles in width. It trends north 55-60 degrees east and extends from east of Georgetown, 23 miles to the northeast. The location of this shear zone roughly corresponds with the southeast margin of the Colorado mineral belt. Shearing activity along this zone is considered to have been the primary cause for development of the younger Precambrian foliation. Movement along the ancient shear zone is also known to have occurred

during the Paleozoic and Mesozoic eras, with minor reactivation during Tertiary time (Tweto and Sims, 1963).

The Central City district contains a complex network of faults with various trends. These faults can be catagorized into five major groups (Sims, 1982). Two of these fault groups were first active in Precambrian time while the other three groups were first displaced during the Laramide Orogeny.

The oldest set of Precambrian faults in the district trends northwest and extends for miles across the Colorado mineral belt. This fault set consists of discrete faults, shear zones, and silicified breccia reefs. Many of these faults underwent extensive reactivation during the Laramide Orogeny and some contain Laramide-related felsic porphyry dikes. Displacement along these faults during the Precambrian was left lateral strike-slip on the order of several hundred feet. Some relatively minor oblique and vertical displacement occurred along these faults during Laramide orogenic activity.

The relatively younger set of Precambrian faults in the Central City district trend north to northeasterly. Displacement along this fault system is thought to be dominantly strike-slip, but the direction of displacement is unknown. These faults also suffered minor reactivation

during the Laramide Orogeny and some have been intruded by Laramide-related felsic porphyry dikes. Since a full understanding of the displacement direction and displacement magnitude of all Precambrian faults has not been attained, the Precambrian stress fields which were active in the district can not be fully defined.

The three sets of faults which were first offset during the Laramide Orogeny are generally short and display small magnitudes of displacement. These Laramide-related faults also host most of the mineralized veins of economic importance. All three fault sets display dominant strike-slip displacement, though local dip-slip is common. Displacement along these faults generally does not exceed a few tens of feet. Most of these faults were formed after the peak of Laramide igneous intrusive activity. Vein mineralization was concurrent with Laramide fault displacement and many veins have been brecciated by syn- or post-depositional fault reactivation.

The three Laramide fault sets from oldest to youngest include an east trending group, an east to northeast trending group, and a northeast trending group. The east trending group displays left lateral displacement while the relatively later east to northeast and northeast trending sets display right lateral displacement (Sims, and others,

1963b). The Laramide fault structures appear to have been formed by regional stresses acting in a general east-northeastward direction (Sims, and others, 1963b; Tweto and Sims, 1963). The fissure vein structures within the study area strike east-northeast and dip steeply to the northwest and southeast. The structures are interpretted to be right lateral strike slip faults with lateral displacement not exceeding one hundred feet.

Three main stages of mineralization occur in the concentrically zoned Central City district (Sims, 1982). The three stages from oldest to youngest are referred to as the uranium stage, the pyrite stage, and the base metal stage. Most of the gold and silver was deposited during the base metal stage. Each mineralizing stage is thought to be separated by a tectonic event which resulted in structural readjustment of the district and reactivation of the hydrothermal system.

The relative brittleness of the wallrocks strongly controlled the fault characteristics and hence the localization of ore. Fracture filling veins commonly occur within simple dilational zones in relatively brittle gneissic units. Where these fractures intersect less brittle, relatively biotite-rich gneissic units, the fractures and veins typically horsetail out, thus becoming

significantly less favorable. The localization of ore in vein fissures is effected and drastically enhanced by abrupt variations in strike or dip or by the intersection of two structures.

Geomorphology

Slopes in the study area range from 20-40 degrees and vegetation is sparse relative to the northeast side of Maryland Mountain. Vegetation consists dominantly of pine, spruce, juniper, aspen, small bushes, and sparse to moderate grass cover. A small perennial stream 2-4 feet wide forms Chase Gulch at the southwest boundary of the study area. The topography is relatively rugged in certain parts of the study area, with a steadily increasing slope to the north toward Maryland Mountain Peak at elevation 9203 feet. In general, the soil profile is poorly developed where it is present at all on the southern portion of Maryland Mountain. A B horizon is present in low, less steep portions of the study area, but on the relatively steep slopes, only a thin C horizon is available for sampling. The soils on the southern portion of Maryland Mountain are juvenile and classified as Entisols (United States Department of Agriculture, 1975).

Numerous erosional surfaces have been described in the Front Range. Five of these from oldest to youngest include

the Flattop, Green Ridge, Cheyenne Mountain, Overland Mountain, and the Bergen Ridge surface. These surfaces are listed in order from highest to lowest elevations (Lovering and Goddard, 1950).

In more recent literature, only two main erosional surfaces are recognized in the Front Range. These are the older Flattop peneplain and the younger Rocky Mountain peneplain. The Rocky Mountain peneplain is also referred to as the Sherman, South Peak, Green Ridge, or Green Mountain peneplain. In the Middle and Northern Rocky Mountains, the younger and older surfaces are given the names Summit and Subsummit peneplains, respectively. This nomenclature is further complicated because the surfaces are also given local geographic names (Thornbury, 1965). Secondary supergene mineral depth extension may be related to some of these geomorphic features in the Front Range.

Economic Geology

History and District Production

Placer gold was first discovered in Colorado near the mouth of Chicago Creek, near Idaho Springs in January of 1859. A few months later, the first gold lode was discovered by John H. Gregory just east of Central City. The first smelter in the region was built at Black Hawk in 1865 and this event signaled the beginning of increased gold

production in the district for years to come. Silver was discovered in 1877 or 1878 at Silver Hill, northeast of Maryland Mountain.

Activity in the area slowly declined after the turn of the century until the end of World War I in 1918, when production was seriously reduced. Renewed activity in the area began in 1933 after the United States went off the gold standard and gold prices increased. Gold mining activity in the district diminished again at the beginning of World War II, but the silver and base metal mining activity was stimulated (Vanderwilt, and others, 1947).

Over 500 mines have been worked in the Central City district with total production since the first discovery exceeding $100,000,000 (Sims, and others, 1963b). Gold has accounted for about 85% of this total dollar value. Silver ores have produced 10% and copper, lead, zinc, and uranium production, in decreasing order of importance, account for the remaining 5% of production (Sims, and others, 1963b).

Fluctuating base and precious metal prices in recent years have triggered renewed interest and re-evaluation of portions of the Central City and adjacent districts. Only minor, small scale, and sporadic mine reactivation has occurred.

Ore Types

Ore mineralogy in the district is relatively simple. The main ore minerals include pyrite, galena, sphalerite, chalcopyrite, and tennantite along with the less common gold tellurides, pitchblende, enargite, and marcasite. Principal gangue components include quartz and microcrystalline silica along with locally occurring fluorite, barite, and carbonate minerals (Table 2).

The veins in the area are divided into two general mineralogical categories by most workers: the pyrite and the galena-sphalerite types. A particular vein often represents a combination of the two types along with other components (Bastin and Hill, 1917). Such composite veins are fairly common and form as a result of multi-staged mineralization events. Telluride and pitchblende veins are present in the district, but in far lesser quantities than the pyrite and galena-sphalerite veins.

The pyrite veins are predominantly composed of pyrite and quartz, though chalcopyrite, tennantite, enargite, sphalerite, and galena are common locally. Gold and silver are most abundant in those pyrite-type veins containing substantial quantities of sphalerite, galena, and copper minerals. Gold is the most important ore metal in the pyrite veins. Gold and silver are associated chiefly with

Table 2. Primary and secondary vein minerals in the Central City district
(from Sims, and others, 1963b)

Primary	*Secondary*
Sulfides:	Sulfides:
Pyrite FeS_2	Chalcocite Cu_2S
Sphalerite ZnS	Covellite CuS
Galena PbS	Chalcopyrite $CuFeS_2$
Chalcopyrite $CuFeS_2$	Bornite Cu_5FeS_4
Marcasite FeS_2	
Molybenite MoS_2	
Bornite Cu_5FeS_4	
Sulfosalts:	Sulfosalts:
Tennantite $(Cu,Fe,Zn,Ag)_{12}As_4S_{13}$	Ruby silver $Ag_3(As,Sb)S_3$
Tetrahedrite $(Cu,Fe,Zn,Ag)_{12}Sb_4S_{13}$	
Enargite Cu_3AsS_4	
Pearcite(?) $(Ag,Cu)_{16}As_2S_{11}$	
Chalcostibite(?) $Cu_2S\ Sb_2S_3$	
Native elements:	Native elements:
Gold Au	Gold Au
Bismuth Bi	Silver Ag
Oxides:	Oxides:
Uraninite (pitchblende) $UO_2\ (UO_3)$	Hydrous iron oxides
Hematite Fe_2O_3	
Tungstates:	
Wolframite (Fe,Mn) WO_4	
Ferberite Fe WO_4	
Tellurides:	
Sylvanite $(Au,Ag)\ Te_2$	
Calaverite(?) $AuTe_2$	
Halides:	
Fluorite CaF_2	
Phosphates:	Phosphates:
	Autunite $Ca(UO_2)_2(PO_4)_2 \cdot 10\text{–}12H_2O$
	Metatorbernite $Cu(UO_2)_2(PO_4)_2 \cdot 8H_2O$
	Torbernite $(Cu(UO_2)_2)(PO_4)_2 \cdot 8\text{–}12H_2O$
	Meta-autunite $(Ca(UO_2)_2)(PO_4)_2 \cdot 10H_2O$
Silicates:	Silicates:
Quartz SiO_2	Quartz SiO_2
	Kasolite $Pb(UO_2)\ SiO_4 \cdot H_2O$
Carbonates:	Carbonates:
Ankerite $Ca\ (Mg,Fe)(CO_3)_2$	Cerussite $PbCO_3$
Siderite $(Fe,Mg,Mn)CO_3$	Smithsonite $ZnCO_3$
Rhodochrosite $(Ca, Mg)(CO_3)_2$	Malachite $Cu_2CO_3\ (OH)_2$
Calcite $CaCO_3$	Azurite $Cu_3\ (CO_3)_2\ (OH)_2$
Sulfates:	Sulfates:
Barite $BaSO_4$	Anglesite $PbSO_4$
	Copper sulfates
	Epsomite(?) $MgSO_4 \cdot 7H_2O$
	Zippe te $(UO_2)SO_4(OH_2)_2 \cdot nH_2O$
	Johannite $(Cu(UO_2)_2(SO_4)_2(OH)_2 \cdot 6H_2O$
	Gypsum $CaSO_4$

chalcopyrite, tennantite, and pyrite, and galena (Bastin and Hill, 1917). Pyritic ore produced in the Central City district during active times averaged 1 to 3 ounces of gold and 4 to 8 ounces of silver per ton. The copper content in the pyrite ores has typically been below 1.5 percent, though some have contained up to 15 percent copper (Vanderwilt, and others, 1947).

The galena-sphalerite veins are composed of galena and sphalerite with limited pyrite, chalcopyrite, tennantite, and bornite (Bastin and Hill, 1917). Silver is common in these veins, becoming enriched locally, while gold is relatively less abundant. Silver in the galena-sphalerite-type veins increases with the amount of tennantite and galena, but locally chalcopyrite and sphalerite may be rich in silver. Gold, when present, is associated with chalcopyrite and tennantite (Sims, and others, 1963b). Silver content in the mined galena-sphalerite veins has ranged from 5.5 to 40 ounces per ton and gold content has ranged from 0.15 to 3.0 ounces per ton. Copper, lead, and zinc, contents have ranged from less than 1 percent for all three, up to 17 percent for copper, 54 percent for lead, and 32 percent for zinc (Vanderwilt, and others 1947). Generally the galena-sphalerite veins contain more silver and lead and less gold and copper relative to the pyrite-

type veins (Sims, and others, 1963b).

The less abundant telluride ores consist of gold and silver tellurides in a gangue of horn quartz with small amounts of purple fluorite, ferruginous calcite, and fine-grained pyrite. Krennerite, petzite, sylvanite, altaite, and coloradoite are the common telluride minerals. Average telluride ore taken from the War Dance Mine in the Central City district, during peak production, had average grades of approximately 16 ounces gold and 13 ounces silver per ton (Bastin and Hill, 1917).

Pitchblende often occurs in veins which have been mined primarily for their gold or silver content. Production of pitchblende in the Central City district has always been of secondary importance relative to gold and silver production.

Ore Zonation and Morphology

Mineralization in the Central City district is part of a well-defined, northeast-southwest elongate, and concentric hypogene zonation feature in plan view (Figure 4). The maximum dimensions are about 7 miles X 11 miles at the surface.

A central zone with a maximum extension of 3 miles is characterized by pyrite veins. Copper minerals in pyrite veins generally increase in abundance outward in this zone. Quartz makes up most of the gangue in the central zone

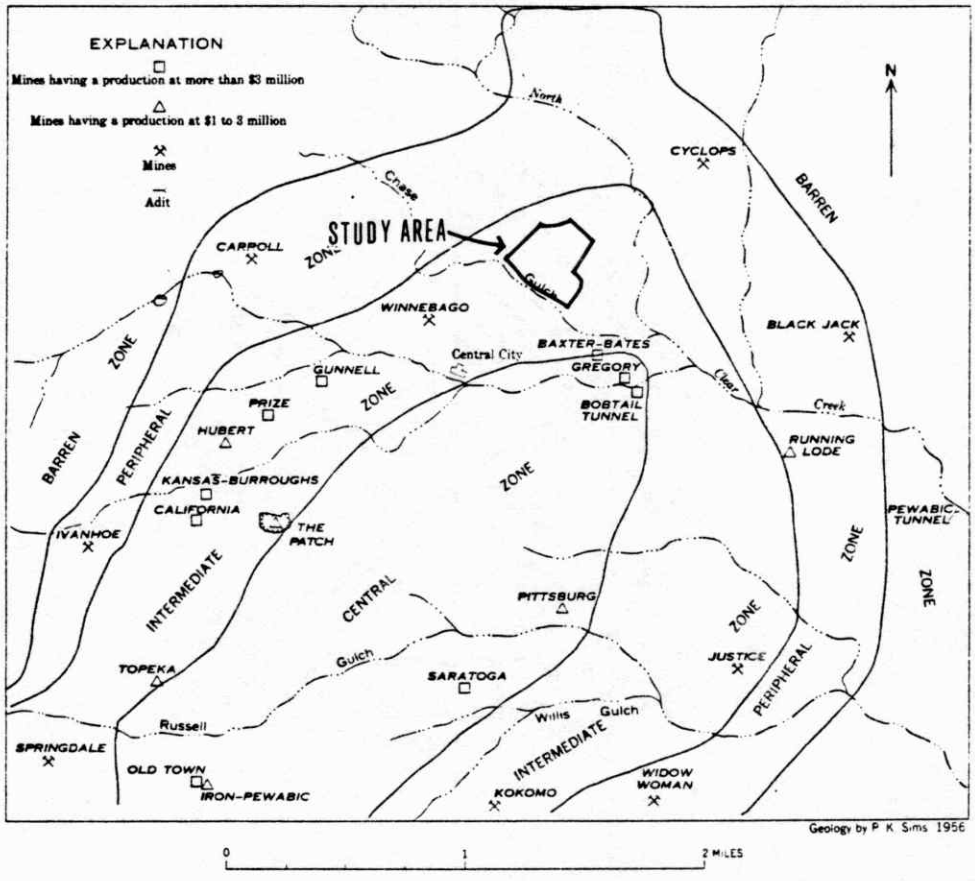

Figure 4. Map of Central City district showing zoning of mineralization
(from Sims, and others, 1963b)

(Rice, and others, 1982b).

A second, intermediate zone, is transitional between the central zone and a third, peripheral zone. The intermediate zone contains pyrite-type veins which include substantial quantities of galena, sphalerite, and copper minerals. The principal gangue in the intermediate zone includes a coarsely crystalline and a chalcedonic quartz with sparse carbonates. The study area is located within the intermediate zone.

The peripheral zone includes chiefly the galena-sphalerite type veins. Silver is the major ore metal produced in this zone. Vein gangues in the peripheral zone are principally chalcedonic quartz, rhombohedral carbonate minerals, along with barite, which is not found in the central or intermediate zones.

Outside the peripheral zone is a fourth, so-called barren zone which has produced only minor amounts of silver ore. Figure 5 shows the distribution of gold, silver, and important minerals in the Central City district relative to the four hypogene zones.

Ores in the area occur as fissure veins and to a lesser degree as stockwork "explosion breccias". Ore morphology in the district ranges from small pods or lenses to more tabular vein-type bodies. The veins in the district are

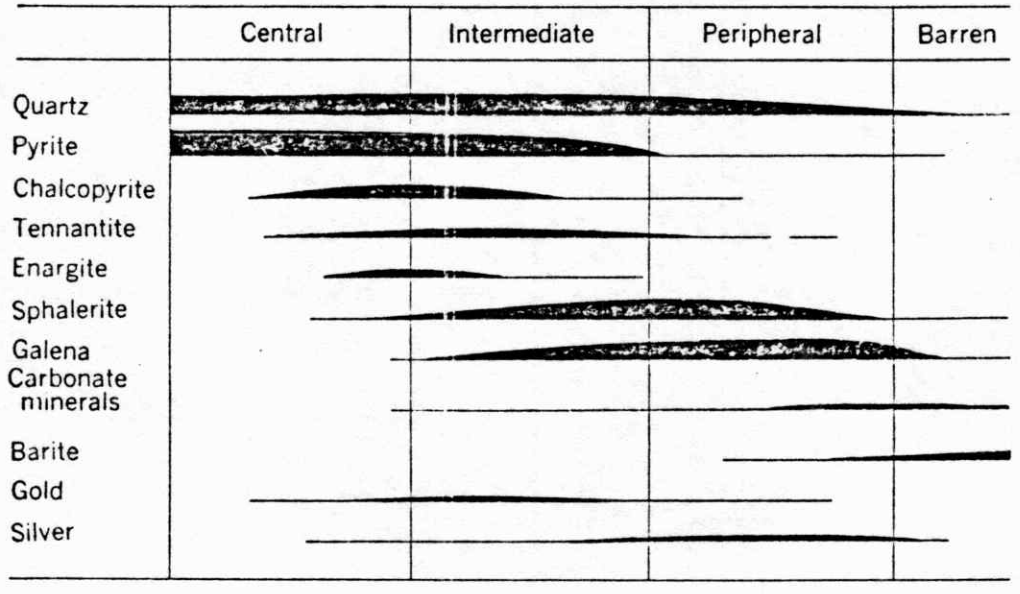

Figure 5. Zonal distribution of vein-forming minerals (from Sims, and others, 1963b)

highly variable, ranging from simple, well-defined filled fissures to complex branching lodes, consisting of subparallel fractures, loops, and horsetailing or feathering fractures (Sims, and others, 1963b).

The ore veins may measure up to 3 feet wide, though they have been observed up to 8 feet wide on a local scale. Ore shoot extension is highly variable in the district. The majority of the bodies have been known to pinch out or become unminable at moderate depths.

The predominant stockwork structure in the area is "the Patch" located about one mile southwest of Central City. This structure plunges steeply to the north. It is oval-shaped in plan view with an east-west axis about 800 feet long and a shorter surface dimension of 500 feet; the wallrocks of the breccia chimney are predominantly Precambrian microcline-bearing gneiss.

Sims, and others, (1963b) postulated that the Patch developed as a result of the explosive upward-movement of a magma body along a zone of rocks weakened by fault activity. They proposed the hypothesis that large volumes of gases emanating from depth during and after the explosive phenomenon eventually resulted in extensive alteration of the breccia zone. Subsequent mineralization by vein-forming fluids produced the stockwork-type ores in the Patch. The

ores in the Central City district are completely fissure-vein types except for the stockworks in the Patch.

Generalized Ore Paragenesis

Mineralization in the Central City district is considered to have been deposited in four temporal stages. The earliest stage was characterized by uranium deposition, primarily in the form of pitchblende. The second stage included deposition of most of the pyrite in the area and the third stage was responsible for base metal deposition. Sparce telluride minerals were deposited in the last stage and these are generally found in the southeast part of the Central City district.

Pitchblende deposited during the first mineralization stage is commonly associated with quartz gangue and intergrown with chalcopyrite and pyrite. The principal minerals deposited during the pyrite stage were pyrite and quartz. The base metal stage was responsible for deposition of most of the sphalerite, chalcopyrite, tennantite, enargite, and galena along with some pyrite in quartz gangues. Some carbonates, fluorite, and barite occur locally as gangue minerals deposited during the base metal stage. Almost all of the silver and gold was introduced during the base metal stage of mineralization (Sims and Barton, 1962; Sims, and others, 1963b).

A paragenetic study of the Smith Vein on the southeast side of Maryland Mountain by Kramer (1984) revealed a sequence of six hypogene stages. These stages include I. hematite, II. early pyrite, III. base metal, IV. galena, V. chalcopyrite, and VI. late pyrite, followed by the effects of supergene alteration. Kramer determined that gold was first introduced during the early pyrite stage and most was deposited during the base metal stage.

Primary ore zonation, from the central zone to the peripheral zone, generally corresponds with a gradation from pyrite to galena-sphalerite veins respectively. This relationship, in turn, is defined by an increase in silver:gold and lead:copper ratios, and in absolute zinc content outward from the central to the peripheral zone.

Temperatures of mineralization were determined by sphalerite fluid inclusion thermometry and found to generally decrease outward from the central pyrite zone (Sims and Barton, 1962). Temperatures measured show a narrow, abrupt lateral geothermal gradient separating a central zone with temperatures around 600^{o}C from a zone including temperatures from 150^{o} to 300^{o}C near the hypogene margins. The abrupt lateral geothermal gradient zone includes the intermediate and peripheral hypogene zones where most of the gold, silver, and sulfides were deposited.

Kramer (1984) found no evidence for boiling in the Smith Vein, which is located within the intermediate zone. Kramer estimated depth of overburden at the time of mineralization to be 4000 feet for a pressure correction of 33 bars, assuming purely lithostatic conditions. She determined primary inclusion homogenization temperatures which ranged from 323° to 345°C and 302° to 325°C for her stage II quartz and stage III sphalerite, respectively.

Sims and Barton (1962) believe that heat-dissipating processes of magma at depth were responsible for the hydrothermal mineral gradation in the area. They also believe that the water in the mineralizing solutions was derived from a mixture of magmatic and meteoric sources. The first mineralizing solutions were transported upward along openings in breccias and along fissures caused by the upward-migrating magma. Solution transport in the area was facilitated during deposition by the reactivation of fissures causing reopening of solution paths. Major episodes of solution path reactivation probably separate the various temporal mineralization stages. Pyritic and galena-sphalerite veins correspond to, and generally define the hypogene zones, while the uranium and telluride mineral distribution has little or no relationship to the zonation model.

Ore deposits in the area are considered to be closely related, temporally and genetically, to prevalent early Tertiary porphyritic intrusions. An age for precious and base metal mineralization was determined by Rice, and others, (1982b) to be 58 to 60 million years before the present. They used direct potassium-argon dating of associated sericites and indirect dating of pre- and post-ore intrusions in the area to determine this age. Rice, and others, (1982a) suggest that known mineralization in the Central City district represents an upper structural level in a magmatic/hydrothermal system which contains a molybdenum-bearing porphyry intrusion at depth.

Alteration and Secondary Enrichment

Successive alteration zones are found enveloping all veins in the district. Local alteration zones around pyrite veins are generally more extensive relative to the galena-sphalerite type veins. Most commonly, sericite alteration occurs adjacent to the vein minerals and the clay minerals become prevalent further out eventually grading into fresh rock (Tooker, 1963). Quartz-sericite-pyrite (QSP) altered rock is the predominant gangue on dumps in the study area. Argillic alteration zones up to 2 feet thick enclose the quartz-sericite-pyrite alteration. Intense sericite alteration is often hard and bleached to a light greenish

gray or white color. Strongly argillized zones are commonly a light-green to white color.

Width of alteration zones may be highly variable, ranging from inches up to an extreme 30 feet (Tooker, 1963). The ratio of alteration zone thickness to vein mineralization thickness is generally greater in the central hypogene zone as compared with the intermediate or peripheral hypogene zones. This is evidence for the hypothesis that hypogene minerals in the district were derived from a central solution source (i.e., alteration is more extensive near the solution source). Generalized mineralogical relationships are represented in Figure 6 showing variations from fresh, unaltered host rocks (Zone 1), to weakly argillized rocks (Zone 2), strongly argillized rocks (Zone 3), and sericitized rocks (Zone 4), to the veins.

Fissure wallrock alteration is considered to predate deposition of vein minerals. Therefore, the presence of sericite or argillite alteration does not necessarily indicate the presence of enclosed vein materials. Primary uranium minerals, however, are thought to have been deposited earlier than precious metal ores, during the late stage of early hydrothermal rock alteration.

Minerals indicative of secondary supergene enrichment

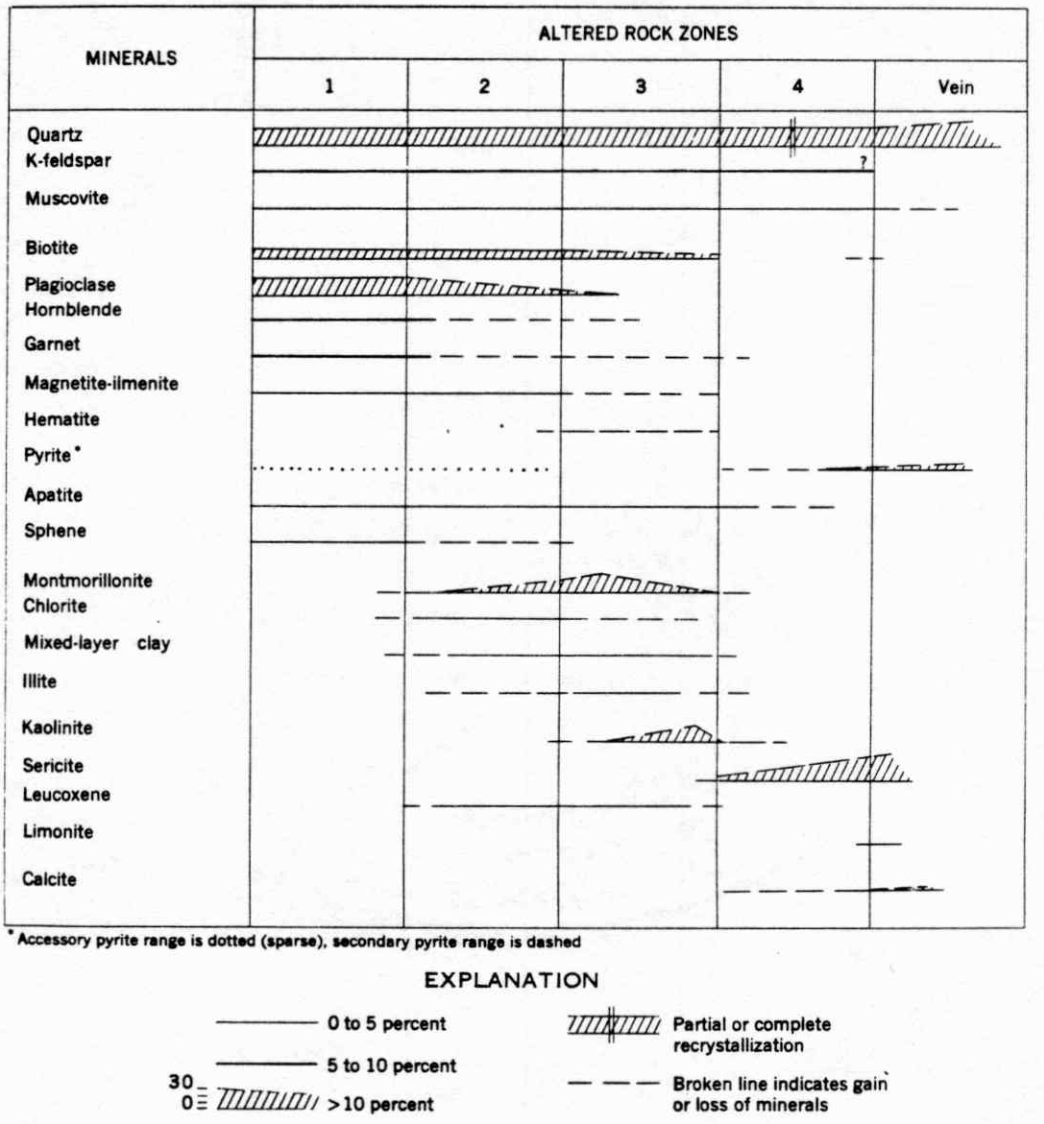

Figure 6. Generalized amounts and ranges of the most common minerals in fresh (1) and altered wallrocks (from Tooker, 1963)

are found at great depths in the district, however, almost all of these occurrences are not economic. Supergene enriched ores are often not readily distinguishable from their hypogene counterparts, but they do account for some local silver and copper enrichment below the zone of oxidation. Secondary enrichment derived from galena-sphalerite veins is important in the Silver Hill area. Silver is present here in native form or as sulfosalts (e.g., proustite and ruby silver, etc.). Gold in some mines in the district is found locally secondarily enriched in upper portions of oxidized veins and generally extending 50 feet and as much as 150 feet below the present surface. Minerals which are typically present and most easily recognizable in supergene enriched zones include limonite, kaolinite, and minor quantities of chalcocite (Table 2).

Geochemistry

Surveying, Soil Sampling, and Sample Preparation

Surveying methods were used to accurately locate all important surficial features including caved and open stopes or shafts, adits, prospect pits, and mine dumps. These and other features are located on Plate I which is a map of the area at a scale of 1 inch = 100 feet. The topographic contour interval on this map is 10 feet. Details of the surveying procedure are presented in Appendix I. The alignment of cultural features including prospect pits, stopes, adits, and dumps was used to establish the locations of structures V1 - V6 shown on Plate I. These structures were used as control for developing the surficial geochemical model and they will be referred to as "control structures" throughout this text.

Soil samples were collected along three traverses oriented perpendicular to structural strike at 10 feet intervals over observed vein structures and at 25 feet intervals where no structures were known. Details of the soil sampling procedure are presented in Appendix II. The soil samples were sized into 3 fractions using stainless steel U.S. Series 10, 60, 80, and 230 sieves. The three size fractions included: -10 to +60, -80, and -230 mesh.

Sample Analysis

The objective of this study was to characterize the trace element dispersion haloes around vein stuctures in a base and precious metal mining district which has been subjected to extensive prospecting and mining activity within the past 100 years. The purpose of the study was to develop a surficial geochemical exploration tool which could be used to locate unexploited mineralization in areas where soil cover disturbance and steep slopes are common. Preliminary analytical steps were carried out in order to determine the most appropriate sample digestion/extraction method to use to meet the objective and purpose. In effect, these preliminary steps reduced the amount of total laboratory work. Certain procedures, elements, and soil size fractions were eliminated from further consideration during preliminary analysis because they resulted in no useful information. Initially, 18 elements were considered for analysis including Ag, As, Au, Bi, Cd, Cu, Fe, Ga, In, Mn, Mo, Pb, Sb, Se, Sn, Te, Tl, and Zn. The procedures which were finally used to analyze all of the soil samples were chosen because they generated a maximum amount of information from a minimum amount of data.

A hot nitric acid digestion was used to leach the -80 mesh soil fraction, but the detection limits of the flame

atomic absorption spectrophotometer were not sufficiently low enough to determine the concentrations of many trace elements of interest (e.g., Ag). The hot nitric acid digestion method was used to analyze all soil samples for Cu, Pb, Zn, Cd, Fe, and Mn. Following this, a series of experimental analytical steps was carried out, which included a hot sulfuric acid-bromate digestion/MAGIC extraction, 24 hour cold HCl digestion/MAGIC extraction, and a 30 minute cold HCl digestion/MAGIC extraction (Clark and Viets, 1981; Clark, personal communication, 1985). The 30 minute cold HCl digestion/MAGIC extraction method was deemed most significant of those tested and all soil samples were analyzed for Ag, As, Au, Cd, Cu, Fe, In, Mn, Mo, Pb, and Zn.

Data Processing

Statistical and spatial data analysis was carried out on the Colorado School of Mines (CSM) DEC-10 main frame computer and on a Texas Instruments personal computer. Coefficients for absorbance-concentration calibration curves were calculated using a least squares fit program called LSQ which is maintained in the CSM Geology Department computer library. These coefficients were then incorporated into the raw absorbance data sets. Concentrations were calculated by executing a polynomial solution program which also accounted for the appropriate dilution factors.

Basic statistics and correlation matrices were generated using program URPSTAT, which is maintained in the CSM Geology Department computer library. Elemental distribution plots presented in Plates II, III, and IV were created using program GRAPHM from the CSM computer library. Program GRAPHM possesses regression capabilities. All plots were plotted with the CSM DP-8 plotter.

Ratio calculations were executed by a program which is written in FORTRAN. This program and its explanation are presented in Appendices Xa and Xb, respectively. Calculated ratio values (Appendix Xc) which exceed 10.0 are assigned this value and these data were run through program GRAPHM and plotted with the DP-8 plotter. The Fe/Mn ratio plots for the hot nitric acid digestion and the 30 minute cold HCl digestion are presented on Plate IV.

Results

Results obtained in this study are described under the following headings: Analytical Data, Averaged Relative Precision, Basic Statistics, Interpretational Considerations, Correlation Analysis, Distribution of Elements in Soil, and Regression Analysis. The discussion of ratio analysis follows in a separate section.

Analytical Data

During the course of these experimental analytical steps (including the hot nitric acid digestion, hot sulfuric acid-bromate digestion/MAGIC extraction, 24 hour cold HCl digestion/MAGIC extraction, and the 30 minute cold HCl digestion/MAGIC extraction) it was determined that the concentrations of trace elements in many samples of the -10 to +60 mesh soil fraction were below detectable limits. The -80 mesh soil fraction was found to contain substantially higher concentrations of all trace elements, relative to the coarser fraction (see Table 3). However, the -230 mesh soil fraction contained the highest concentrations of metals and it allowed for a slight improvement in analytical precision over the other two fractions (see Tables 3 and 4). This fraction was therefore chosen as best for all subsequent analytical procedures.

Bismuth, Ga, Sb, and Sn were eliminated from analytical

Table 3 Preliminary Soil Analysis: Concentration Ranges and (Arithmetic Means)

Method:	24 Hr. HCl/MAGIC	24 Hr. HCl/MAGIC	24 Hr. HCl/MAGIC
Fraction:	-10/+60	-80	-230
element			
Ag	0.05-0.90 (0.16)	0.19-3.72 (0.72)	0.16-3.48 (0.81)
As	0.36-1.83 (0.91)	0.69-6.06 (2.70)	0.78-8.22 (3.30)
Au	0.002-0.035 (0.004)	0.002-0.258 (0.057)	0.002-0.384 (0.120)
Bi	0.03-0.26 (0.14)	0.15-1.26 (0.61)	0.15-1.74 (0.72)
Cd	0.15-1.86 (0.54)	0.30-6.60 (1.70)	0.35-7.50 (2.00)
Cu	1.8-30.0 (7.3)	7.8-111.0 (34.0)	9.8-120.0 (35.0)
Ga	0.20-0.66 (0.39)	0.51-1.71 (0.97)	0.54-1.56 (0.99)
In	0.01-0.18 (0.03)	0.02-0.60 (0.10)	0.20-0.69 (0.11)
Mo	0.17-0.65 (0.36)	0.50-2.64 (0.90)	0.60-2.12 (0.99)
Pb	9.9-531.0 (74.0)	27.9-1320.0 (230.0)	24.0-1620.0 (260.0)
Sb	0.03-0.54 (0.12)	0.10-1.80 (0.54)	0.10-2.19 (0.62)
Sn	0.08-0.48 (0.23)	0.30-1.20 (0.61)	0.60-1.92 (1.00)
Zn	19.5-351.0 (64.0)	51.0-1680.0 (230.0)	53.1-1690.0 (240.0)

All numbers are expressed in parts per million (ppm)

Table 4 Preliminary Soil Analysis: Averaged Relative Precision of Analytical Duplicates (in percent)

Method:	24 Hr. HCl/MAGIC	24 Hr. HCl/MAGIC	24 Hr. HCl/MAGIC
Fraction:	-10/+60	-80	-230
element			
Ag	7.39	4.07	3.41
As	7.12	7.06	6.34
Au	17.98 ***	29.62 *	43.25 *
Bi	10.82 *	5.82	5.65
Cd	6.33 *	8.58	12.75 *
Cu	9.34	6.41	2.44
Ga	4.64	4.64	3.09
In	19.55 **	13.49	6.60
Mo	9.06	7.09	7.77
Pb	9.60	6.80	3.26
Sb	9.06 *	3.89	2.34
Sn	7.79	7.71	5.79
Zn	8.69	3.55	2.34

Number of duplicate pairs analyzed by 24 Hr. HCl/MAGIC method used to determine averaged relative precision of analytical duplicates = 4

(Relative Precision of Duplicate Pair) in percent=

$[[X_1-((X_1+X_2)/2)]/[(X_1+X_2)/2]](100).$

(X_2=duplicate of X_1)

Average Relative Precision = Averaged Absolute Values of (Relative Precision of Duplicate Pairs)

The number of asterisks after precision values indicate the number of duplicate pairs which include one or both concentrations at or below the detection limit.

consideration after it was determined that the concentrations of these elements are low in both the soils and in the mineralized rocks, relative to other elements. Those elements in the soils and/or mineralized rock samples which were present in concentrations at or below the detection limits of the Perkin-Elmer 360 atomic absorption spectrophotometer equipped with an HGA-2100 graphite furnace were eliminated from subsequent analytical procedures (e.g., Se, Te, and Tl). The concentration of molybdenum in mineralized rock was much higher in the unconcentrated -200 mesh pulp fraction (18.27 ppm) relative to the concentrated -60 mesh fraction (0.93 ppm, see Appendix Table VIa). The molybdenum in the mineralized rock probably occurs in a platy or flaky form locked within silicates. The molybdenum-bearing silicates would have been less dense relative to the coarser sulfide phases in the rock so they were undoubtedly lost during heavy mineral separation using the Wilfley Table. The fact that molybdenum was present in fairly high concentrations in the unconcentrated mineralized rock made it interesting enough to consider in subsequent analytical steps.

Data obtained using different digestion methods revealed that free sulfides are present in abundance in the soils near areas where the ground was disturbed by mining

activity. This was further confirmed by wet panning of soil collected near surficial workings. Pyrite was present in these concentrates in visible quantities along with very sparse quantities of galena. In addition to sulfides, small pieces of rusty scrap iron were found. The sulfides present in and around the mine dumps and stopes may have been exposed to the processes of weathering for as long as 100 years (since mining was initiated in the district).

It was hypothesized that the sulfides which have become exposed to surface weathering in a semi-arid climate in this district as a result of mining have not been completely transformed to oxyhydroxides during the century which has passed since the initiation of mining. It was also hypothesized that metal-bearing Fe-Mn oxyhydroxide surface coatings on the soil grains may retain substantial and interpretable trace metal concentrations. Furthermore, the concentrations of the trace metals contained in or adsorbed on the Fe-Mn oxyhydroxides may not have been influenced to a significant degree by trace metal contributions resulting from the oxidation of sulfides which were dispersed as a result of mining activity.

From these facts/hypotheses it was determined that a partial chemical digestion/extraction of trace elements which are coprecipitated with or adsorbed on Fe-Mn

oxyhydroxides in these soils may be the ultimate (and perhaps the only) tool for defining reasonable geochemical trends in a contaminated area such as the Central City district. A very weak digestion procedure which would attack the oxyhydroxide coatings, but which would not significantly oxidize the sulfides was considered the most appropriate for the analysis of these soils.

The 30 minute cold hydrochloric acid digestion was chosen as the best method of those tested because it selectively dissolves a substantial proportion of the Fe-Mn oxyhydroxides in the soil, whereas dissolution of base metal sulfides is minimal and the dissolution of pyrite is virtually nil. The 30 minute cold HCl digestion was integrated with the MAGIC extraction system (Clark, personal communication, 1985) and the concentrations of Ag, As, Au, Cd, Cu, Fe, In, Mn, Mo, Pb, and Zn were determined in all samples. Flame and graphite furnace atomic absorption spectrophotometric methods were used to analyze the extracted trace elements in aqueous and organic solutions. The -230 mesh soil fraction was the most appropriate choice for analysis because it possesses the highest relative total grain surface area and it contains the highest concentration of Fe-Mn oxyhydroxide coatings.

Averaged Relative Precision

Precision is the ability to reproduce or repeat the same result. Accuracy is the approach to the true value or content. In general, good precision is much more important than good accuracy in geochemical exploration (Levinson, 1980).

Precision can be calculated using a variety of equations. These equations usually involve the determination of a given sample's variance from the mean of duplicate samples. The relative precision of a duplicate pair (in percent) =

$$[[X_1-((X_1+X_2)/2)]/[(X_1+X_2)/2]](100)$$

where X_2 is the duplicate of X_1. The averaged relative precision equals the averaged absolute values of the relative precision of duplicate pairs. The values of precision are expressed in percent and may be positive or negative. The closer the calculated value approaches zero, the better the precision.

Analytical precision is evaluated in order to estimate the variation resulting from analytical procedures. Selected samples were prepared, split, and then analyzed individually. These data provide the basis for calculation of the averaged relative analytical precision.

Field precision is evaluated in order to estimate the variation at the sample site. Selected field sites were sampled in duplicate, prepared separately, and analyzed individually. These data provide the basis for calculation of the averaged relative field variability. Field variability consists of both analytical and sample site variability.

Most workers consider the analytical precision of a given data set to be acceptable if the absolute value of the precision is less than 15 percent (Closs and Sado, 1982). Field duplicate precision is considered acceptable if the absolute value of the precision is less than 25 percent.

If the precision of a data set appears to be unacceptable, the data are not necessarily unusable for the purposes of interpretation. A lack of good precision may be caused by a few samples whose concentrations are near the upper or lower ends of the analytical method's working range. In this case, the bulk of the data may possess acceptable precision and the data set may therefore be utilized for a reasonable interpretation.

In the analysis of variance, the total variability equals regional variability plus sample variability plus analytical variability (Miesch, 1964). Regional variability is measured indirectly and it is related to the probability

of reproducing the survey and obtaining similar results. Since the reproduction of the survey and obtaining similar results are desirable, regional variability should ideally account for a high proportion (>50%) of the total variability. Sample variability reflects the character of elemental dispersion at the sample site, and analytical variability is that proportion of the total variability which results from human and instrumental error.

Tabular representations of averaged relative precision for hot nitric acid digestion and 30 minute cold HCl digestion/MAGIC extraction soil elemental concentration data are presented in Appendix VII. The averaged relative precision is calculated for analytical duplicate pairs and field duplicate pairs. The averaged absolute values of the relative precision in Appendix VII are expressed in percentages.

Hot Nitric Acid Digestion Method

The analytical duplicate reproducibility for elements analyzed using the hot nitric acid digestion method is generally acceptable although that for Cd (16.89 percent, Appendix Table VIIa) is somewhat high. The field duplicate reproducibility for elements analyzed using the hot nitric acid leach method is acceptable with no values exceeding 21 percent (Appendix Table VIIb).

30 Minute Cold HCl Digestion/MAGIC Extraction

The analytical duplicate reproducibility for elements analyzed using the 30 minute cold HCl digestion/MAGIC extraction method is well within acceptable limits, except that for Au (Appendix Table VIIa). Gold is typically distributed inhomogeneously in soils. The field duplicate reproducibility for Au analyzed using the 30 minute cold HCl digestion/MAGIC extraction is relatively poor (38.82 percent, Appendix Table VIIb). Otherwise, the field duplicate reproducibility for the other elements analyzed by this method is very good. All other averaged relative precision of field duplicates values analyzed by the this method are less than 19 percent (Appendix Table VIIb).

Basic Statistics

The basic statistics for the soil elemental concentration data are presented in tabular form in Appendix VIII. These statistics were utilized during regression and ratio analyses.

Interpretational Considerations

Specific soil samples were chosen for preliminary analysis in order to provide quantitative information about elemental concentration ranges. These samples were collected directly over known mineralized vein structures as

well as over areas thought to be barren of mineralization. It was hypothesized that the concentrations of base and precious metals would be higher in soils overlying mineralization relative to soils overlying barren rock. If this was found to be true, then elemental threshold concentrations could be estimated. Such threshold concentration levels would separate background concentrations over barren rock from anomalous concentration levels over mineralized rock. This was not, however, found to be true from the preliminary analytical data. Many of the base and precious metal elemental concentrations in soils over "barren rock" were higher than those over "mineralized rock." This condition is caused by the close spacing of the mineralized structures and the mechanical downslope creep of the soils.

Much information was missing along the sample traverses since the preliminary samples chosen for analysis were 100-200 feet apart. Following definition of the most appropriate analytical procedure, soil fraction, and elements to be analyzed, all samples from all three traverses were analyzed using the 30 minute cold HCl digestion/MAGIC extraction method. Once this was done, raw data elemental concentration profile plots on the traverses could be used to resolve the locations of known

mineralization (Plate III). It was thought that subtle "rolls" or anomalous sample groupings would be found over the known structures. This was found to be true in the cases where the known mineralized structures are exposed or where they subcrop on gentle slopes (Plate III). At first, resolution of the locations of structures on steep slopes seemed to be impossible, since no obvious anomalous sample groupings existed in soils over these structures.

A data analysis technique applicable to the soil geochemical data was sought which could resolve the locations of mineralized structures on gentle slopes as well as on steep slopes. Correlation and regression analysis were carried out upon these soil geochemical data with limited success. Brief summaries of these procedures and their results follow. After correlation and regression analysis, ratio analysis was used to define the locations of known mineralized structures as well as the locations of some previously unknown or unexploited structures. The logic used to substantiate the utility of the ratios considered is discussed in the following section of this text.

Correlation Analysis

Correlation matrices for the raw soil data are presented in Appendix IX. Correlation coefficient values in

these matrices can theoretically range from -1.0 to +1.0. The correlation coefficients are a statistical measure of the similarity between elemental concentration variables. A correlation coefficient of +1.0 between two variables indicates a 100 percent direct correlation. A correlation coefficient of 0.0 indicates no linear correlation and a correlation coefficient of -1.0 indicates a 100 percent inverse correlation between two variables.

Correlation analysis indicates that the precious metal concentrations (i.e., Ag and Au) vary sympathetically, though gold is more sporadic relative to any other element analyzed (Appendix Table IXb). This is undoubtedly due to the characteristic inhomogeneity of gold dispersion in the soil medium. Base metal concentrations obtained using the hot nitric acid digestion and the 30 minute cold HCl digestion/MAGIC extraction methods are highly correlated with each other (Appendix Tables IXa and IXb).

Correlation analysis indicates that there is a weak positive relationship between Fe and Mn concentrations in soils (correlation coefficient = 0.311 for the 30 minute cold HCl digestion, Appendix Table IXb). Molybdenum appears to be strongly scavenged by Fe, a relationship supported by a strong positive correlation coefficient (correlation coefficient = 0.798 for the 30 minute cold HCl digestion,

Appendix Table IXb).

Distribution of Elements in Soil

All three traverses are represented on Plates II and III. Plate II includes 6 elements (Cd, Cu, Fe, Mn, Pb, and Zn) which were analyzed by the hot nitric acid digestion method. Plate III includes 11 elements (Ag, As, Au, Cd, Cu, Fe, In, Mn, Mo, Pb, and Zn) which were analyzed by the 30 minute cold HCl digestion/MAGIC extraction method. Both of these plates include a topographic profile which displays the projected control vein structures and the surface locations of any trails. The x-axis of all topographic and elemental profiles has increments of 100 feet with an origin at the lowest numbered soil sample station of that traverse (i.e., station 1 for traverse 1, station 68 for traverse 2, and station 148 for traverse 3). The y-axis of the elemental profiles represents concentration and it has increments of base 10 log cycles to allow for a reasonable Y-axis dimension. All elemental concentration units are parts per million (ppm), except iron, which is represented in units of percent.

Hot Nitric Acid Digestion

Cadmium, Cu, Pb, and Zn are superimposed onto one set of axes on Plate II, labeled "BASE METALS." Iron and

manganese are represented on two separate sets of axes.

Base Metal Suite

Cadmium is grouped with the base metal elemental profiles on Plate II because it is highly correlated with all three base metals, especially Zn (Appendix Table IXa). In general, Cd, Cu, Pb, and Zn, categorized as base metals on Plate II, display similar contrast in all three soil sample traverses. The only low correlation coefficient (i.e., <0.50) exists for Cu and Zn (Appendix Table IXa). Copper is only moderately correlated with Zn, but the contrast of Cu is approximated by that of Zn in the raw data plots on Plate II.

The soils overlying control structure V1 are positively anomalous in Cd, Cu, Pb, and Zn in traverses 1 and 2. Structure V3 is unresolved by contrast of the base metal suite raw data in traverses 1 and 2 on Plate II. Anomalous concentrations of all four base metals occur within 70 feet of V3, but these are on the other side of a drainage from V3. Structure V6 is crossed by all three traverses, but is resolved only in traverse 1 by positively anomalous concentrations of all four base metals in the soil. Prior to sampling, it was apparent that many structures cross traverse 3. It was for this reason that the major portion of this traverse was sampled at 10 feet intervals. It is

possible that the geochemical signature of structure V6 is masked in traverse 3 on Plate II by the dispersion of base metals from nearby structures.

Iron

Iron is most strongly correlated with Zn (correlation coefficient = 0.590). Other correlations (i.e., Cd, Cu, Mn, and Pb) with Fe are relatively weak (Appendix Table IXa). The location of structure V1 is well-resolved in traverse 2 by a positive soil Fe anomaly (Plate II). Structure V1 occurs at the beginning of traverse 1, where the first Fe concentration value is high, relative to adjacent samples. Control structure V3 appears to be indicated by the Fe content of one soil sample in traverse 1, but it is unresolved in traverse 2 (Plate II). As with the base metals, the concentration of iron is anomalously high, downslope from V3 about 70 feet and across a small drainage. The location of control structure V6 is indicated by high iron concentrations in the soils from all three traverses.

Iron concentrations in soils determined using the hot nitric acid digestion method are derived from the dissolution of Fe hydroxides as well as Fe sulfides. Since QSP alteration is common around known mineralized structures, the positive anomalous responses over control structures probably reflects pyrite concentrations. The

concentration of pyrite in some structures (e.g., V3) is apparently low, however, since the Fe concentrations are not anomalously high in soils overlying these structures (Plate II).

Manganese

Manganese correlates most strongly with Cu (correlation coefficient = 0.646 for hot nitric acid digestion, Appendix Table IXa). The correlations between Mn and Pb and Mn and Zn are positive, but weak (Appendix Table IXa).

Initially, it was thought that the relative depletion of Mn in the first 400 feet of traverse 2 (Plate II) could be attributed to a condition of disturbed soil resulting from the excavation and construction of the Gilpin County Tram grade just above this portion of traverse 2. A very similar trend of Mn depletion is also observed in the first 400 feet of traverse 1 on Plate II, however, and no substantial cultural contamination is indicated in this area. The soil profile is better developed in these areas relative to the steeper sloped areas. This soil profile variation probably accounts for the Mn depletion in the first 400 feet of traverses 1 and 2 on Plate II.

There is no consistent pattern of manganese contrast variations in soils overlying the control structures on Plate II. Manganese anomalies occur, but they are both

positive and negative and they are generally displaced away from the structures a few tens of feet.

30 Minute Cold HCl Digestion/MAGIC Extraction

Silver and Au are superimposed onto the same set of axes on Plate III, labeled "PRECIOUS METALS." Arsenic, Cd, Cu, In, Pb, and Zn are plotted upon the same set of axes, labeled "BASE METALS." Iron and Mo are also superimposed upon one set of axes and Mn is plotted onto a separate set of axes.

Precious Metal Suite

In hydrothermal systems, Ag and Au generally have a strong geochemical affinity. The correlation coefficient between Ag and Au in soils (0.509) is only moderate, however (Appendix Table IXb). The dispersive habits of Ag and Au are drastically different in the surficial environment and this accounts for the lack of strong correlation. Silver is commonly transported in the surficial environment by hydromorphic processes while the transport of gold is predominantly by mechanical processes (Levinson, 1980). Gold is characteristically inhomogeneous in its distribution in the primary environment as well as in the surficial soil environment. The inhomogeneous behavior of gold in soils is evidenced by the averaged relative precision of field

duplicates for gold (38.82 percent, Appendix Table VIIb). This is the poorest sampling reproducibility of all elements determined. The raw data plots for gold in soils from all three traverses on Plate III show the erratic distribution of gold.

There is no apparent increase in Ag or Au over control structure V1 on traverse 1, though a definite positive anomaly in both metals exists in soils overlying this structure in traverse 2 on Plate III. Structure V3, crossed by traverses 1 and 2, is apparently deficient in precious metals. Control structure V6 is crossed by all three traverses, but a silver anomaly in traverse 1 is the only obvious precious metal response in soils over this structure (Plate III).

Silver and gold may be their own best pathfinders, but gold is a difficult element to sample and analyze for in soils. Gold is highly correlated with copper, perhaps making copper a more reliable pathfinder for gold (Appendix Table IXb). Gold is commonly associated with chalcopyrite in this district (Bastin and Hill, 1917). Silver is highly correlated with Cd, Cu, In, Pb, and Zn (Appendix Table IXb).

Base Metal Suite

Cadmium is grouped with the base metal elemental profiles on Plate III because it is highly correlated with

Cu, Pb and especially Zn (Appendix Table IXb). This is easily accounted for by the fact that Cd is known to substitute very readily for Zn within the sphalerite lattice. Arsenic is highly correlated with the base and precious metal suites on Plate III, but it is more positively correlated with the base metals so As is categorized with the base metals.

The relative contrasts of As, Cd, Cu, In, Pb, and Zn are all very similar in the raw data plots on Plate III. This situation is comparable to that which exists for the base metals on Plate II, analyzed by the hot nitric acid digestion method.

Control structure V1 is indicated by positive base metal anomalies in soils from traverse 2, but not traverse 1 (Plate III). Structure V3 is indicated by very small positive base metal anomalies in soils from traverse 2, but not traverse 1. Structure V6 is indicated by strong positive base metal anomalies in traverse 1, but it is indicated by weak negative base metal anomalies in traverse 2. The location of V6 on traverse 3 is unresolved by the soil base metal geochemistry (Plate III).

Copper, Pb, and Zn are probably their own best pathfinders in the surficial soil environment. Arsenic, Cd, and In probably substitute into the lattices of one or more

Cu-Pb-Zn sulfide phases.

Iron and Molybdenum

Iron and Mo are grouped together on Plate III because of their strong correlation. This correlation is exhibited qualitatively on Plate III as well as in the quantitative correlation matrix (Appendix Table IXb). The Fe hydroxides in the soil are scavengers of Mo in the surficial environment and this is the reason for the strong Fe-Mo correlation (Levinson, 1980).

Control structure V1 is indicated by a strong positive Fe and Mo concentration anomaly in soils from traverse 2 but not from traverse 1 (Plate III). Structure V3 is essentially unresolved by Fe or Mo contrast in soils from traverses 1 and 2. A strong positive Fe and Mo anomaly occurs in the soil 70 feet downslope from V3 in traverse 2 and across a drainage. Structure V6 is indicated geochemically by weak negative Fe and Mo anomalies in soils from traverse 2 and 3, but it is indicated in traverse 1 as a strong positive Fe and Mo anomaly (Plate III). These positive anomalies in soils over structure V6 from traverse 1 are displaced downslope from structure V6. The geochemical responses of Fe and Mo are very inconsistent over known mineralized structures. This makes the definition of a geochemical model from these raw data very

difficult.

Manganese

Manganese correlates most strongly with As, Cd, and Cu (Appendix Table IXb). The depletion of Mn in the first 400 feet of traverses 1 and 2 is even more pronounced in samples analyzed using the 30 minute cold HCl digestion/MAGIC extraction method relative to those analyzed using the hot nitric acid digestion method. Once again, this variation in manganese concentrations in soils on steep slopes versus those on gentle slopes probably results from differences in soil profile development between these two areas.

Control structure V1 is indicated by a strong positive soil Mn anomaly in traverse 2, but not in traverse 1 (Plate III). Manganese concentration contrast in soils overlying structure V3, crossed by traverses 1 and 2, is weakly negatively anomalous. Structure V6 appears to be indicated by weak negative Mn anomalies in all three traverses (Plate III). Manganese concentrations in soils analyzed using the 30 minute cold HCl digestion/MAGIC extraction method are predominantly negatively anomalous, though weak, over known mineralized structures.

Regression Analysis

The program GRAPHM in the CSM computer library has the

capability of fitting a polynomial regression curve up to degree 10 to a set of data points on an x-y coordinate system. This program has a 9 inch by 9 inch physical limit. Because of this, the input data sets for elements in traverses 1 and 2 had to be split if the scale of plate I was to be maintained. Concentration data for representative elements on Plate III were fit with polynomial regression curves. The statistical significance of these curves was checked by running the data through a least squares fit program (program LSQ in the CSM Geology Department computer library). This program outputs the residuals and an F-ratio parameter for the polynomial of a given degree. The curves were considered significant: (1) if the residuals lacked a tendency to autocorrelate, and (2) if the F-ratio parameter exceeded tabular values reported in statistical tables for the given degrees of freedom at an 0.05 level of confidence (Davis, 1973). The positions of the polynomial regression curve inflections on the x-axis of the representative elemental profiles were then used to fit a regression curve to the entire length of all three traverses in Plate III.

Regression analysis can be used for delineating general elemental concentration trends. The smoothing affect of regression analysis is of little use in resolving the locations of mineralized structures, however. The general

location (i.e., a 100 foot interval) of the large known mineralized structures can be defined by locating spatial groupings of anomalous samples in the raw data elemental profiles without the use of regression analysis. Regression analysis of geochemical traverse data is therefore not recommended for survey data analysis.

Discussion of Ratio Analysis

Limitations of Single Element Plots

The raw data plots on Plate III are useful for defining the general positions of the control structures on gentle slopes, but the utility of these raw data for this purpose is severely limited where topographic slopes exceed 20 degrees. For example, 3 of the 6 control structures are crossed by traverse 2 and their positions are indicated on the topographic profile on Plate III. The vein structures which are exposed on gentle slopes in the traverse are indicated by increasing concentrations of most of the elements analyzed from soils overlying those structures. Where the structures are exposed on steeper slopes, however, their geochemical signature is effectively transported downslope, making geochemical resolution of the structures' locations impossible. This problem was resolved in this study by ratioing statistically standardized Fe and Mn concentrations. The following paragraphs rationalize the logic and natural processes underlying this interpretative methodology.

Rationale for Ratio Analysis

Quartz-sericite-pyrite is the predominant gangue material which can be found on mine dumps in the Central City district. This pyrite-rich alteration envelopes

virtually every mineralized vein in the district. Pyrite and other sulfide minerals in the Central City district are exposed as a result of natural weathering processes and also by mining activity. Chemical weathering eventually breaks down these sulfides to form relatively stable products, which include iron hydroxides and a byproduct of sulfuric acid. These iron hydroxides can adsorb or coprecipitate trace metals which are released from other weathering sulfides. The sulfuric acid produced can significantly lower the soil pH. Pyrite, exposed to chemical weathering, first forms ferrous sulfate. The ferrous sulfate further reacts to form ferric hydroxides. The ferric hydroxides may then react further to form products which may include goethite or lepidocrocite (Levinson, 1980).

Completion of the sulfide breakdown reaction is slow in semi-arid environments, such as the Central City district. Mining activity has resulted in the increased concentration of sulfides (especially pyrite) in soils near mine dumps and stopes or shafts. The sulfide breakdown reaction is slow enough that it cannot be completed in the 100 years which have passed since the initiation of mining activity. This is evidenced by the presence of abundant visible pyrite in soils near the mine dumps.

The mobility and dispersion of elemental species is

often strongly controlled by the pH of the medium in which they exist (Garrels and Christ, 1965; Hansuld, 1967). Figure 7 is an Eh-pH diagram which shows the relative mobilities of Fe and Mn oxyhydroxide species under surface conditions. The boundaries on this diagram were calculated from thermochemical data from Baas Becking, and others (1960); Langmuir (1969); Wagman, and others (1969); Crerar and Barnes (1974); and Baes and Mesmer (1976). This diagram can be used qualitatively to explain Fe and Mn dispersive processes in soils. In general, soils in the Central City district are oxidizing and acidic. The stippled parallelogram in Figure 7 encloses an Eh-pH field representing natural oxidizing and acidic soil environments. The oxidizing potential, or Eh, of the soils in the district will be virtually constant, since the climate and soil moisture conditions are constant, so that variations in the mobility of Fe and Mn species are controlled mainly by changes in pH. Two arrows, labeled A and B, are drawn across the stippled areas at constant Eh in order to demonstrate species mobility changes with pH. The pH limits defined by arrows A and B in Figure 7 will also be considered in Figure 8. Manganese is soluble, assuming a metal concentration of 10^{-5} molarity, across the entire field indicated by arrows A and B and it is increasingly

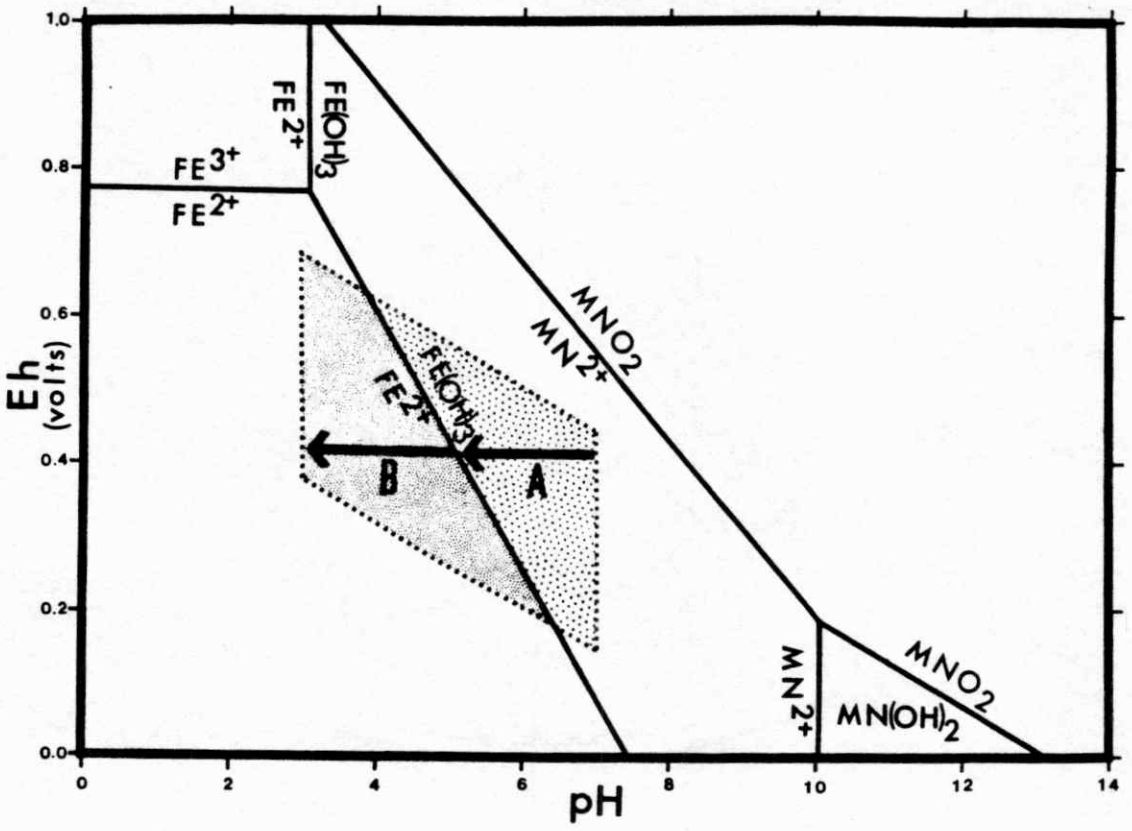

Figure 7. Eh-pH diagram for the simple ions and oxyhydroxides of iron and manganese at 25°C. Molarity of metal ions = 10^{-5}. Thermochemical data from: Baas Becking, and others (1960); Langmuir (1969); Wagman, and others (1969); Crerar and Barnes (1974); and Baes and Mesmer (1976)

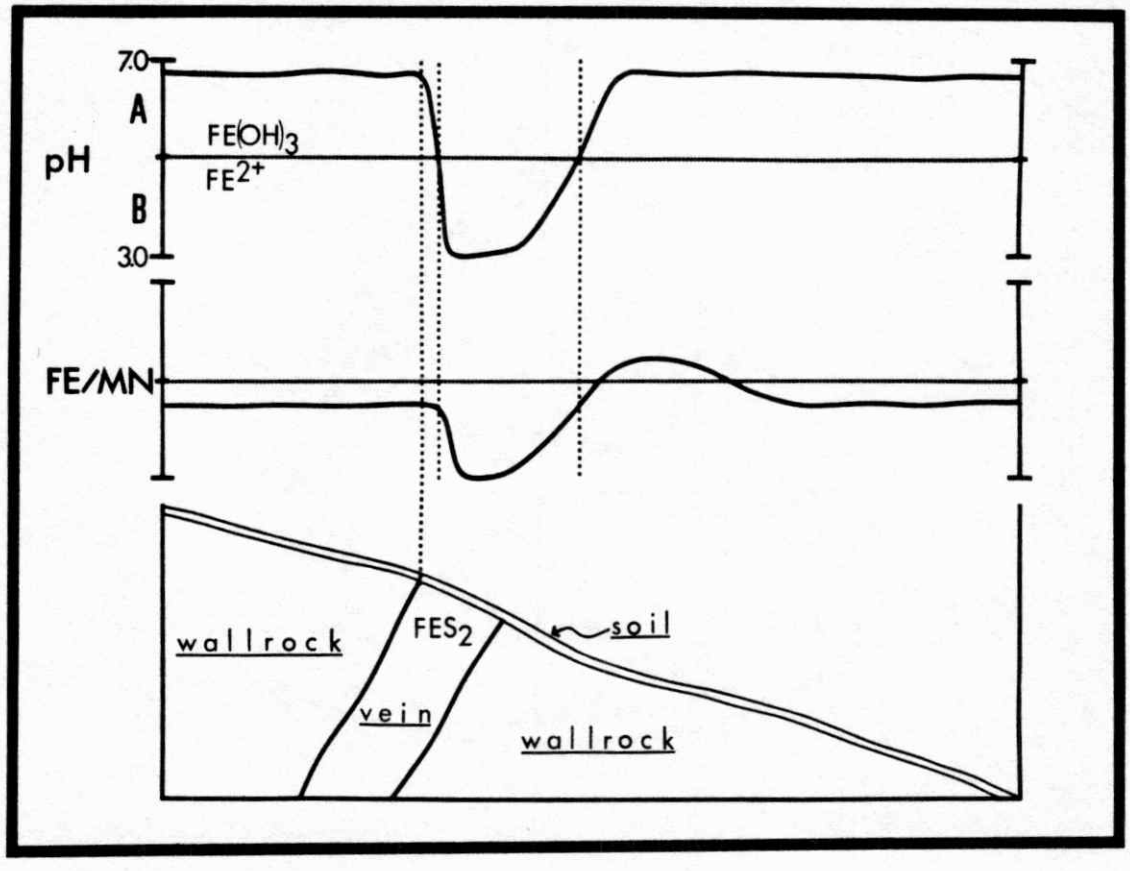

Figure 8. Hypothetical pH and Fe/Mn variance in soils overlying an oxidizing sulfide-bearing vein structure on a steep slope.

soluble as the pH of the soil decreases. Iron on the other hand is insoluble, assuming a metal concentration of 10^{-5} molarity, as a hydroxide phase where the pH limits of arrow A exist. This ferric hydroxide is soluble at low pH levels, indicated by the limits of arrow B.

The upper diagram on Figure 8 shows a hypothetical representation of pH in soils. The pH range on the vertical axis corresponds with the limits indicated by arrows A and B on Figure 7. The horizontal reference line on the upper diagram in Figure 8 separates insoluble ferric hydroxide at relatively high pH's from the soluble Fe at the lower pH's for the conditions given in Figure 7. Manganese is assumed to be soluble over this entire pH range. The solid curve in the upper diagram represents idealized pH as it varies in soils over unmineralized wallrock and an oxidizing sulfide-bearing vein structure on a steep slope. This vein structure is illustrated in the lower diagram on Figure 8. The middle diagram on Figure 8 shows a curve representing Fe/Mn variations in the soils overlying unmineralized wallrock and the vein structure. The Fe and Mn concentrations are controlled by pH since these data are assumed to represent oxyhdroxide phases and not sulfide phases. In the upper diagram of Figure 8, as the pH is varied across the ferric hydroxide/soluble Fe reference

line, the magnitude of Fe in the Fe/Mn ratio is directly effected. A decrease in pH across the ferric hydroxide/soluble Fe reference line reduces the concentration of Fe relative to Mn in the soil and this decreases the Fe/Mn ratio.

Oxidizing sulfide-bearing structures produce sulfuric acid. This sulfuric acid significantly lowers the pH of the soils which overly this structure. The low pH in the soil can result in the dissolution of any ferric hydroxides present. In effect, the Fe in soluble form migrates downslope away from the oxidizing sulfide-bearing structure. This results in a decrease in the Fe/Mn ratio in soils directly over the vein structure. Immediately downslope from the vein structure, the pH of the soil is low, but it increases progressively and relatively rapidly downslope. Hydrogen ions react with feldspars and micas present in the wallrocks in low temperature hydrolysis reactions similar to those described by Hemley and Jones (1964). Reactions with the sulfide-free wallrock neutralizes the soil pH a short distance downslope from the vein structure. When the pH increases downslope to a level in which ferric hydroxide becomes less soluble, the ferric hydroxide precipitates. This produces an Fe/Mn ratio increase. The level of the Fe/Mn ratio at this point may actually exceed levels reached

upslope. This situation is dependent upon how much Fe was actually dissolved from the structure itself. Abundant Fe dissolution at the vein structure site will most likely result in a distinct ferric hydroxide increase downslope and this is reflected by a distinctive positive Fe/Mn ratio peak. To summarize the utility of Figure 8, a sharp decrease in the measured Fe/Mn ratio pinpoints the location of a low pH environment which indicates the presence of oxidizing sulfides. A sharp increase in the measured Fe/Mn ratio indicates the presence of a low pH environment immediately upslope from the increase. The Fe/Mn decrease and increase may occur over a structure and downslope from a structure, respectively, but they may not always occur together.

Application of Ratio Analysis

Actual Fe/Mn ratio data are presented on Plate IV. The Fe and Mn concentrations analyzed using the 30 minute cold HCl digestion/MAGIC extraction method are uniquely useful for the purpose of ratio analysis in resolving structure locations since they are derived from oxyhydroxide phases and not sulfides. Only these data will be considered here. It is important to note that the Fe/Mn ratios referred to throughout this text do not merely represent the ratios of raw concentration data. The data must first be

statistically standardized (Davis, 1973) and made positive before reasonable ratio values will result. The computer program used to calculate the ratios and its explanation are given in Appendices Xa and Xb, respectively. Soil sample traverse 2 is chosen for the purpose of discussion in the following paragraph.

The Fe/Mn ratios in traverse 2 on Plate IV are drastically different in the gently sloping areas compared to the steeply sloping areas. This results from variations in soil profile development between the two areas. The information sought involves data point contrast and not just ratio magnitudes, making the Fe/Mn information from both areas equally useful. Three of the 6 control structures identified in the study area are intersected by traverse 2. Control structure V1 is pinpointed by a relative low in the Fe/Mn ratios. Structure V3 is also indicated by a relative low in the Fe/Mn ratios. Structure V6, on the steep slope, is also indicated by a small, but distinct low in the Fe/Mn ratios. In summary, the use of this Fe/Mn ratio method, can be used to pinpoint the locations of known control structures on gentle slopes and on very steep slopes. It is apparent from the Fe/Mn ratio data on Plate IV that the locations of some additional structures are indicated by the presence of other Fe/Mn ratio lows along with Fe/Mn ratio

highs.

After consideration of the locations of additional unexplained prospect pits and stopes, along with the Fe/Mn ratio data, the locations of numerous other structures were inferred upon Plates IV and I. Twenty-six structures are designated as V1 - V26 on Plate I. Structures V1-V6 are the "control structures" which were used to define the geochemical model. All vein structures indicated on Plate I are not necessarily mineralized. The ratioing methodology developed here identifies altered structures which are only potentially mineralized. Analysis of base and precious metals in soil and rock along the strike of the newly identified structures must be carried out in order to gain information about possible locations of mineralized dilational zones within the structures.

Iron/manganese ratio lows on Plate IV which are greater than 2.0 are considered possibly anomalous and those less than 2.0 are considered definitely anomalous. The choice of a 2.0 Fe/Mn ratio cut-off is arbitrary. It is observed, however, in traverse 2 on Plate IV that relative lows of Fe/Mn occur below 2.0 and above 3.0, but not between 2.0 and 3.0. As of yet, there is no physiochemical explanation for this observation and it may in fact only be coincidental.

Many small vein structures are intersected by the

Bonanza Adit (Cullar, personal communication, 1985). The strike of V14 (Hyde Vein) underground is east-west and the dip is 75°N (Cullar, personal communication, 1985). The mineralization carried by this structure in the Bonanza Adit is relatively minor (i.e., approximately 1 inch wide). There are no known cultural surface expressions of V14 (Cullar, personal communication, 1985). The 75°N dip is assumed to be constant from where it is measured underground and the plane of this structure was projected upward from the level of the Bonanza Adit (Cullar, 1981). The structural trace of V14 on the surface, determined from the Fe/Mn ratio geochemistry of soils from traverses 1 and 2, is drawn to intersect the trace of the Adit where the projection from V14 underground intersects the surface.

The distribution of simple and complex trace element ratios (e.g., Mo:Mn, Mo:Cu, Mo+Fe:Mn, Mo+In:Mn, Mo+In+Zn:Mn, Mo+In+Zn+Pb:Mn) were evaluated. No discussion of these results is provided since it was concluded that the resolution of structures obtained using only Fe and Mn was the best and the easiest to explain.

Summary and Conclusions

Selective extraction procedures can be used to discriminate between coexisting processes (i.e., cultural and natural) in the semi-arid surficial geochemical environment of the Central City district. The interpretation of selective extraction data using statistically standardized ratio combinations can resolve the locations of chemically weathered sulfide-bearing structures in this contaminated district. This ratioing exercise allows for the geochemical resolution of the known structure locations even where slopes are steep.

The surficial geochemical exploration method developed is very effective, but it is an indirect indicator of mineralization. The method defines known structures on the basis of the pH-controlled mobility of Fe and Mn species. The pH conditions which indicate the presence of a structure result from the weathering of the characteristic QSP alteration around the veins as well as the mineralization itself. Mineralization is never present without the QSP alteration, but the alteration may occur without significant mineralization. Even though the method developed is indirect and reveals no information about the exact type of mineralization, it does reveal the locations of altered structures which may be mineralized and this advantage is

important.

A 30 minute cold HCl digestion (without the MAGIC extraction) of the -230 mesh soil fraction and analysis of Fe-Mn concentrations by flame atomic absorption spectrophotometric methods can be carried out efficiently and economically. These data can be interpreted through a series of simple calculations and plots made most efficiently and effectively with a computer. The potential amount of information obtained from a minimal amount of data is great. Attention to detail during surveying of the study area was necessary to define the model, but such detail is probably not necessary for the successful exploration application of the Fe/Mn ratio method. A sample spacing of 15-20 feet is necessary, however, if the locations of the small closely-spaced structures are to be resolved.

Even though questions remain and additional research is necessary, the Fe/Mn ratio methodology developed here can be used today (even as close as 75-100 feet to dumps) to locate altered structures containing mineralization which have gone unnoticed. The influence of dump tailings is significantly reduced over short distances because of silicate wallrock pH buffering. The potential utility of surficial geochemical exploration methods in contaminated districts, such as the Central City district, is great and additional work

considering the concepts addressed in this thesis should be carried out.

Implications for Exploration and Prospect Evaluation

The 30 minute cold HCl digestion, applied to the -230 mesh soil fraction, was necessarily integrated with the MAGIC extraction so that the low level concentrations of the various trace elements could be determined. This integration effectively complicates the procedure and undoubtedly reduces analytical precision. The 30 minute cold HCl digestion (without the MAGIC extraction) should be applied to the -230 mesh fraction of soil samples collected in equal-sample-space traverses and these solutions should be analyzed for Fe and Mn. Once interesting areas in the traverse are defined using the Fe/Mn ratioing method, samples over these areas should by analyzed for base and precious metals using the 30 minute cold HCl digestion integrated with the MAGIC extraction. This methodology would be the most efficient approach for defining mineralization concealed by soil cover in this contaminated base and precious metal mining district.

Structure traces V11 and V12 give strong geochemical responses. The degree of exploitation of these structures underground is questionable. Any one of the structural traces identified with the Fe/Mn ratioing method may dilate within a short distance down dip or along strike. Sampling along strike should be carried out along these traces.

Recommendations For Further Work

Additional research should be carried out in the laboratory in order to better define the degree to which the various Fe-Mn species, iron sulfide, and base metal sulfide phases are being effected by the 30 minute cold HCl digestion. Some methods described by Chao and Theobald (1976) which might be tested include:

1 - Mn oxides: 0.1 M hydroxylamine hydrochloride in 0.01 M HNO_3 at room temperature, 30 minutes;

2 - Fe oxides (amorphous): 0.25 M hydroxylamine hydrochloride in 0.25 HCl at 70°C, 30 minutes;

3 - Fe oxides (crystalline): sodium dithionite extraction at pH=4.75 at 50°C, 30 minutes.

Chao (1984) presents an overview of partial dissolution techniques including those applicable to Fe-Mn oxyhydroxides.

Since the Fe/Mn ratio method developed is based upon the selective extraction of specific Fe and Mn species, it is not effected by mining activity contamination. A great deal of experimental-analytical and theoretical work will be neccessary to substantiate this statement. How long does pyrite (and other sulfides), which becomes exposed as a result of mining activity, remain in the surficial weathering environment before it is oxidized to a

substantial degree in a given climatic/physiographic setting? There are many complicated processes which interact to oxidize sulfides during weathering. These processes will have to be examined in future studies if a suitable answer to this question is to be realized.

The collection of soil pH data on sampling traverses would be very useful for substantiating some of the statements made in this study concerning variable mobilities of elemental species. Direct pH measurement of soil samples from the traverses may in fact be a more effective method of resolving the locations of weathering sulfide-bearing structures.

Sampling on the northern portion of Maryland Mountain should be attempted. This side of the mountain is considerably steeper than the southern portion and the likelihood of encountering slumped masses of soil is great. Such a study might locate some of the large structures which have been projected into this area.

Many large ore bodies have been discovered and mined from the structural intersection or junction of two veins (Sims, and others, 1963b). Several intersections exist between structures on Plate I. The locations of these intersections should be examined closely for potential mineralization.

Soil sampling across one or more of the breccia features exposed at the surface should be carried out. The breccia body which is intersected by V2 (Plate I) should yield some interesting results.

This study was carried out in the intermediate hypothermal zone of the Central City district (Figure 4). This zone possesses QSP alteration. The central hypothermal zone possesses QSP alteration which is more intense than the intermediate zone. The peripheral and barren hypothermal zones possess QSP alteration which is less intense than the intermediate zone. Logical interpretative modifications of the Fe/Mn method might be necessary for its successful application in these areas within this district. For example, the predominance of iron hydroxide as an immobile phase in the soil environment may be decreased in the central hypothermal zone relative to the intermediate zone. In the peripheral and barren hypothermal zones, iron hydroxide is probably the predominant stable iron species in the surficial environment.

Further, this study was carried out in a semi-arid climatic environment. Modification of the methodology developed in this study may be necessary when the methodology is applied in other climatic environments.

References Cited

Baas Becking, L.G.M., Kaplan, I.R., and Moore, D., 1960, Limits of the natural environment in terms of pH and oxidation-reduction potentials: Journal of Geology, v. 68, p. 243-284.

Baes, C.F., Jr., and Mesmer, R.E., 1976, The hydrolysis of cations: Wiley, New York, 489 p.

Bastin, E.S., and Hill, J.M., 1917, Economic geology of Gilpin County and adjacent parts of Clear Creek and Boulder Counties, Colorado: U.S. Geological Survey Professional Paper 94, 379 p.

Budge, Suzanne, 1982, Trace element distribution around precious and base metal veins, Idaho Springs District, Colorado: Colorado School of Mines, Master of Science thesis, 152 p.

Chao, T.T., 1984, Use of partial dissolution techniques in geochemical exploration: Journal of Geochemical Exploration, v. 20, p. 101-135.

Chao, T.T., and Theobald, P.K., Jr., 1976, The significance of secondary iron and manganese oxides in geochemical exploration: Economic Geology, v. 71, p 1560-1569.

Clark, J. Robert, 1984-1985, Personal communication.

Clark, R.J., and Viets, J.G., 1981, Multielement extraction system for the determination of 18 trace elements in geochemical samples: Analytical Chemistry v. 53, p. 61-65.

Closs, L.G., and Sado, E.V., 1982, Bedrock and overburden geochemistry. Investigations in Midlothian Lake and Natal Lake areas, district of Sudbury and Timiskaming: Ontario Geological Survey Geoscience Study 24, 68 p.

Collins, G.E., 1910, Lessons from Gilpin County practice: Mining and Science Press, v. 101, p. 366-371.

Crerar, D.A., and Barnes, H.L., 1974, Deposition of deep-sea manganese nodules: Geochimica Cosmochimica et Acta, v. 38, p. 279-300.

Cullar Geologic Services, Van Cullar - Geologist, 1981: Preliminary report of the "Bonanza Tunnel Group", confidential unpublished report.

Cullar, Van, March, 1985: Personal communication.

Davis, John C., 1973, Statistics and data analysis in geology: John Wiley and Sons, New York, 550 p.

Garrels, R.M., and Christ, C.L., 1965, Solutions, minerals, and equilibria: Freeman, Cooper, and Company, San Fransisco, California, 450 p.

Hansuld, J.A., 1967, Eh and pH in geochemical prospecting: Geological Survey Canada Paper 66-54, p. 172-187.

Hedge, C.E., 1967, Precambrian geochronology of the central Colorado Front Range, Colorado [abs.]: Geological Society of America, Rocky Mountain Section 20th Annual Meeting Program, p. 39.

Hedge, C.E., 1970, Whole-rock Rb-Sr age of the Pikes Peak Batholith, Colorado: U.S. Geological Survey Professional Paper 700-B, p. B86-B89.

Hemley, J.J., and Jones, W.R., 1964, Chemical aspects of hydrothermal alteration with emphasis on hydrogen metasomatism: Economic Geology, v. 59, p. 538-569.

Hutchinson, R.M., 1959, Ar^{40}/K^{40} determinations of the north end of Pikes Peak Batholith, Jefferson, Douglas, and Park Counties, Colorado [abs.]: Geological Society of America Bulletin, v. 70, no. 12, p. 1779.

Hutchinson, R.M., and Hedge, C.E., 1967, Pikes Peak Batholith and basement rocks of the Central Colorado Front Range and its 700 million year history: Geological Society of America, Rocky Mountain Section, Guide Book Field Trip No. 1, Colorado School of Mines Publications, p. 1-51.

Hutchinson, R.M., and Hedge, C.E., 1976, Precambrian geochronology of western and central Colorado and southern Wyoming: In professional contributions of Colorado School of Mines - Studies in Colorado field study, No. 8, edited by Epis, R.C., and Weimer, R.J., p. 73-77.

Kramer, Ann M., 1984, Paragenetic and fluid inclusion study of the Smith Vein, Smith Mine, Blackhawk, Colorado: Colorado School of Mines, Master of Science thesis, 108 p.

Langmuir, Donald, 1969, The Gibbs free energies of substances in the system $Fe-O_2-H_2O-CO_2$ at 25°C: U.S. Geological Survey Professional Paper 650B, p. 180B-184B.

Levinson, A.A., 1980, Introduction to exploration geochemistry, 2nd ed., Applied Publishing Ltd., Wilmette, Illinois, 924 p.

Lovering, T.S., 1929, Geologic history of the Front Range, Colorado: Colorado Scientific Society Proceedings, v. 12, no. 4, p. 59-111.

Lovering, T.S., 1930, Localization of ore in the schists and gneisses of the Mineral Belt of the Front Range, Colorado: Colorado Scientific Society Proceedings, v. 12, no. 7, p. 234-268.

Lovering, T.S., 1935, Structure controls deposition of ore in Front Range areas: Engineering and Mining Journal, v. 136, no. 8, p. 411-413.

Lovering, T.S., and Goddard, E.N., 1938, Larimide igneous sequence and differentiation in the Front Range, Colorado: Geological Society of America Bulletin, v. 49, p. 35-68.

Lovering, T.S., and Goddard, E.N., 1950, Geology and ore deposits of the Front Range, Colorado: U.S. Geological Survey Professional Paper 233, 319 p.

Lovering, T.S., and Tweto, Ogden, 1953, Geology and ore deposits of the Boulder County tungsten district, Colorado: U.S. Geological Survey Professional Paper 245, 199 p.

Meisch, A.T., 1964, Effects of sampling and analytical error in geochemical prospecting: Computers in the minerals industries, Part 1, Stanford University Publications in the Geological Sciences, v. 9, no. 1, p. 156-170.

Moench, R.H., Harrison, J.E., and Sims, P.K., 1962, Precambrian folding in the Idaho Springs - Central City area, Front Range, Colorado: Geological Society of America Bulletin, v. 73, no. 1, p. 35-58.

Rice, C.M., Harmon, R.S., and Shepard, T.S., 1982a, Porphyry molybdenum style mineralization near Central City, Colorado [abs.]: Geological Society of America, Annual Meeting, v. 14, no. 7, p. 598.

Rice, C.M., Lux, D.R., and Macintyre, R.M., 1982b, Timing and mineralization and related intrusive activity near Central City, Colorado: Economic Geology, v. 77, p. 1655-1666.

Rickard, Forbes, 1898, Notes on the vein formation and mining of Gilpin County, Colorado: American Institute of Mining Engineering Transactions, v. 28, p. 108-126.

Rogers, A.M., 1883, The mines and mills of Gilpin County, Colorado: American Institute of Mining Engineering Transactions, v. 11, p. 29-55.

Sims, P.K., 1982, Geology of the Central City area, Colorado - A Laramide mining district: in Proceedings of the Denver Region Exploration Geologists Society Symposium - The genesis of Rocky Mountain ore deposits: changes with time and tectonics, November 4-5, Denver, Colorado, p. 95-100.

Sims, P.K., and Barton, P.D., Jr., 1961, Some aspects of the geochemistry of sphalerite, Central City district, Colorado: Economic Geology, v. 56, p. 1211-1237.

Sims, P.K., and Barton, P.D., Jr., 1962, Hypogene zoning and ore genesis, Central City district, Colorado: Geological Society of America, Buddington Volume, p. 373-395.

Sims, P.K., and others, 1963a, Geology of uranium and associated ore deposits, central part of Front Range Mineral Belt, Colorado: U.S. Geological Survey Professional Paper 371, 119 p.

Sims, P.K., Drake, A.A., Jr., and Tooker, E.W., 1963b, Economic geology of the Central City district, Gilpin County, Colorado: U.S. Geological Survey Professional Paper 359, 231 p.

Sims, P.K., Drake, A.A., Jr., and Tooker, E.W., 1964, Geologic map of the Central City quadrangle, Colorado: U.S. Geological Survey GQ-267, scale 1:24,000.

Spurr, J.E., George, H.G., and Ball, S.H., 1908, Economic geology of the Georgetown quadrangle (together with the Empire district), Colorado: U.S. Geological Survey Professional Paper 63, 411 p.

Taylor, R.B., 1976, Geologic map of the Black Hawk quadrangle Gilpin, Jefferson, and Clear Creek Counties, Colorado: U.S. Geological Survey GQ-1248, scale 1:24,000.

Thornbury, W.D., 1965, Regional geomorphology of the United States, John Wiley and Sons, Inc., New York, 609 p.

Tooker, E.W., 1963, Altered wall rocks in the central part of the Front Range Mineral Belt, Gilpin and Clear Creek Counties, Colorado: U.S. Geological Survey Professional Paper 439, 102 p.

Tweto, Ogden, 1975, Laramide (Late Cretaceous-early Tertiary) Orogeny in the southern Rocky Mountains: in Cenozoic history of the southern Rocky Mountains, Geological Society of America Memoir 144, Curtis, B.F., editor, p. 1-44.

Tweto, Ogden, and Sims, P.K., 1963, Precambrian ancestry of the Colorado Mineral Belt: Geological Society of America Bulletin, v. 74, no. 8, p. 991-1014.

United States Department of Agriculture, 1975, Soil Survey Staff, Soil Taxonomy Handbook No. 436, Washington, D.C.

United States Department of the Interior Geological Survey, 1972, 7.5 minute series topographic map, Black Hawk quadrangle, Colorado, scale 1:24,000.

United States Department of the Interior Geological Survey, 1972, 7.5 minute series topographic map, Central City quadrangle, Colorado, scale 1:24,000.

Vanderwilt, J.W., editor, Burbank, W.S., and Traver, W.M., Jr., 1947, Mineral resources of Colorado, Denver, Colorado, Mineral Resources Board, 547 p.

Wagman, D.D., Evans, W.H., Parker, V.B., Halow, I., Bailey, S.M., Schumm, R.H., and Churney, K.L., 1971, Selected values of chemical thermodynamic properties: National Bureau of Standards Technical Note 270-5.

Appendix I - Surveying Procedure

An electronic distance meter and theodolite were used to survey two closed traverses in the area. A survey elevation datum was located 45 feet S7°E of the Bonanza Adit portal and was estimated to be 8280 feet above sea level from United States Department of Interior Geological Survey 7.5 minute Central City, Colorado quadrangle (1972). The Bonanza Adit is a cross-cut tunnel and its portal is located near the southern boundary of the study area. The adit is accessible and it extends 1,155 feet N7°W of the portal with a slight incline upward to the northwest. A solar bearing was shot with the theodolite in order to determine true north. Magnetic declination was assumed to be approximately 13.5°E (as determined from the United States Department of Interior Geological Survey Central City, Colorado quadrangle, 1972). Auxiliary survey control stations were shot from the closed traverse stations using the electronic distance meter and theodolite. In all, 69 survey control stations exist throughout the area at which the elevations are known. These stations were marked by wooden stakes with a 3 feet long vertical wire, flagging, and an aluminum tag with the station number.

The 69 survey control stations were then used as set-up points for alidade-plane table topographic mapping at a scale of 1 inch = 100 feet (Plate I). The contour interval for this map is 10 feet. The locations of several vein structures are indicated by the presence of mine stopes or shafts to the surface. Details on the plane table map include the locations of caved and open stopes or shafts, adits, prospect pits, and mine dumps. The abandoned Gilpin County Tram grade which passes through the study area is accurately located on the map. Trails which connect the various mine workings in the area to the railroad grade are also carefully mapped. An unimproved road is located at lower elevations at the southwest boundary of the mapping area. This road is parallel to Chase Gulch Creek, which is not shown on the map. Abandoned and occupied buildings are also located on the map.

Appendix II - Soil Sampling Procedure

Three soil sample traverse locations were chosen. The sample traverses were located using a Brunton Compass. The available control stations which were adjacent to the sample traverses were used to check and correct for errors in the compass readings. Each sample traverse was completely surveyed prior to sampling and station locations were labeled with blue surveying tape, marked with the appropriate number.

Soil sample traverse 1 trends N32°W; traverse 2 trends N25°W; and traverse 3 trends N9°W. Sample station numbers in traverse 1 include #1-#67; station numbers in traverse 2 include #68-#147; and station numbers in traverse 3 include #148-#174 (Plate I). Traverse 1 is on a constant bearing and on a single line except for one offset 25 feet to the northeast for samples #54-#67. This offset is necessary because of the lack of soil cover. Traverse 2 possesses one offset of 100 feet between samples #84 and #85. This offset was necessary because of the sample line's intersection with the Gilpin County Tram grade. Both legs of soil sample traverse 2 trend N25°W. Traverse 3 is continuous.

The paint on the blades of the sampling shovels was completely removed prior to sampling in order to reduce the probability of sample contamination. One composite sample was collected from each station and placed in a geochemical paper envelope. At least three separate holes were dug at each station in order to collect representative samples at each station. Duplicate samples were collected at every tenth station on each of the 3 sample traverses.

The samples consisted of soil collected from depths as shallow as 1-2 inches and as deep as 16 inches. The shallow samples were generally collected at sample stations where the slope was steep, i.e., where the soil cover was poorly developed. In some cases it was possible to identify a B horizon which was generally lighter brown in color, relative to the A horizon. The B horizon exists at sample stations at low elevations between the intermittent stream drainages, especially in traverses 1 and 2. There was an attempt during sampling to remove large fragments which were greater than 1/4 inch in diameter and any visible free organic matter.

In an attempt to obtain information about soil trace element background concentration levels, 18 soil samples

were collected 500 feet west of the western boundary of the study area at elevations between approximately 8550 feet and 8700 feet. Nine sample station holes were dug and two sample envelopes were filled from each of these holes with soil from the B horizon.

Appendix III - Analytical Apparatus

A Perkin-Elmer Model 303 atomic absorption spectrophotometer equipped with a flame burner was used for flame analyses of the high concentration elements including Cd, Cu, Pb, and Zn. A Perkin-Elmer Model 360 atomic absorption spectrophotometer equipped with an HGA-2100 graphite furnace was used for the flameless determinations of low concentration elements. An air-acetylene flame was used for all flame atomic absorption determinations. An internal furnace flow of argon gas was used for all flameless atomic absorption determinations. A Fisher Recordall Series 5000 strip chart recorder with a Pilot Razor Point felt tip pen was used to record the Perkin-Elmer Model 360 absorption responses on Omniscribe 5 x 10 chart paper at a rate of 0.5"/minute. Eppendorf digital micropipettes were used to accurately measure and inject samples into the HGA-2100 graphite furnace. Lamps used for analyses included both hollow cathode and electrodeless discharge types. The hollow cathode lamps included Ag, As, Au, Cu, Ga, In, Mo, and Zn. The electrodeless discharge lamps included Cd, Pb, Sb, Se, Sn, Te, and Tl. The Sb lamp was substituted for a Bi lamp. Soil samples were weighed on a Scientech 3300 electronic top-loading balance which has a working range of 0.001-300.00 grams.

Appendix IV - Analytical Methods

Three digestion/extraction methods are described on the following pages. The first method described is the hot nitic acid digestion which was used for the analysis of the -80 mesh soil fraction during initial stages of laboratory work. The second extraction procedure described is the hot sulfuric acid-bromate digestion/MAGIC extraction (Clark and Viets, 1981) which was used for the analysis of the mineralized rock samples. The third extraction procedure described is the 30 minute cold HCl digestion/MAGIC extraction (Clark, personal communication, 1985) which was used to analyze the -230 mesh soil fraction samples. The 24 hour cold HCl digestion/MAGIC extraction method is a modification of method #3. This modification is explained in "Method #3" in this Appendix.

METHOD #1 - Hot Nitric Acid Digestion

1- Weigh 1.00 g sample into test tube.

2- Add 4.0 ml 50% HNO_3.

3- Vortex sample and place in hot water bath for 3 hours, vortexing the sample every 1/2 hour.

4- Remove sample from bath and allow to cool.

5- Filter sample and dilute to 10.0 ml with H_2O.

dilution factor=10.0
(additional dilutions may be necessary)

METHOD #2 -
Hot Sulfuric Acid-Bromate Digestion/MAGIC Extraction
EXTRACTION PROCEDURE

1- Put 0.9 to 1.1 g of $KBrO_3$ in a 18 mm x 150 mm disposable test tube or a 20 mm disposable screw cap culture tube.

2- Weigh 3 g ($\pm$.03g) of sample. Use only 1.0 g if the sample is 1% to 5% sulfides and 0.5 g if the sample is greater than 5% sulfides. The samples should be ground to -200 mesh.

3- Place the sample in the test tube and mix the powder with a vortex mixer.

4- Place the entire rack of test tubes in an ice water bath filled up to the level of the top of the rack.

5- Add one ml of H_2O_2 (unstabilized) to the bottle of H_2SO_4-Mn solution and shake briefly. Add 3 ml of dilute H_2SO_4-Mn solution to each test tube. Cover each test tube with a Kim-Kap. Keep tubes covered at all times during digestion, except when adding reagents. This solution is 5% H_2SO_4 and 0.5% Mn.

6- After 10 minutes place the rack in a warm water bath at about 50°C. After 2 hours, check samples for Mn ppt, vortex and leave in 50°C bath overnight.

7- Place the rack in an ice water bath. Allow samples to cool down. Excess $KBrO_3$ will crystallize at the sediment-water interface.

8- Add 0.5 ml concentrated formic acid. Allow the reaction to proceed for about 30 minites, vortex and let stand in the cold water bath for another 15 minutes. Then return the rack of samples to the 50°C bath for about 30 minutes.

9- Place the rack of samples in a cold water bath and add 1.0 ml concentrated (30%) H_2O_2 (UNSTABILIZED!!). After about 15 minutes, vortex and return the samples to the 50°C bath for about 1 hour.

10- Repeat the H_2O_2 step two (2) more times, making sure that the peroxide is getting to the bottom of the sediment pile. Heat the samples the last time for 2 hours. Then place the rack in a boiling water bath for 15 minutes or until all the tubes have ceased vigorous bubbling.

11- Check each test tube for new black or brown MnO_2 ppt below the water line or on the sediment particles. If it is present all the excess oxidizing potential has not been consumed. In this case add 0.1 ml of formic acid, vortex and heat for 1/2 hour. Then add 0.2 ml of H_2O_2, vortex and reheat the sample in the 50°C bath for 1/2 hour. Repeat the boiling water bath step for 15 minutes. If the black ppt forms again you probably added too much $KBrO_3$ or missed a step.

12- Place the rack of samples in a cold water bath and allow to cool. Add 5.0 ml conc. HCl to each sample.

13- The sample can be stoppered and stored indefinitely at this point. The following extraction steps should be carried out without interruption.

14- Add 4.5 ml of MP-1 to each tube (total aqueous phase is 14 ml). Vortex and let stand for 1/2 hour to allow for complete reduction of the sample.

15- Add 3 ml of MP-2 organic phase to each tube and cap the tubes.

16- Shake each tube by hand to make sure that the sediment is mixing well.

17- Shake the rack mechanically for 1 minute.

18- Immediately, centrifuge the samples at 2000 rpm for 5 minutes. Samples that do not yield at least 2.5 ml of recovered organic extract due to the formation of a sediment-organic clot should be tapped gently against the heel of your hand to break up the clot and centrifuged again.

19- Allow the rack to stand overnight. Most As, Sb, and Se precipitates will dissolve in the organic phase during this time.

20- Samples that are exceptionally high in Ag, Cu, Hg, Pb, or any other element that tends to form insoluble iodides will have a white ppt around the sides of the organic phase. These samples should be run at a greater dilution factor or the ppt can be forced to dissolve in the extract by adding KI, one gram at a time, and shaking. This addition of KI will cause slight shifts in the extraction curves for other elements such as Zn.

21- If the samples are going to be stored for a week or more prior to use it is best to keep them refrigerated.

METHOD #2 -
Hot Sulfuric Acid-Bromate Digestion/MAGIC Extraction
STARTER SOLUTION
H_2SO_4-Mn STARTER SOLUTION (5% H_2SO_4 and 0.5% Mn)

1- Add 21 g of Reagent grade $MnCO_3$ to a one liter volumetric flask.

2- Add 10 ml concentrated H_2SO_4 to the flask and swirl until reaction ceases. Then add more concentrated H_2SO_4, 1 ml at a time, and swirl until all the carbonate has reacted.

3- Add 1 ml 30% H_2O_2 (UNSTABILIZED!) and swirl to reduce all the MnO_2 to Mn^{2+}. (Add more peroxide if needed to complete this reduction.)

4- Add 100 ml concentrated H_2SO_4.

5- Dilute solution to one liter with D.I. H_2O.

6- Transfer the solution to a clean 5 pint reagent bottle.

7- Add one more liter of D.I. H_2O, cap bottle, and mix solution.

METHOD #2 -
Hot Sulfuric Acid-Bromate Digestion/MAGIC Extraction
MAGIC POTIONS
MP-1 (MAGIC POTION #1)

1- Add 400 g of potassium iodide into a clean dark brown reagent bottle.

2- Add 400 g of ascorbic acid.

3- Add 100 g of potassium chloride.

4- Add 100 g of potassium bromide.

5- Add one liter of D.I. H_2O.

6- Cap and mix frequently until completely dissolved. This may take one hour or more.

7- Makes about 1.5 liters of solution.

note: The shelf life of MP-1 may be weeks or months. The solution should be kept in the dark brown reagent bottle in a cool dark place. The MP-1 solution has gone bad when brown particles are noted in the solution and/or the solution has a color which is darker than that of a manila folder.

MP-2 (MAGIC POTION #2)

1- Add 50 ml of Alamine 336 to a one liter flask.

2- Add 100 ml of Aliquat 336.

3- Add 100 ml of heptane.

4- Dilute to one liter with Methyl Iso-Butyl Ketone while swirling the contents of the flask.

5- Cap and mix thoroughly.

note: The shelf life of the MP-2 solution should be on the order of months if it is kept in a cool dark place.

METHOD #2 -
Hot Sulfuric Acid-Bromate Digestion/MAGIC Extraction
STANDARD PREPARATION

Low and high standards were prepared by dissolving the metal, oxide of the metal, or chloride salt of the metal in HBr. The low combined standard containing 1.0 ppm Ag, As, Au, Bi, Cu, Hg, Ga, In, Mo, Tl, Sb, Se, Sn, Te, Pb and 10.0 ppm Cu and Zn was mixed 33% (W/V) in HBr. The high combined standard containing 100.0 ppm Ag, As, Au, Bi, Cu, Hg, Ga, In, Mo, Tl, Sb, Se, Sn, Te, Pb and 1000.0 ppm Cu and Zn was mixed 33% (W/V) in HBr. Aqueous standards for Fe and Mn were prepared by diluting commercial stock solutions and stabilizing these solutions with to 5% HCl.

1- Add 3.0 ml H_2SO_4-Mn starter solution to test tube

2- Add 3.0 ml H_2O

3- Add specified volume standard (see below)

4- Add 3.5 ml conc. HCl

5- Add 4.5 ml MP-1

6- Add 3.0 ml MP-2

7- allow to sit 24-48 hours unrefrigerated before stripping.

#	volume of low standard	resulting concentration of elements
1	10 microliters	0.0033 ppm (0.033 ppm for Zn and Cu)
2	20 microliters	0.0067 ppm (0.067 ppm for Zn and Cu)
3	30 microliters	0.010 ppm (0.10 ppm for Zn and Cu)
4	60 microliters	0.020 ppm (0.20 ppm for Zn and Cu)
5	100 microliters	0.033 ppm (0.33 ppm for Zn and Cu)
6	200 microliters	0.067 ppm (0.67 ppm for Zn and Cu)
7	300 microliters	0.100 ppm (1.00 ppm for Zn and Cu)
8	600 microliters	0.200 ppm (2.00 ppm for Zn and Cu)

#	volume of high standard	resulting concentrations of elements
9	10 microliters	0.333 ppm (3.33 ppm for Zn and Cu)
10	20 microliters	0.667 ppm (6.67 ppm for Zn and Cu)
11	30 microliters	1.00 ppm (10.0 ppm for Zn and Cu)
12	60 microliters	2.00 ppm (20.0 ppm for Zn and Cu)
13	100 microliters	3.33 ppm (33.3 ppm for Zn and Cu)
14	200 microliters	6.67 ppm (66.7 ppm for Zn and Cu)
15	300 microliters	10.0 ppm (100 ppm for Zn and Cu)
16	600 microliters	20.0 ppm (200 ppm for Zn and Cu)

METHOD #2 -
Hot Sulfuric Acid-Bromate Digestion/MAGIC Extraction
STRIPPING PROCEDURE

Step #1: for Fe and Mn

Remove 1.0 ml of aqueous phase from extraction test tube. Dilute to 25% concentration with H_2O (additional dilutions may be necessary). Analyze by flame AA. This solution should be analyzed within 48 hours after the leach is completed. Dilution Factor = (ml of aqueous dilutant/grams of sample) X 4.0.

Step #2: for Cd, Cu, Pb, and Zn

Combine 0.2 ml extract with 1.8 ml dilutant (10% Aliquat-336, 90% MIBK). Analyze by flame AA. Refrigerate stripped samples when analyses are not being carried out.

Step #3: for Mo

Analyze directly by flameless AA (i.e., no stripping is necessary). Refrigerate samples when analyses are not being carried out.

Step #4: 1st strip for As and Ga (aqueous phase) and Ag, Sn, and Tl (organic phase)

Add 1.0 ml extract to 1st strip test tube, add 1.0 ml 6% H_2SO_4 and wash (shake tube with cap on), let phases separate. Remove 0.5 ml of organic phase and place in 2nd strip test tube. Seal 2nd strip test tube and refrigerate for later use. Remove 0.5 ml of the dilute H_2SO_4 from 1st strip test tube and discard. Add 20.0 microliters unstabilized H_2O_2 to 1st strip test tube and shake tube with cap on. Separate the aqueous from the organic phases prior to analysis. Analyze by flameless AA. Refrigerate stripped samples when analyses are not being carried out. Analyze Sn and Tl within 4 days after stripping and analyze Ag within 5 days after stripping.

Step #4: 2nd strip for Bi, Cd, In, Sb, Se, Te (aqueous phase) and Au (organic phase)

One-half ml of organic is present in 2nd strip test tube as a result of the 1st strip procedure. Add to this 0.5 ml of solution containing 5% HNO_3 and 5% Acetic Acid in 30% unstabilized H_2O_2. Shake tube with cap on and allow phases to separate. Separate the aqueous from the organic phases prior to analysis. Analyze by flameless AA. Refrigerate stripped samples when analyses are not being carried out. Analyze Bi, Sb, and Se within 4 days after striped extracts turn very pale yellow in color. Analyze Au

within 4 days after stripping.

METHOD #2 - Hot Sulfuric Acid-Bromate Digestion/MAGIC Extraction

MATRIX MODIFIERS

Ag - 5% (W/V) ammonium thiocyanate (NH_4SCN), 1% (W/V) ascorbic acid, 10% (V/V) acetic acid in MEOH

e.g., 5 g NH_4SNC, 1 g acsorbic acid, 10 ml acetic acid, dilute to 100 ml with MEOH.

As - 1000 ppm Ni in MEOH

e.g., 0.495 g nickelous nitrate ($Ni(NO_3)_2(6H_2O)$), dilute to 100 ml with MEOH.

Au - 5% (W/V) ammonium thiocyanate (NH_4SCN), 5% (W/V) urea in MEOH

e.g., 5 g NH_4SCN, 5 g urea, dilute to 100 ml with MEOH.

Bi - 1% (W/V) ammonium molybdate, 1% (W/V) ammonium citrate, 500 ppm Cu and 30% (V/V) acetic acid in H_2O

e.g., 1 g ammonium molybdate, 1 g ammonium citrate, 0.183 g cupric nitrate ($Cu(NO_3)_2(nH_2O)$), and 30 ml acetic acid, dilute to 100 ml with H_2O.

In - 0.5% (W/V) ammonium meta-tungstate and 10% (W/V) ammonium citrate in H_2O.

e.g., 1 g ammonium meta-tungstate, 10 g ammonium citrate, dilute to 100 ml with H_2O.

Ga - 1000 ppm Ni, 0.1% (W/V) ammonium meta-vanadate, 1% (W/V) ascorbic acid, 30% (V/V) acetic acid in 2-3% HCl. A fresh matrix modifier solution should be prepared each day.

e.g., first add 2-3 ml concentrated HCl to 0.1 g ammonium meta-vanadate (NH_4VO_3) and swirl until it is dissolved, then add 0.495 g nickelous nitrate ($Ni(NO_3)_2(6H_2O)$), 1 g ascorbic acid, 30 ml acetic acid, swirl until solids are dissolved and dilute to 100 ml with H_2O.

Mo - no matrix modifier is necessary, although sample memory may be significant so atomize for at least 10 seconds at

2700°C.

Sb - 500 ppm Ni, 1000 ppm Cr, and 1% (W/V) ammonium meta-tungstate in H_2O

e.g., 0.248 g nickelous nitrate ($Ni(NO_3)_2(6H_2O)$), 0.192 g CrO_3, and 1 g ammonium meta-tungstate, dilute to 100 ml with H_2O.

Se - 1000 ppm Zn and 200 ppm Cu in H_2O

e.g., 0.455 g zinc nitrate ($Zn(NO_3)_2(6H_2O)$) and 0.073 g cupric nitrate ($Cu(NO_3)_2(nH_2O)$), dilute to 100 ml with H_2O.

Sn - First, in order to make an organic W-rich extract, make a solution containing 5% (V/V) Alamine-336 and 10% Aliquat-336 in MIBK

e.g., 5 ml Alamine-336 and 10 ml Aliquat-336, dilute to 100 ml with MIBK.

Next, add 1 g ammonium meta-tungstate and 2.0 ml 6N HCl to a test tube. Add 8.0 ml of the Alamine-336, Aliquat-336, MIBK solution to the test tube, cap test tube, shake, and centrifuge. Remove and save the organic W-rich extract in another test tube

Now, make the Sn matrix modifier solution containing 1% (V/V) organic W-rich extract and 1% (W/V) ascorbic acid in MEOH

e.g., 0.5 ml organic W-rich extract, 0.5 g ascorbic acid, dilute to 50 ml with MEOH.

Condition each new graphite tube by running it through 5 furnace program cycles, injecting 20 microliters of organic W-rich extract before each cycle or until peak absorption stabilizes. Maintain the tungsten carbide surface in the graphite tube by injecting 20 microliters of organic W-rich extract and running through the furnace program cycle following every 20 determinations.

Te - 200 ppm Ni and 100 ppm Cu in H_2O

e.g., 0.198 g nickelous nitrate ($Ni(NO_3)_2(6H_2O)$) and 0.073 g cupric nitrate ($Cu(NO_3)_2(nH_2O)$), dilute to 200 ml with H_2O.

Tl - First, in order to make an organic W-rich extract, make a solution containing 5% (V/V) Alamine-336 and 10% Aliquat-336 in MIBK

e.g., 5 ml Alamine-336 and 10 ml Aliquat-336, dilute to 100 ml with MIBK.

Next, add 1 g ammonium meta-tungstate and 2.0 ml 6N HCl to a test tube. Add 8.0 ml of the Alamine-336, Aliquat-336, MIBK solution to the test tube, cap test tube, shake, and centrifuge. Remove and save the organic W-rich extract in another test tube

Next, make an organic W-rich extract and E+OH solution for the Tl matrix modifier solution. First, make a 10% (W/V) Cr (as CrO_3) solution in H_2O.

e.g., 10 g CrO_3, dilute to 100 ml with H_2O.

Place 5 g urea in a 125 ml polyethylene bottle (not glass), add 95 ml E+OH, cap bottle and agitate until the urea is dissolved (a slow process). Add 1.0 ml concentrated HNO_3 to bottle, cap bottle, and mix. Add 1.0 ml of 10% Cr solution. This produces a a bright green solution. Wait for solution to turn blue. Add 3.0 ml of organic W-rich extract to the solution.

Condition each new graphite tube by running it through 5 furnace program cycles, injecting 20 microliters of organic W-rich extract before each cycle or until peak absorption stabilizes. Maintain the tungsten carbide surface in the graphite tube by injecting 20 microliters of organic W-rich extract and running through the furnace program cycle following every 20 determinations.

METHOD #3 - 30 Minute Cold HCl Digestion/MAGIC Extraction
[24 Hour Cold HCl Digestion/MAGIC Extraction]
EXTRACTION PROCEDURE

1- Weigh 1g (±0.01 g) of sample and place in a 18mm x 150mm disposable test tube.

2- Add 4.0 ml H_2O to each tube.

3- Add 4.0 ml conc. HCl.

4- Add 4.0 ml MP-1 (total aqueous phase is 12.0 ml, 4.0 HCl Normality). Vortex and let stand for 20 minutes.

5- Add 3.0 ml MP-2 organic phase to each tube.

6- Seal tube with cap and shake each tube by hand for 1.5 minutes.

7- Immediately, centifuge the samples at 2000 rpm for 5 minutes. Samples that do not yield at least 2.5 ml of recovered organic extract due to the formation of a sediment-organic clot should be tapped gently against the heel of your hand to break up the clot and centrifuged again.

8- Immediately, decant aqueous phase, organic clot, and organic phase into a clean test tube. The 10 minutes of reaction time not accounted for in step 4 occur during steps 5, 6, and 7.

It is crucial to the end result that each sample reacts for an equal amount of time. The 174 samples plus analytical duplicates, field duplicates, blanks, and standards were digested in one laboratory session. This session lasted over 10 hours since the centrifuge used holds a maximum of 8 samples. Eight samples were started through the procedure above every 20 minutes and each step was carefully timed with a watch so that absolute reaction time between soil and HCl did not vary by more than a few minutes for all samples.

Important note: Since the sample weight is 1 gram and the original method was developed for 3 grams of sample, dilution factor of 3.0 must be applied.

*[Preliminary analyses were carried out on soil samples using a 24 hour cold HCl leach/MAGIC extraction. The only

difference between this method and METHOD #3 described is a modification in step 8 of the Extraction Procedure. These soil samples were allowed to digest for a full 24 hours before the aqueous phase, organic clot, and organic phase were decanted into a clean test tube. Elemental concentration ranges and means are reported in Table 3 in this text. Averaged relative precision of analytical duplicates are reported in Table 4 in this text.]

METHOD #3 - 30 Minute Cold HCl Digestion/MAGIC Extraction STARTER SOLUTION-none

METHOD #3 - 30 Minute Cold HCl Digestion/MAGIC Extraction MAGIC POTIONS-same as Method #2

METHOD #3 - 30 Minute Cold HCl Digestion/MAGIC Extraction STANDARD PREPARATION-high, low, and aqueous standards are prepared as in Method #2.

1- Add 4.0 ml H_2O

2- Add specified volume standard (same as Method #2)

3- Add 4.0 ml concentrated HCl

4- Add 4.0 ml MP-1

5- Add 3.0 ml MP-2

6- allow to sit 24-48 hours unrefrigerated before stripping. (4.0 HCl Normality)

METHOD #3 - 30 Minute Cold HCl Digestion/MAGIC Extraction STRIPPING PROCEDURE-same as Method #2

METHOD #3 - 30 Minute Cold HCl Digestion/MAGIC Extraction MATRIX MODIFIERS-same as Method #2

Appendix V - Analytical Conditions

Appendix Table Va
Flame Atomic Absorption Conditions

element	wavelength (nm)	slit (nm)	lamp (watts)
Cd	228.8	0.7	5
Cu	324.7	0.7	20
Fe	248.3	4.0	30
Mn	279.5	4.0	30
Pb	283.0	0.7	10
Zn	213.9	0.7	18

Appendix Table Vb
Flameless Atomic Absorption Conditions

elem.	wavelength (nm)	argon flow rate (cc/min.)	graphite tube	slit (nm)	lamp (watts)	program cycles (time(sec) x temp(^{o}C)) dry	char	atom	sample volume (ul)	mat. mod. volume (ul)
Ag	328.1	235	pyro.	0.7	20	15x95	25x800	6x2500	5.0	5.0
As	193.7	105	pyro.	0.7	8	15X95	22X1400	7X2700	7.5	7.5
Au	242.8	50	pyro.	0.7	14	40x100	26x1200	7x2700	20.0	20.0
Bi	223.1	55	pyro.	0.2	8.5	35x100	20x500	6x2700	7.5	7.5
Ga	287.4	200	pyro.	0.7	20	20x100	30x900	7x2700	7.5	7.5
In	303.9	55	pyro.	0.7	25	30x115	22x800	7x2600	10.0	10.0
Mo	313.3	200	pyro.	0.2	35	25x100	30x1800	10x2800	10.0	none
Sb	217.6	50	pyro.	0.7	8	50x100	26x900	6x2550	10.0	10.0
Se	196.0	50	pyro.*	0.7	5.5	40x100	26x850	7x2700	10.0	10.0
Sn	224.6	55	pyro.	0.7	8	20x95	35x800	6x2700	20.0	20.0
Te	214.3	50	pyro.*	0.7	8	30x115	22x850	6x2700	10.0	10.0
Tl	276.8	50	pyro.	0.7	7	20x95	30x900	7x2500	20.0	20.0

* - The pyrolytically coated graphite tube is treated with W-rich extract every 20 determinations.

Appendix Table Vc
Soil Analyses Detection Limits
(all detection limits in ppm, except Fe which is in pct)

Method:	Hot Nitric Acid Leach	24 Hr. HCl/MAGIC	30 Min. HCl/MAGIC
Fraction:	-80	-10/+60,-80,-230	-230
element			
Ag	1.00	0.010	0.02
As	----	0.06	0.12
Au	----	0.0024	0.0033
Bi	----	0.030	----
Cd	0.30	0.15	0.15
Cu	2.5	1.0	1.00
Fe	0.05	----	0.05
Ga	----	0.06	----
In	----	0.010	0.0067
Mn	5.0	----	5.0
Mo	----	0.01	0.067
Pb	5.0	1.0	6.7
Sb	----	0.030	----
Se	----	0.100	----
Sn	----	0.02	----
Te	----	0.060	----
Tl	----	0.010	----
Zn	15.0	2.0	15.0

Number of blank samples used to determine detection limit for the Hot Nitric Acid Leach = 7

Number of blank samples used to determine detection limit for the 24 Hr. HCl/MAGIC method = 2

Number of blank samples used to determine detection limit for the 30 Min. HCl/MAGIC method = 7

Most samples analyzed using the Hot Nitric Acid Leach for Ag were at or below the detection limit.

Most samples analyzed using the 24 Hr. HCl/MAGIC method for Se, Te, and Tl were at or below the detection limits.

Appendix VI - Raw Data

Appendix Table VIa
Mineralized Rock Data
Hot Sulfuric Acid-Bromate Digestion/MAGIC Extraction
(all elements in ppm)

#	Ag	As	Au	Bi	Cd	Cu	Ga	In
R9	0.225	1.35	0.0090	0.147	0.23	216.0	5.79	0.027
R12	9.225	26.04	0.0129	0.735	72.90	183.0	1.95	0.960
R9C	0.330	0.60	0.0039	0.147	0.23	183.0	2.55	0.018
R12C	57.000	515.70	0.5955	2.760	443.10	942.0	0.45	6.917

#	Mo	Pb	Sb	Se	Sn	Te	Tl	Zn
R9	3.96	7.0	0.030	0.201	3.72	<0.060	0.102	21.0
R12	18.27	7350.0	2.010	0.468	3.60	0.120	0.010	5460.0
R9C	0.51	25.0	0.048	0.528	1.34	<0.060	0.054	20.0
R12C	0.93	32655.0	31.110	0.465	0.31	0.204	0.018	14805.0

Sample R9 was collected on the surface at breccia outcrop
Sample R12 was collected underground in the Hyde drift (V14).
Samples R9 and R12 were ground to -200 mesh.
Samples R9C and R12C were ground to -60 mesh and they represent the heavy mineral fraction (minus magnetite) of samples R9 and R12, respectively.

Appendix Table VIb
Raw Soil Data - Hot Nitric Acid Digestion
(all elemental concentrations expressed in ppm, except Fe which is in percent)

#	D	Cd	Cu	Fe	Mn	Pb	Zn
1	0	1.16	8.0	1.74	200.3	11.1	75.5
2	25	0.68	8.4	1.28	262.4	17.6	68.5
3	50	1.22	30.6	1.41	1109.2	33.9	130.0
4	75	0.62	9.5	2.16	580.3	7.8	95.4
5	85	0.62	8.4	1.88	240.8	7.8	88.5
6	95	0.47	8.4	1.63	242.6	11.1	86.4
7	105	0.54	20.6	1.52	590.5	40.4	122.0
8	115	0.56	9.9	1.38	240.8	14.3	88.5
9	125	0.33	9.9	1.60	169.1	17.6	85.2
10	135	0.50	12.3	1.87	310.4	24.1	108.7
11	145	0.98	8.0	1.78	235.4	145.9	130.3
12	155	1.07	10.3	1.70	316.1	40.4	120.3
13	165	0.94	5.6	1.88	253.3	20.8	109.9
14	175	1.01	8.4	1.53	255.1	73.1	156.2
15	200	0.96	6.0	1.04	231.9	40.4	126.8
16	225	0.81	8.4	1.27	210.7	40.4	149.5
17	250	0.83	6.8	1.66	291.7	24.1	126.2
18	275	1.05	9.9	1.93	284.3	20.8	132.1
19	300	0.81	13.6	1.56	387.0	37.1	129.3
20	310	0.77	9.9	1.70	253.3	27.3	126.9
21	320	1.36	17.7	2.38	370.8	37.1	143.5
22	330	1.05	11.5	1.27	308.6	37.1	130.4
23	340	1.05	8.0	1.39	288.0	37.1	132.0
24	350	1.05	14.0	1.46	341.1	50.2	130.8
25	360	1.20	11.1	1.57	212.5	50.2	128.4
26	370	1.29	19.3	1.65	771.6	76.4	237.8
27	380	1.44	50.6	1.57	816.0	109.4	259.5
28	390	0.90	20.2	1.17	430.9	89.6	162.7
29	400	1.76	27.1	1.31	600.9	132.6	264.0
30	425	2.00	54.0	1.41	832.3	152.6	271.8
31	450	2.91	34.2	1.37	665.6	216.7	313.2
32	475	2.05	28.4	1.30	723.1	152.6	231.5
33	500	1.78	37.9	1.33	671.2	145.9	217.4
34	525	2.33	24.5	1.51	474.9	156.0	258.4
35	550	2.51	33.3	1.57	649.0	334.7	353.2
36	575	1.01	11.1	1.29	543.0	53.5	145.9
37	600	2.30	36.0	1.49	657.2	254.4	335.1
38	610	2.74	41.1	1.45	696.8	261.3	339.6
39	620	5.68	78.5	1.84	699.7	971.7	842.3
40	630	2.95	42.5	1.85	504.8	586.7	519.9
41	640	3.16	45.8	1.55	577.8	223.5	387.2
42	650	2.12	21.9	1.39	474.9	149.3	258.4
43	660	1.53	18.5	1.30	555.2	92.9	150.0

#	D	Cd	Cu	Fe	Mn	Pb	Zn
44	670	1.85	25.3	1.36	671.2	112.7	171.4
45	680	1.91	34.2	1.37	744.0	112.7	178.7
46	690	1.53	26.6	1.37	590.5	102.8	150.5
47	700	1.89	26.6	1.41	720.1	109.4	160.3
48	725	1.58	24.0	1.34	632.7	92.9	140.6
49	750	1.85	32.4	1.57	790.4	199.7	174.9
50	775	1.98	31.0	1.44	803.1	89.6	162.1
51	800	1.78	24.5	1.51	696.8	63.3	141.3
52	815	2.10	31.9	1.51	720.1	109.4	162.7
53	850	1.94	35.1	1.52	765.4	76.4	150.0
54	875	1.62	26.2	1.58	671.2	79.7	137.1
55	900	2.12	21.0	1.50	676.8	89.6	136.6
56	910	1.58	29.3	1.52	793.6	89.6	154.1
57	920	1.73	27.9	1.58	777.8	89.6	151.0
58	930	1.55	23.2	1.59	714.2	86.3	147.7
59	940	2.10	33.7	1.55	812.8	119.3	187.4
60	950	1.89	32.8	1.58	838.9	116.0	174.9
61	960	2.00	35.1	1.71	903.6	135.9	174.2
62	970	2.46	29.7	1.66	691.0	79.7	154.6
63	980	2.74	21.5	1.68	622.0	66.6	142.4
64	990	2.14	29.7	1.53	777.8	83.0	132.0
65	1000	2.70	41.1	1.49	845.6	132.6	147.2
66	1025	1.62	30.6	1.52	852.2	102.8	132.9
67	1050	1.89	42.0	1.57	921.3	109.4	134.8
68	0	1.76	92.5	2.99	572.7	424.6	346.5
69	25	0.98	32.8	2.02	251.5	203.1	185.8
70	50	0.90	18.5	1.83	488.6	46.9	143.9
71	75	0.68	16.8	1.69	196.8	66.6	125.1
72	100	0.94	9.1	1.73	170.8	33.9	124.9
73	110	0.90	11.9	1.69	179.4	73.1	132.7
74	120	2.26	23.2	2.03	318.0	629.7	452.2
75	130	2.26	21.5	2.17	286.2	693.5	514.5
76	140	4.19	45.3	2.32	720.1	876.3	526.6
77	150	1.60	33.3	1.93	335.3	417.3	463.5
78	160	1.49	12.3	1.77	165.6	119.3	308.6
79	170	0.98	11.5	1.71	167.4	109.4	159.1
80	180	0.90	14.4	1.78	216.0	132.6	134.1
81	190	0.92	13.6	1.69	210.7	112.7	129.6
82	200	0.68	14.4	1.76	200.3	79.7	141.6
83	225	0.71	16.0	1.66	210.7	60.0	153.5
84	250	1.36	15.2	2.29	319.9	53.5	135.3
85	275	0.71	4.9	1.67	210.7	40.4	130.8
86	300	0.90	8.0	1.88	275.1	50.2	148.1
87	325	1.18	10.7	2.29	289.9	89.6	373.2
88	350	0.73	9.9	1.77	237.2	53.5	137.1
89	375	0.58	10.7	2.15	195.0	43.7	120.8
90	400	0.79	20.2	1.71	288.0	89.6	148.1

#	D	Cd	Cu	Fe	Mn	Pb	Zn
91	425	4.02	23.2	3.34	1056.6	102.8	1658.6
92	435	2.14	18.9	2.49	416.0	37.1	564.9
93	445	3.97	38.8	2.70	622.0	506.3	709.8
94	455	4.19	31.9	1.70	422.4	220.1	609.4
95	465	1.69	16.0	1.66	288.0	76.4	197.7
96	475	2.58	25.8	1.80	502.4	112.7	343.1
97	485	1.67	19.8	1.64	372.8	79.7	181.0
98	495	1.64	20.2	1.55	318.9	89.6	199.5
99	505	1.55	20.2	1.54	283.2	73.1	195.9
100	515	2.16	27.1	1.52	390.1	102.8	317.8
101	525	2.10	27.1	1.50	355.9	106.1	298.2
102	550	2.81	37.9	1.70	464.9	126.0	390.4
103	575	3.73	45.8	2.01	479.2	192.9	436.9
104	600	1.85	27.1	1.56	450.8	92.9	248.5
105	625	0.88	18.1	1.50	335.2	60.0	143.1
106	650	1.87	33.3	1.58	498.7	119.3	249.6
107	675	2.10	31.9	1.59	533.9	116.0	247.4
108	700	1.85	20.6	1.50	472.1	79.7	177.2
109	725	2.26	36.5	1.60	554.6	139.3	284.4
110	750	1.49	30.2	1.46	539.0	89.6	226.4
111	775	1.71	34.2	1.51	594.9	83.0	223.3
112	800	1.76	27.1	1.46	523.7	89.6	229.4
113	825	1.09	10.3	1.41	362.2	46.9	164.6
114	850	1.78	14.8	1.47	546.8	86.3	242.0
115	875	1.62	15.2	1.46	557.3	60.0	202.2
116	885	2.16	18.5	1.47	584.0	73.1	227.4
117	895	2.77	36.9	1.48	654.3	106.1	275.2
118	905	2.46	24.5	1.50	597.6	102.8	248.5
119	915	2.05	16.4	1.44	484.1	92.9	212.5
120	925	2.79	22.7	1.44	581.3	182.8	303.9
121	935	1.49	9.9	1.46	714.4	40.4	167.2
122	945	2.16	43.0	1.59	762.0	92.9	230.5
123	955	1.94	21.5	1.44	654.3	89.6	207.7
124	965	1.67	13.6	1.45	669.0	50.2	160.9
125	975	1.71	17.7	1.47	672.0	56.7	163.3
126	1000	1.62	20.2	1.49	531.3	86.3	147.2
127	1025	2.46	39.2	1.54	907.0	112.7	195.0
128	1050	1.78	39.2	1.74	853.1	92.9	147.2
129	1075	0.92	17.2	1.62	501.2	40.4	127.7
130	1100	0.83	10.7	1.54	491.4	17.6	125.5
131	1125	1.73	30.2	1.52	745.9	83.0	151.0
132	1135	0.79	19.8	1.56	686.9	40.4	130.0
133	1145	0.94	37.4	1.57	811.7	53.5	136.3
134	1155	1.05	36.5	1.50	839.2	69.9	143.1
135	1165	0.98	31.0	1.48	794.9	53.5	139.9
136	1175	0.56	12.7	1.50	648.5	17.6	127.8
137	1185	0.94	17.7	1.57	801.6	33.9	130.6

#	D	Cd	Cu	Fe	Mn	Pb	Zn
138	1195	1.58	26.6	1.64	775.0	69.9	144.3
139	1205	1.71	30.6	1.63	903.3	89.6	160.9
140	1215	0.71	22.3	1.51	672.0	66.6	135.5
141	1225	0.73	21.5	1.50	581.3	79.7	132.9
142	1250	0.54	6.8	1.35	194.1	33.9	120.0
143	1275	1.60	26.6	1.48	998.2	76.4	138.0
144	1300	0.79	10.3	1.37	686.9	40.4	121.6
145	1325	1.73	31.9	1.53	1200.0	99.5	142.4
146	1350	1.09	17.2	1.43	808.3	60.0	125.5
147	1375	1.42	28.8	1.49	1014.0	119.3	134.4
148	0	1.89	40.6	1.72	794.9	139.3	167.9
149	10	1.96	42.0	1.74	899.7	226.9	177.9
150	20	1.73	53.0	1.80	815.1	145.9	184.2
151	30	2.37	90.3	1.88	986.4	189.6	267.3
152	40	2.84	80.1	1.74	1306.4	192.9	283.2
153	50	0.77	9.1	1.54	349.7	92.9	133.9
154	60	0.79	14.4	1.40	258.0	142.6	127.3
155	70	0.96	15.2	1.73	603.1	119.3	143.1
156	80	0.47	6.8	1.49	333.1	102.8	133.1
157	90	0.60	6.0	1.42	239.0	126.0	128.3
158	100	0.94	6.4	1.49	295.0	106.1	130.1
159	110	0.83	9.5	1.54	263.8	89.6	135.3
160	120	1.11	12.3	1.41	455.5	76.4	139.6
161	130	1.07	15.2	1.35	362.2	109.4	137.4
162	140	1.05	8.0	1.31	233.3	179.4	131.3
163	150	1.36	18.9	1.63	368.6	109.4	247.4
164	160	1.29	12.7	1.53	281.2	106.1	148.1
165	170	0.68	14.0	1.53	175.6	149.3	127.8
166	180	0.68	13.6	1.41	231.4	189.6	130.1
167	190	0.54	18.1	1.38	205.2	149.3	126.1
168	200	0.43	13.6	1.37	201.5	149.3	129.2
169	225	1.38	29.7	1.72	518.7	169.4	274.1
170	250	1.03	39.7	1.48	581.3	132.6	190.7
171	275	0.58	16.0	1.74	351.7	66.6	125.1
172	300	0.50	10.7	1.50	225.8	40.4	119.8
173	325	0.35	6.4	1.41	331.1	33.9	119.5
174	350	0.90	24.9	1.51	586.7	53.5	130.7
R9		0.83	172.0	2.88	211.0	15.7	7.5
R12		41.56	118.0	6.30	1650.8	4097.8	9573.6
R9C		0.79	117.0	1.91	90.3	22.2	7.5
R12C		297.66	700.9	34.59	728.7	1275.2	60755.7
GXR2		2.93	52.1	1.03	676.8	502.5	424.2
GXR4		1.05	306.5	1.93	90.3	27.3	7.9
GXR5		1.01	198.1	1.87	131.3	11.1	7.5
GXR6		0.60	31.5	2.95	507.1	53.5	75.5
SB1		0.62	11.1	1.58	598.3	56.7	127.4
SB2		1.40	10.3	1.70	555.2	112.7	154.6

#	Cd	Cu	Fe	Mn	Pb	Zn
SB3	1.78	15.2	2.70	470.4	83.0	348.7
SB5	1.18	10.3	1.26	393.1	142.6	130.1
SB6	1.16	9.5	1.60	493.2	56.7	134.6
SB7	0.43	8.4	1.75	202.0	33.9	117.2
SB8	1.89	37.4	1.69	869.1	159.3	216.4
SB10	1.58	16.4	2.87	454.9	69.9	358.8
SB11	0.41	9.1	1.63	550.3	53.5	128.1
SB12	1.42	9.5	1.75	184.6	46.9	120.6
SB13	0.96	9.5	1.57	418.2	11.1	129.6
SB15	1.01	14.0	1.38	277.0	20.8	130.1
SB16	0.88	10.7	1.73	509.5	69.9	142.7
SB18	1.09	14.8	1.76	488.6	30.6	138.0
B-1	0.00	0.6	0.01	0.0	2.1	9.6
B-2	0.00	0.6	0.01	0.0	2.1	9.3
B-3	0.00	0.6	0.01	0.0	2.1	9.1
B-4	0.00	0.6	0.01	0.0	2.1	9.0
B-5	0.00	0.6	0.01	0.0	2.1	9.0
B-6	0.00	0.6	0.01	0.0	2.1	9.0
B-7	0.00	0.6	0.01	0.0	2.1	9.0
6D	0.88	6.4	1.76	262.4	20.8	97.2
14D	1.05	8.0	1.51	256.9	63.3	162.1
25D	0.66	9.9	1.50	212.5	40.4	127.6
31D	1.38	31.9	1.43	616.6	209.9	309.7
39D	5.80	74.8	1.73	603.5	923.7	796.1
54D	0.79	27.5	1.58	654.5	63.3	138.0
58D	2.35	24.0	1.54	723.1	89.6	150.5
73D	1.03	12.3	1.62	184.6	73.1	135.8
81D	0.98	12.3	1.79	210.7	156.0	130.8
89D	0.96	11.1	2.21	223.0	40.4	122.2
100D	2.26	26.2	1.55	427.8	92.9	323.6
106D	1.71	32.8	1.52	513.6	106.1	219.3
119D	2.14	18.1	1.46	503.7	96.2	228.4
126D	0.79	19.8	1.51	549.4	79.7	145.1
140D	1.16	19.3	1.46	758.8	66.6	136.6
10B	1.03	13.1	2.59	207.2	20.8	107.5
20B	0.79	14.0	1.61	393.1	37.1	127.8
30B	1.25	19.8	1.33	468.2	86.3	181.8
40B	1.87	30.2	1.54	486.3	338.2	371.0
50B	2.10	32.4	1.51	738.0	112.7	181.8
60B	1.31	27.9	1.41	714.2	126.0	163.3
77B	1.20	10.3	1.78	196.8	76.4	405.0
87B	1.33	11.9	2.59	271.5	179.4	762.2
97B	3.90	29.7	2.16	543.0	179.4	486.3
107B	1.40	25.3	1.49	414.3	69.9	148.1
117B	2.46	24.0	1.55	642.7	89.6	313.2
127B	1.76	21.0	1.54	768.5	60.0	156.8
137B	1.01	16.4	1.64	680.9	30.6	132.3

#	Cd	Cu	Fe	Mn	Pb	Zn
147B	1.27	18.1	1.37	853.1	83.0	126.6
157B	0.88	11.1	1.42	252.3	122.6	130.3
167B	0.83	20.6	1.44	476.8	159.3	152.0

R# - Mineralized Rock Sample.
R#C - Mineralized Rock Sample Concentrate.
D - Distance (in feet) from station 1 for traverse #1, distance from station 68 for traverse #2, and distance from station 148 for traverse #3.
GXR# - Soil U.S.G.S. Reference Sample.
SB# - Soil Background Sample collected outside study area.
B-# - Soil Analytical Blank Sample.
#D - Soil Analytical Duplicate Sample.
#B - Soil Field Duplicate Sample.

Samples R9, R9C, and GXR-5 are below the detection limit for zinc of 15.0 ppm, so concentrations for these samples are set at 1/2 the detection limit (7.5 ppm)

Appendix Table VIc
Raw Soil Data -
30 Minute Cold HCl Digestion/MAGIC Extraction
(all elemental concentrations expressed in ppm, except Fe which is in percent)

#	D	Ag	As	Au	Cd	Cu	Fe	In	Mn	Mo	Pb	Zn
1	0	0.18	0.72	0.0017	0.19	4.43	0.73	0.0214	9.7	0.714	14.7	27.4
2	25	0.12	1.18	0.0050	0.36	5.97	0.47	0.0187	16.1	0.557	20.0	27.8
3	50	0.34	4.35	0.0172	0.88	30.15	0.62	0.0368	79.5	0.846	34.8	78.3
4	75	0.15	0.80	0.0131	0.22	4.43	0.70	0.0200	15.8	0.966	12.5	26.6
5	85	0.15	0.80	0.0017	0.40	5.44	0.83	0.0214	15.0	0.932	14.7	27.8
6	95	0.14	1.00	0.0056	0.41	7.20	0.65	0.0242	18.2	0.800	20.5	29.7
7	105	0.46	3.95	0.0213	0.75	19.72	0.74	0.0566	54.9	0.780	57.2	54.6
8	115	0.16	0.91	0.0063	0.47	5.84	0.61	0.0174	13.1	0.563	16.5	28.6
9	125	0.20	0.71	0.0017	0.36	5.19	0.75	0.0200	7.9	0.681	13.7	26.6
10	135	0.37	0.83	0.0043	0.47	8.34	0.93	0.0272	23.5	0.866	22.8	36.2
11	145	1.67	0.61	0.0017	0.29	5.58	0.58	0.0174	10.8	0.734	98.9	40.8
12	155	0.47	1.29	0.0179	0.42	9.07	0.63	0.0335	20.0	0.681	35.8	39.3
13	165	0.49	0.51	0.0158	0.29	3.69	0.55	0.0214	10.8	0.681	18.6	29.3
14	175	1.64	0.69	0.0017	0.47	4.80	0.47	0.0174	11.2	0.681	51.0	45.0
15	200	0.35	0.74	0.0017	0.52	4.80	0.37	0.0161	11.0	0.550	27.1	40.8
16	225	0.24	0.61	0.0381	0.41	6.65	0.42	0.0149	9.3	0.583	33.1	55.4
17	250	0.21	0.97	0.0611	0.50	6.24	0.47	0.0242	13.4	0.708	23.8	39.7
18	275	0.21	0.56	0.0017	0.29	4.43	0.46	0.0149	5.0	0.576	16.7	31.2
19	300	0.26	1.17	0.0389	0.52	11.52	0.48	0.0214	23.7	0.497	24.7	40.8
20	310	0.17	1.15	0.0017	0.39	5.31	0.45	0.0187	8.0	0.458	20.3	28.9
21	320	0.20	1.16	0.0063	0.56	12.96	0.64	0.0242	18.2	0.616	30.7	48.1
22	330	0.28	0.97	0.0036	0.73	8.78	0.45	0.0149	18.2	0.504	29.2	44.6
23	340	0.29	1.57	0.0017	0.64	6.51	0.51	0.0257	16.7	0.471	28.8	51.1
24	350	0.33	1.21	0.0043	0.67	11.84	0.58	0.0272	19.7	0.550	38.1	56.1
25	360	0.51	0.75	0.0017	0.52	6.78	0.51	0.0272	8.9	0.484	37.2	44.6
26	370	0.64	1.87	0.0144	1.26	21.56	0.74	0.0644	65.7	0.583	79.6	123.6
27	380	0.98	4.03	0.1236	1.59	59.05	0.72	0.1086	81.4	0.622	118.8	131.9
28	390	0.83	2.57	0.0611	0.98	17.38	0.52	0.0368	37.0	0.386	77.6	92.7
29	400	0.91	4.79	0.0269	1.71	25.18	0.63	0.0870	54.2	0.504	132.0	147.8
30	425	1.42	6.16	0.1279	2.44	65.03	0.64	0.1325	78.9	0.517	160.0	194.2
31	450	1.18	6.07	0.1134	2.66	36.59	0.60	0.1537	56.2	0.616	302.3	211.7
32	475	0.82	5.41	0.0360	2.06	31.17	0.57	0.1107	72.7	0.550	168.4	143.3
33	500	0.78	4.64	0.0438	1.56	44.40	0.57	0.0977	62.4	0.758	158.6	138.3
34	525	0.73	2.24	0.0137	1.62	20.27	0.55	0.0644	40.9	0.744	158.8	134.0
35	550	1.59	5.99	0.1279	2.71	37.66	0.91	0.1659	74.0	1.043	386.7	211.7
36	575	0.44	1.71	0.0070	1.15	11.84	0.62	0.0242	53.4	0.582	76.2	68.6
37	600	1.09	5.26	0.1439	2.67	42.86	0.77	0.1832	70.4	0.880	336.4	228.2
38	610	1.29	5.36	0.0276	3.08	52.99	0.76	0.0807	71.7	1.074	354.3	254.3
39	620	2.91	7.62	0.1848	9.10	95.06	1.25	0.5280	48.0	2.089	1291.1	741.4
40	630	2.52	6.82	0.0632	4.71	52.53	1.22	0.3840	37.4	1.679	820.6	438.8
41	640	1.41	4.99	0.1047	3.22	63.10	0.98	0.2003	51.9	1.590	297.3	241.4

#	D	Ag	As	Au	Cd	Cu	Fe	In	Mn	Mo	Pb	Zn
42	650	0.88	3.24	0.0241	2.40	20.45	0.63	0.1107	39.5	0.813	177.2	133.0
43	660	0.63	4.04	0.0199	2.25	20.45	0.70	0.0566	47.0	1.093	106.8	94.0
44	670	0.85	3.93	0.0792	2.75	29.14	0.66	0.0664	66.4	1.043	148.5	126.2
45	680	1.15	5.41	0.0668	2.65	40.24	0.63	0.1020	74.0	0.860	151.6	126.7
46	690	0.67	3.99	0.0206	1.89	25.77	0.55	0.0472	59.8	0.786	114.3	87.5
47	700	0.88	3.80	0.0705	2.11	26.75	0.62	0.0765	66.9	0.887	132.2	100.2
48	725	0.81	3.74	0.0290	2.11	28.14	0.60	0.0604	64.3	0.751	130.1	91.4
49	750	1.14	7.68	0.0269	2.59	38.09	0.65	0.0765	74.8	1.080	320.4	125.1
50	775	1.09	4.63	0.0828	2.95	41.55	0.68	0.0870	90.0	1.017	146.9	134.6
51	800	0.60	4.85	0.0792	2.21	29.14	0.62	0.0624	75.6	1.074	109.0	98.4
52	815	1.22	8.54	0.0654	2.84	36.59	0.68	0.0934	66.7	1.255	157.6	119.1
53	850	1.15	7.85	0.1568	2.77	52.76	0.71	0.0724	88.7	1.196	139.0	114.7
54	875	0.56	4.38	0.0325	1.47	33.44	0.62	0.0436	66.4	0.979	104.2	83.7
55	900	0.72	3.75	0.0381	2.22	23.45	0.55	0.0401	72.2	1.074	118.1	99.8
56	910	1.12	5.52	0.0923	2.40	34.07	0.63	0.0566	75.3	0.998	131.6	113.3
57	920	1.19	5.64	0.0705	2.78	41.33	0.67	0.0724	91.2	1.196	143.6	117.6
58	930	0.92	5.08	0.0741	2.60	31.38	0.64	0.0547	72.7	1.074	126.1	111.4
59	940	1.38	7.55	0.1496	3.64	48.20	0.66	0.0684	80.9	1.244	192.6	141.6
60	950	1.10	6.35	0.0734	2.94	41.11	0.60	0.0849	74.0	1.136	150.6	124.6
61	960	1.28	6.70	0.0539	3.06	48.20	0.78	0.0849	88.7	1.166	163.5	109.9
62	970	0.75	4.28	0.1626	2.39	39.38	0.64	0.0547	65.0	0.867	106.4	91.0
63	980	0.48	2.62	0.0438	1.88	23.07	0.63	0.0257	47.4	0.639	67.3	74.7
64	990	0.78	5.42	0.0531	1.61	34.91	0.60	0.0491	76.4	0.854	104.2	83.7
65	1000	1.10	6.35	0.0431	2.08	54.83	0.57	0.0664	64.5	0.914	155.1	109.9
66	1025	0.83	5.31	0.0339	1.81	35.96	0.57	0.0745	78.6	1.005	129.0	83.7
67	1050	0.93	5.58	0.0517	1.82	46.41	0.57	0.0454	90.0	0.894	138.0	87.1
68	0	1.68	25.22	0.1200	1.32	156.12	2.06	0.2778	54.2	2.965	650.3	248.2
69	25	1.15	7.64	0.0916	0.69	47.53	1.27	0.1020	16.4	1.750	343.5	147.8
70	50	0.37	1.77	0.0311	0.59	24.41	0.77	0.0137	32.4	1.782	66.9	83.3
71	75	0.30	1.33	0.0117	0.41	11.68	0.48	0.0187	7.9	1.203	68.0	44.2
72	100	0.07	0.65	0.0185	0.37	3.34	0.33	0.0103	2.5	0.813	38.7	40.8
73	110	0.15	0.85	0.0262	0.46	6.78	0.43	0.0125	2.5	0.741	86.1	57.3
74	120	0.91	3.55	0.0339	2.02	20.08	0.76	0.0624	13.9	1.677	684.7	256.1
75	130	1.19	2.03	0.0560	1.81	15.64	0.72	0.0368	9.0	2.235	717.4	256.1
76	140	1.23	3.37	0.2171	3.92	46.85	0.89	0.0828	46.8	2.096	832.4	317.5
77	150	0.68	3.19	0.1061	1.44	37.02	0.73	0.0436	19.4	1.092	468.6	221.0
78	160	0.33	0.80	0.0075	1.03	6.11	0.38	0.0200	2.5	0.629	119.2	129.8
79	170	0.26	0.67	0.1282	0.50	5.58	0.36	0.0242	2.5	0.562	107.9	47.7
80	180	0.31	0.90	0.0046	0.55	6.92	0.41	0.0303	2.5	0.562	151.0	44.6
81	190	0.45	1.19	0.0033	0.55	6.92	0.41	0.0401	5.1	0.562	140.9	45.0
82	200	0.50	1.05	0.0107	0.56	7.76	0.38	0.0257	2.5	0.518	97.3	48.8
83	225	0.26	1.78	0.0036	0.57	9.97	0.43	0.0351	6.4	0.551	74.2	65.9
84	250	0.55	1.71	0.0071	0.78	16.33	0.83	0.0228	15.3	0.796	56.5	73.9
85	275	0.29	0.63	0.0071	0.61	2.99	0.41	0.0161	2.5	0.523	41.1	40.4
86	300	0.21	0.71	0.0017	0.61	4.43	0.48	0.0200	5.5	0.490	47.3	39.7
87	325	0.62	1.67	0.0043	1.03	8.34	0.72	0.0472	13.9	0.713	96.5	93.6

#	D	Ag	As	Au	Cd	Cu	Fe	In	Mn	Mo	Pb	Zn
88	350	0.28	1.08	0.0096	0.64	5.71	0.43	0.0257	11.2	0.484	47.4	42.3
89	375	0.31	1.14	0.0017	0.54	6.51	0.62	0.0272	5.6	0.607	44.7	36.6
90	400	0.62	2.45	0.0089	0.82	20.27	0.54	0.0454	15.5	0.635	93.2	71.4
91	425	1.03	1.20	0.0075	4.80	28.14	1.44	0.0624	80.3	2.876	137.8	780.6
92	435	1.26	1.24	0.0085	2.48	23.26	1.31	0.0303	41.3	1.538	50.5	410.3
93	445	2.98	6.97	0.1624	4.46	57.17	1.74	0.5124	35.8	2.491	717.4	654.0
94	455	2.70	2.08	0.0182	6.01	39.16	0.75	0.1639	27.1	0.964	283.2	556.1
95	465	1.23	1.63	0.0398	1.54	15.13	0.60	0.0303	14.6	0.590	86.5	110.9
96	475	1.23	3.33	0.0140	3.07	31.58	0.72	0.1719	35.4	0.886	139.5	218.7
97	485	0.96	1.91	0.0064	1.61	20.82	0.63	0.0547	25.0	0.735	93.2	115.7
98	495	0.83	2.27	0.0271	2.09	20.63	0.62	0.0724	41.9	0.869	101.0	128.8
99	505	0.86	2.08	0.0252	1.62	21.94	0.57	0.0745	37.2	0.724	87.7	127.7
100	515	1.02	2.78	0.0220	2.97	33.86	0.63	0.1216	47.8	0.769	120.6	237.2
101	525	1.48	4.20	0.1130	3.16	35.33	0.72	0.2019	40.7	0.902	152.3	229.0
102	550	0.75	4.82	0.0465	4.46	55.76	0.89	0.3398	63.3	0.936	222.0	330.5
103	575	2.97	3.62	0.0965	5.26	71.91	1.07	0.2520	55.1	0.992	297.3	388.3
104	600	1.14	3.52	0.0457	2.31	29.14	0.62	0.1260	45.6	0.568	110.7	162.6
105	625	0.60	1.73	0.0067	1.29	15.47	0.52	0.0509	32.8	0.507	76.7	82.1
106	650	1.06	4.46	0.0482	2.35	37.66	0.67	0.1738	61.4	0.707	134.9	162.6
107	675	0.78	5.25	0.0373	2.35	33.44	0.68	0.1921	51.0	0.741	118.5	182.5
108	700	0.53	2.92	0.0148	1.91	19.53	0.59	0.0644	48.5	0.635	75.4	117.6
109	725	0.99	7.06	0.0144	3.56	43.74	0.75	0.2520	58.0	0.919	152.1	235.5
110	750	0.68	4.33	0.0197	2.28	32.20	0.62	0.1238	60.1	0.649	85.7	160.8
111	775	0.87	4.16	0.0291	2.63	41.33	0.64	0.0956	63.3	0.829	87.0	168.8
112	800	1.12	4.76	0.1061	2.91	35.96	0.64	0.1260	63.1	0.712	97.3	173.9
113	825	0.46	1.25	0.1292	1.36	6.78	0.42	0.0214	26.1	0.453	44.7	91.4
114	850	0.41	2.36	0.0118	2.24	12.48	0.48	0.0454	43.7	0.723	68.0	143.9
115	875	0.43	2.29	0.0046	2.46	14.29	0.56	0.0384	58.2	0.739	59.4	148.4
116	885	0.72	3.13	0.0057	2.88	21.00	0.60	0.0335	57.6	0.675	72.6	170.1
117	895	1.34	5.61	0.1126	4.22	44.63	0.65	0.0807	66.9	0.845	118.5	242.2
118	905	0.91	4.07	0.0201	3.32	28.34	0.57	0.0786	56.7	0.750	102.5	190.7
119	915	0.95	3.18	0.0096	2.60	18.09	0.55	0.0604	44.5	0.819	88.6	148.4
120	925	1.55	4.12	0.0586	3.76	25.77	0.64	0.1173	54.0	0.914	154.7	253.4
121	935	0.55	1.27	0.0542	1.63	7.06	0.41	0.0174	38.3	0.521	37.6	94.9
122	945	1.10	6.92	0.0599	2.99	50.70	0.68	0.0913	78.3	1.026	98.8	172.7
123	955	0.88	5.07	0.0256	2.28	23.26	0.66	0.0745	59.4	0.829	93.6	143.9
124	965	0.38	2.63	0.0085	1.55	11.36	0.60	0.0436	61.9	0.819	54.9	99.8
125	975	0.46	3.25	0.0209	1.70	18.27	0.64	0.0401	56.9	0.739	62.9	103.4
126	1000	0.91	4.14	0.0762	1.64	19.90	0.64	0.0604	56.7	0.829	91.2	93.6
127	1025	1.03	6.96	0.0423	3.03	46.85	0.78	0.1346	99.5	1.206	137.8	160.8
128	1050	0.96	8.26	0.0299	1.78	41.76	0.77	0.1020	78.9	1.211	108.5	102.5
129	1075	0.57	3.47	0.1016	1.17	16.68	0.58	0.0491	48.2	0.819	52.9	65.9
130	1100	0.24	1.40	0.0057	0.82	7.76	0.58	0.0187	42.9	0.734	30.7	48.8
131	1125	0.83	6.57	0.1093	2.24	29.95	0.64	0.0870	68.4	1.163	100.4	114.2
132	1135	0.53	3.55	0.1648	1.54	18.99	0.63	0.0624	63.3	0.914	56.3	75.1
133	1145	0.64	6.47	0.0248	1.73	41.76	0.64	0.0807	75.1	1.084	73.1	82.9

#	D	Ag	As	Au	Cd	Cu	Fe	In	Mn	Mo	Pb	Zn
134	1155	0.81	6.98	0.0415	2.17	40.24	0.65	0.0977	97.4	1.057	90.1	103.4
135	1165	0.67	6.54	0.0209	2.06	37.87	0.70	0.0828	80.6	1.047	88.1	105.3
136	1175	0.19	2.14	0.0057	1.05	11.05	0.64	0.0257	55.3	0.957	37.4	100.7
137	1185	0.33	3.25	0.0189	1.42	18.09	0.76	0.0419	72.2	0.824	54.6	82.5
138	1195	0.54	6.07	0.0252	1.95	25.96	0.64	0.0828	67.7	1.153	89.7	99.8
139	1205	0.92	7.02	0.1061	2.41	32.82	0.71	0.1194	83.2	1.238	129.5	128.2
140	1215	0.47	4.98	0.0651	1.72	23.07	0.63	0.0547	73.0	1.073	66.4	91.4
141	1225	0.44	3.97	0.0201	1.33	16.51	0.56	0.0604	48.9	0.962	74.4	73.0
142	1250	0.15	1.49	0.0017	0.44	4.06	0.33	0.0114	6.6	0.521	25.1	33.2
143	1275	0.97	5.52	0.0263	2.43	32.82	0.61	0.0724	97.7	0.845	84.1	104.3
144	1300	0.25	2.76	0.0060	0.91	11.05	0.48	0.0242	60.5	0.638	38.2	50.0
145	1325	1.04	6.73	0.1455	2.13	32.20	0.53	0.0913	103.6	1.015	104.9	99.8
146	1350	0.44	4.05	0.0082	0.87	16.68	0.49	0.0368	64.0	0.712	53.7	51.5
147	1375	0.77	6.58	0.0465	1.47	28.74	0.59	0.0870	93.9	0.994	115.6	85.4
148	0	1.07	10.04	0.0678	2.08	34.91	0.86	0.1411	53.8	1.466	145.2	104.3
149	10	1.17	15.50	0.0423	1.98	35.96	0.86	0.2040	52.1	2.453	295.6	117.6
150	20	1.15	10.23	0.0381	2.09	49.56	0.88	0.1699	60.5	1.413	158.6	122.1
151	30	1.84	10.04	0.1648	2.68	77.23	0.78	0.1886	67.2	0.808	258.6	157.2
152	40	1.72	10.14	0.1273	3.83	88.08	0.89	0.2064	111.3	1.068	286.7	191.4
153	50	0.57	1.39	0.0060	0.89	7.06	0.45	0.0214	15.8	0.702	54.1	52.3
154	60	1.16	2.50	0.0163	0.99	9.97	0.55	0.0303	12.3	0.675	73.0	40.4
155	70	0.93	2.67	0.0100	1.33	13.62	0.71	0.0454	40.5	0.840	103.2	59.2
156	80	0.53	1.02	0.0050	0.89	4.30	0.51	0.0187	14.6	0.781	69.9	46.5
157	90	0.56	0.86	0.0096	1.02	4.68	0.45	0.0214	8.4	0.622	96.0	42.7
158	100	0.56	1.08	0.0017	1.02	4.43	0.54	0.0257	12.3	0.744	82.6	40.0
159	110	0.30	0.99	0.0224	0.94	6.11	0.72	0.0214	9.2	0.686	65.4	45.0
160	120	0.29	1.85	0.0046	1.26	10.12	0.47	0.0351	29.1	0.755	67.6	51.9
161	130	0.43	1.71	0.0060	1.25	9.97	0.43	0.0351	19.2	0.633	97.7	49.2
162	140	0.96	1.09	0.0053	1.15	5.71	0.35	0.0528	8.8	0.559	144.6	42.7
163	150	0.89	1.82	0.0111	1.71	13.79	0.51	0.0454	21.8	0.654	105.5	83.7
164	160	0.84	0.83	0.0033	1.13	8.63	0.43	0.0384	11.6	0.585	90.3	53.4
165	170	0.68	0.73	0.0017	0.75	6.92	0.32	0.0174	2.5	0.580	126.3	38.5
166	180	1.18	0.88	0.0151	0.95	9.22	0.34	0.0384	9.0	0.511	234.2	47.3
167	190	1.80	1.18	0.0100	1.07	16.16	0.40	0.0287	7.5	0.644	145.9	52.7
168	200	1.15	1.21	0.0071	0.98	10.43	0.36	0.0335	6.3	0.453	140.1	49.6
169	225	1.26	4.68	0.0361	2.60	40.24	0.84	0.1281	47.0	1.100	290.3	175.2
170	250	1.25	3.21	0.2113	2.31	98.53	0.72	0.0828	62.1	1.339	225.5	159.6
171	275	1.08	2.22	0.0078	1.15	22.50	0.67	0.0335	28.9	0.723	88.5	65.5
172	300	0.40	0.74	0.0036	0.71	6.65	0.35	0.0161	7.2	0.553	33.3	35.5
173	325	0.28	0.63	0.0017	0.68	4.55	0.39	0.0137	15.9	0.431	27.3	30.5
174	350	0.47	2.20	0.0155	1.29	21.94	0.53	0.0419	45.8	0.665	56.8	64.7
GXR2		17.33	12.93	0.0269	3.24	72.42	1.03	0.0228	57.1	0.813	745.1	466.0
GXR4		2.36	24.57	0.0916	0.43	3482.39	1.05	0.0644	5.7	168.900	33.3	60.4
GXR5		0.79	5.48	0.0076	0.27	337.12	2.42	0.0187	12.1	31.784	11.0	50.7
GXR6		0.23	132.86	0.0792	0.32	43.30	3.16	0.0161	54.9	1.296	64.3	66.3
SB1		0.46	1.18	0.0017	0.69	8.63	0.80	0.0436	51.9	1.085	61.5	62.3

#	Ag	As	Au	Cd	Cu	Fe	In	Mn	Mo	Pb	Zn
SB2	0.61	1.40	0.0424	0.60	9.82	0.68	0.0585	37.0	1.212	109.4	82.9
SB3	0.73	1.29	0.0110	1.04	18.09	1.14	0.0528	33.4	1.951	86.8	163.8
SB5	1.76	1.45	0.0017	0.80	7.20	0.58	0.0200	27.1	1.132	130.9	77.5
SB6	0.24	1.60	0.0017	0.91	9.07	0.73	0.0242	40.9	0.992	68.5	84.1
SB7	0.51	1.05	0.0165	0.51	5.19	0.71	0.0125	5.4	1.024	40.7	41.2
SB8	1.21	4.63	0.3625	2.79	36.38	0.81	0.0849	84.7	1.397	237.7	150.1
SB10	0.69	1.24	0.0103	1.42	19.72	1.35	0.0472	34.1	1.934	102.5	176.5
SB11	0.57	1.33	0.0063	0.78	9.22	0.75	0.0287	55.3	1.062	69.2	58.1
SB12	0.48	1.01	0.0199	0.37	5.84	0.58	0.0125	5.0	0.860	42.2	41.6
SB13	0.61	1.06	0.0192	0.64	8.05	0.87	0.0149	56.7	1.287	46.9	67.5
SB15	0.83	1.49	0.0060	0.78	11.68	0.46	0.0149	18.1	0.936	61.9	73.4
SB16	0.28	1.84	0.0193	1.19	8.92	0.77	0.0214	41.9	1.075	73.5	82.5
SB18	0.55	1.30	0.0017	0.78	8.63	0.85	0.0200	32.6	1.092	48.6	69.4
B-1	0.01	0.06	0.0004	0.12	0.65	0.00	0.0031	0.6	0.009	0.8	12.9
B-2	0.01	0.07	0.0017	0.10	0.37	0.00	0.0031	0.6	0.028	0.8	12.1
B-3	0.01	0.10	0.0030	0.11	0.37	0.00	0.0031	0.4	0.053	0.4	9.3
B-4	0.01	0.10	0.0029	0.11	0.27	0.00	0.0031	0.4	0.059	1.6	10.1
B-5	0.01	0.10	0.0010	0.08	0.09	0.00	0.0031	0.4	0.061	0.5	11.7
B-6	0.01	0.08	0.0001	0.13	0.09	0.00	0.0031	0.4	0.038	4.5	10.9
B-7	0.01	0.08	0.0005	0.05	0.09	0.00	0.0031	0.5	0.066	2.6	10.1
6D	0.11	1.03	0.0131	0.30	7.48	0.59	0.0228	19.7	0.800	21.1	29.3
14D	1.63	0.58	0.0070	0.51	4.68	0.50	0.0161	10.6	0.622	51.2	42.3
25D	0.50	0.73	0.0103	0.43	6.78	0.52	0.0228	9.8	0.439	35.3	44.6
31D	1.13	6.10	0.0510	2.79	37.87	0.77	0.1903	57.3	1.024	290.3	202.1
39D	2.98	6.49	0.0945	10.93	95.63	1.13	0.5850	48.7	1.782	132.2	763.0
54D	0.85	3.68	0.0389	1.60	34.70	0.62	0.0436	65.9	0.992	101.9	85.8
58D	0.86	5.07	0.0290	2.56	31.79	0.81	0.0547	75.1	1.030	125.3	111.4
73D	0.23	0.88	0.0308	0.58	6.51	0.35	0.0187	2.5	0.735	85.9	52.7
81D	0.56	1.28	0.0377	0.55	7.20	0.52	0.0214	5.5	0.573	137.4	41.6
89D	0.31	0.99	0.0612	0.48	6.38	0.59	0.0242	5.8	0.607	44.4	31.6
100D	1.07	2.75	0.0118	2.93	34.70	0.68	0.1411	47.2	0.735	123.0	237.2
106D	0.95	4.46	0.0216	2.55	36.38	0.65	0.1516	51.2	0.856	105.1	168.2
119D	0.91	3.35	0.0155	2.73	17.91	0.53	0.0604	53.4	0.803	89.7	148.4
126D	0.71	3.50	0.0159	1.51	18.63	0.61	0.0604	50.6	0.819	81.7	89.7
140D	0.44	4.59	0.0185	1.61	22.88	0.60	0.0566	69.4	1.116	69.8	94.0
10B	0.44	1.36	0.0056	0.58	10.43	0.99	0.0384	28.2	1.059	33.8	44.2
20B	0.21	1.08	0.0017	0.43	5.97	0.50	0.0228	9.2	0.432	24.1	30.9
30B	0.66	2.89	0.0625	1.43	34.70	0.52	0.0419	67.2	0.406	89.0	124.1
40B	3.03	5.83	0.1141	8.09	78.01	1.22	0.5090	51.0	2.187	1136.0	648.2
50B	1.09	5.42	0.0403	3.04	48.20	0.69	0.0828	79.2	1.074	156.6	152.4
60B	1.00	5.73	0.2358	2.50	34.28	0.60	0.0870	74.3	1.290	139.3	109.9
77B	0.72	2.69	0.0763	1.53	26.36	0.70	0.0585	19.0	1.231	401.1	283.0
87B	0.46	0.94	0.0017	0.87	4.80	0.62	0.0287	11.7	0.674	88.5	75.1
97B	0.92	2.38	0.0377	2.13	26.75	0.69	0.0807	38.3	0.702	109.2	152.4
107B	0.50	2.76	0.0114	1.39	19.90	0.50	0.0604	38.5	0.467	68.0	88.0
117B	1.00	3.95	0.0163	2.57	22.31	0.57	0.0644	51.0	0.766	82.6	155.4

#	Ag	As	Au	Cd	Cu	Fe	In	Mn	Mo	Pb	Zn
127B	1.16	6.72	0.1016	2.77	41.98	0.74	0.1107	87.7	1.148	126.5	150.1
137B	0.25	2.94	0.0064	1.01	12.80	0.72	0.0287	75.1	1.026	43.1	77.1
147B	0.45	3.19	0.0129	1.07	20.82	0.53	0.0436	81.4	0.835	101.7	67.1
157B	0.43	1.49	0.0033	1.00	5.31	0.45	0.0228	10.0	0.728	101.2	46.9
167B	1.81	1.38	0.0107	1.18	13.79	0.42	0.0335	9.4	0.521	230.7	51.1

D - distance (in feet) from station 1 for traverse #1, distance from station 68 for traverse #2, and distance from station 148 for traverse #3.
GXR# - Soil U.S.G.S. Reference Sample.
SB# - Soil Background Sample collected outside study area.
B-# - Soil Analytical Blank Sample.
#D - Soil Analytical Duplicate Sample.
#B - Soil Field Duplicate Sample.

Samples 1, 5, 9, 11, 14, 15, 18, 20, 23, 25, 86, 89, 142, 158, 165, 173, SB-1, SB-5, SB-6, SB-18, 20B, and 87B are below the detection limit for gold of 0.0033 ppm, so concentrations for these samples are set at 1/2 the detection limit (0.0017 ppm)

Samples 72, 73, 78, 79, 80, 82, 85, 165, and 73D are below the detection limit for manganese of 5.0 ppm, so concentrations for these samples are set at 1/2 the detection limit (2.5 ppm)

Appendix VII - Averaged Relative Precision

Appendix Table VIIa
Averaged Relative Precision of Analytical Duplicates
(in percent)

Method:	Hot Nitric Acid Digestion	30 Min. HCl/MAGIC
Fraction:	-80	-230
element		
Ag	----	6.59
As	----	3.69
Au	----	46.35 **
Cd	16.89	5.19
Cu	3.64	1.33
Fe	1.72	4.92
In	----	6.90
Mn	2.75	3.13 *
Mo	----	4.11
Pb	6.84	7.53
Zn	1.79	1.96

Number of duplicate pairs analyzed by Hot Nitric Acid Leach used to determine averaged relative precision of analytical duplicates = 15

Number of duplicate pairs analyzed by 30 Min. HCl/MAGIC method used to determine averaged relative precision of analytical duplicates = 15

(Relative Precision of Duplicate Pair) in percent= $[[X_1-((X_1+X_2)/2)]/[(X_1+X_2)/2]](100)$.
(X_2=duplicate of X_1)

Average Relative Precision = Averaged Absolute Values of (Relative Precision of Duplicate Pairs)

The number of asterisks after precision values indicate the number of duplicate pairs which include one or both concentrations at or below the detection limit.

Appendix Table VIIb
Averaged Relative Precision of Field Duplicates
(in percent)

Method:	Hot Nitric Acid Digestion	30 Min. HCl/MAGIC
Fraction:	-80	-230
element		
Ag	----	11.53
As	----	15.98
Au	----	38.82 *
Cd	15.90	12.12
Cu	18.55	15.70
Fe	4.78	4.29
In	----	18.17
Mn	13.29	8.64
Mo	----	7.89
Pb	20.30	12.00
Zn	11.84	11.60

Number of duplicate pairs analyzed by Hot Nitric Acid Leach used to determine averaged relative precision of field duplicates = 16

Number of duplicate pairs analyzed by 30 Min. HCl/MAGIC method used to determine averaged relative precision of field duplicates = 16

(Relative Precision of Duplicate Pair) in percent= $[[X_1-((X_1+X_2)/2)]/[(X_1+X_2)/2]](100)$.
(X_2=duplicate of X_1)

Average Relative Precision = Averaged Absolute Values of (Relative Precision of Duplicate Pairs)

The number of asterisks after precision values indicate the number of duplicate pairs which include one or both concentrations at or below the detection limit.

Appendix VIII - Basic Statistics

Appendix Table VIIIa
Soil Data - Summary Statistics
Hot Nitric Acid Digestion

VAR	UNITS	N	ARITH MEAN	STD DEV	CV %	SKEW	GEOM MEAN	LOG 10 MEAN	STD DEV
Cd	ppm	174	1.5	0.84	0.5E+02	1.	1.3	0.13	0.23
Cu	ppm	174	24.	15.	0.6E+02	2.	20.	1.3	0.26
Fe	pct	174	1.6	0.29	0.2E+02	3.	1.6	0.20	0.68E-01
Mn	ppm	174	0.52E+03	0.25E+03	0.5E+02	0.4	0.46E+03	2.7	0.22
Pb	ppm	174	0.12E+03	0.13E+03	0.1E+03	4.	84.	1.9	0.35
Zn	ppm	174	0.21E+03	0.16E+03	0.8E+02	5.	0.18E+03	2.3	0.20

Appendix Table VIIIb
Soil Data - Summary Statistics
30 Minute Cold HCl Digestion/MAGIC Extraction

VAR	UNITS	N	ARITH MEAN	STD DEV	CV %	SKEW	GEOM MEAN	LOG 10 MEAN	STD DEV
Ag	ppm	174	0.82	0.53	0.7E+02	2.	0.66	-0.18	0.30
As	ppm	174	3.6	3.0	0.8E+02	3.	2.6	0.42	0.36
Au	ppm	174	0.43E-01	0.48E-01	0.1E+03	1.	0.21E-01	-1.7	0.57
Cd	ppm	174	1.8	1.2	0.7E+02	2.	1.4	0.15	0.32
Cu	ppm	174	26.	21.	0.8E+02	2.	19.	1.3	0.37
Fe	pct	174	0.65	0.23	0.4E+02	3.	0.62	-0.21	0.13
In	ppm	174	0.75E-01	0.78E-01	0.1E+03	3.	0.52E-01	-1.3	0.36
Mn	ppm	174	44.	28.	0.6E+02	0.1	31.	1.5	0.43
Mo	ppm	174	0.89	0.43	0.5E+02	2.	0.82	-0.84E-01	0.17
Pb	ppm	174	0.14E+03	0.17E+03	0.1E+03	4.	94.	2.0	0.37
Zn	ppm	174	0.12E+03	0.12E+03	0.9E+02	3.	93.	2.0	0.31

Appendix VIIIc
Soil Data - Ranges and Percentiles
Hot Nitric Acid Digestion

VAR	UNITS	N	MIN VALUE	50TH	75TH	90TH	95TH	99TH	MAX VALUE
				PERCENTILE					
Cd	ppm	174	0.334	1.54	1.96	2.58	2.91	4.19	5.69
Cu	ppm	174	4.92	20.7	32.0	40.7	45.9	90.4	92.6
Fe	pct	174	1.04	1.55	1.71	1.89	2.17	3.00	3.35
Mn	ppm	174	166.	531.	700.	839.	907.	0.120E+04	0.131E+04
Pb	ppm	174	7.86	89.6	126.	200.	335.	876.	972.
Zn	ppm	174	68.5	150.	229.	343.	464.	842.	0.166E+04

Appendix VIIId
Soil Data - Ranges and Percentiles
30 Minute Cold HCl Digestion/MAGIC Extraction

VAR	UNITS	N	MIN VALUE	50TH	75TH	90TH	95TH	99TH	MAX VALUE
				PERCENTILE					
Ag	ppm	174	0.720E-01	0.783	1.11	1.39	1.68	2.98	2.99
As	ppm	174	0.513	3.20	5.26	6.97	7.86	15.5	25.2
Au	ppm	174	0.200E-02	0.250E-01	0.610E-01	0.124	0.150	0.211	0.217
Cd	ppm	174	0.192	1.63	2.44	3.09	3.93	6.02	9.10
Cu	ppm	174	2.99	21.0	36.6	49.6	59.1	98.5	156.
Fe	pct	174	0.329	0.626	0.717	0.861	0.985	1.75	2.06
In	ppm	174	0.100E-01	0.530E-01	0.870E-01	0.170	0.204	0.512	0.528
Mn	ppm	174	2.50	47.0	66.5	79.5	90.0	104.	111.
Mo	ppm	174	0.387	0.797	1.03	1.26	1.75	2.88	2.97
Pb	ppm	174	12.5	97.7	145.	296.	387.	832.	0.129E+04
Zn	ppm	174	26.7	98.5	144.	237.	318.	741.	781.

Appendix IX - Correlation Matrices

Appendix Table IXa
Correlation Coefficients for Raw Soil Data - Hot Nitric Acid Digestion

	Cd	Cu	Fe	Mn	Pb	Zn
Cd	1.000	0.645	0.279	0.474	0.623	0.711
Cu	0.645	1.000	0.219	0.646	0.509	0.369
Fe	0.279	0.219	1.000	-0.021	0.339	0.590
Mn	0.474	0.646	-0.021	1.000	0.110	0.194
Pb	0.623	0.509	0.339	0.110	1.000	0.560
Zn	0.711	0.369	0.590	0.194	0.560	1.000

Appendix Table IXb
Correlation Coefficients for Raw Soil Data - 30 Minute Cold HCl Digestion/MAGIC Extraction

	Ag	As	Au	Cd	Cu	Fe	In	Mn	Mo	Pb	Zn
Ag	1.000	0.489	0.509	0.767	0.672	0.565	0.743	0.331	0.485	0.673	0.716
As	0.489	1.000	0.497	0.462	0.817	0.597	0.602	0.640	0.607	0.440	0.317
Au	0.509	0.497	1.000	0.519	0.660	0.391	0.500	0.459	0.419	0.519	0.403
Cd	0.767	0.462	0.519	1.000	0.660	0.510	0.757	0.559	0.491	0.621	0.842
Cu	0.672	0.817	0.660	0.660	1.000	0.677	0.712	0.620	0.588	0.585	0.557
Fe	0.565	0.597	0.391	0.510	0.677	1.000	0.672	0.311	0.798	0.587	0.693
In	0.743	0.602	0.500	0.757	0.712	0.672	1.000	0.353	0.527	0.706	0.738
Mn	0.331	0.640	0.459	0.559	0.620	0.311	0.353	1.000	0.316	0.117	0.289
Mo	0.485	0.607	0.419	0.491	0.588	0.798	0.527	0.316	1.000	0.659	0.637
Pb	0.673	0.440	0.519	0.621	0.585	0.587	0.706	0.117	0.659	1.000	0.694
Zn	0.716	0.317	0.403	0.842	0.557	0.693	0.738	0.289	0.637	0.694	1.000

Appendix Table IXc
Correlation Coeffecients for Raw Soil Data - 30 Minute Cold HCl Digestion/MAGIC Extraction (XxM) Versus Hot Nitric Acid Digestion (XxN)

	CdM	CuM	FeM	MnM	PbM	ZnM
CdN	0.898	0.621	0.544	0.463	0.661	0.845
CuN	0.657	0.941	0.607	0.629	0.597	0.533
FeN	0.137	0.244	0.671	-0.131	0.369	0.474
MnN	0.518	0.587	0.326	0.936	0.168	0.297
PbN	0.553	0.472	0.480	0.044	0.972	0.633
ZnN	0.651	0.374	0.605	0.145	0.582	0.914

Appendix X - Ratio Analysis Procedure

Appendix Xa
Ratio Analysis Program

```
C       THIS PROGRAM READS THE 30 MINUTE COLD
C       HCL/MAGIC EXTRACTION AND NITRIC EXTRACTION
C       DATA.  IT THEN CALCULATES SEVERAL VARIABLES
C       FOR EACH OF THESE ELEMENTS WHICH ARE USED TO
C       CALCULATE THE Z-SCORES OF EACH DATA POINT.
C       THIS STANDARDIZATION OF THESE DATA ALLOWS FOR
C       THEIR COMPARISON.  THE Z-SCORES ARE THEN
C       RATIOED.  THE PROGRAM WRITES THE SAMPLE
C       STATION NUMBER, THE DISTANCE THAT THE STATION
C       IS LOCATED FROM THE FIRST STATION IN THE
C       TRAVERSE, AND THE RATIO OF THE SELECTED Z-
C       SCORE MINUS THE LOWEST Z-SCORE FOR THAT
C       VARIABLE SET.  SAMPLE POPULATION = 174.
C
        REAL N,D,FE,MN,FEN,MNN,R,MFE,MMN,MFEN,MMNN
     *  LZFE,LZMN,LZFEN,LZMNN
100     READ (10,*,END=250)N,D,FE,MN,FEN,MNN
C       CALCULATE SUMS OF ELEMENTS
        SUMFE=SUMFE+FE
        SUMMN=SUMMN+MN
        SUMFEN=SUMFEN+FEN
        SUMMNN=SUMMNN+MNN
C       CALCULATE SUMS OF SQUARES OF ELEMENTS
        SSQFE=SSQFE+FE**2
        SSQMN=SSQMN+MN**2
        SSQFEN=SSQFEN+FEN**2
        SSQMNN=SSQMNN+MNN**2
        GO TO 100
C       CALCULATE SQUARE OF SUMS OF ELEMENTS
250     SQSFE=SUMFE**2
        SQSMN=SUMMN**2
        SQSFEN=SUMFEN**2
        SQSMNN=SUMMNN**2
C       CALCULATE VARIANCE OF ELEMENTS
        VFE=(174*SSQFE-SQSFE)/(174*173)
        VMN=(174*SSQMN-SQSMN)/(174*173)
        VFEN=(174*SSQFEN-SQSFEN)/(174*173)
        VMNN=(174*SSQMNN-SQSMNN)/(174*173)
C       CALCULATE STANDARD DEVIATION OF ELEMENTS
        SDFE=SQRT(VFE)
        SDMN=SQRT(VMN)
        SDFEN=SQRT(VFEN)
```

```
      SDMNN=SQRT(VMNN)
C     CALCULATE MEANS OF ELEMENTS
      MFE=SUMFE/174
      MMN=SUMMN/174
      MFEN=SUMFEN/174
      MMNN=SUMMNN/174
      CLOSE (10)
275   READ (10,*,END=400)N,D,FE,MN,FEN,MNN
C     CALCULATE Z-SCORES FOR ELEMENT
      ZFE=(FE-MFE)/SDFE
      ZMN=(MN-MMN)/SDMN
      ZFEN=(FEN-MFEN)/SDFEN
      ZMNN=(MNN-MMNN)/SDMNN
C     FIND LOWEST Z-SCORE FOR EACH ELEMENT AND
C     LABEL IT LZXX
      IF(ZFE.LT.LZFE)LZFE=ZFE
      IF(ZMN.LT.LZMN)LZMN=ZMN
      IF(ZFEN.LT.LZFEN)LZFEN=ZFEN
      IF(ZMNN.LT.LZMNN)LZMNN=ZMNN
      GO TO 275
400   CLOSE (10)
450   READ (10,*,END=500)N,D,FE,MN,FEN,MNN
      ZFE=(FE-MFE)/SDFE
      ZMN=(MN-MMN)/SDMN
      ZFEN=(FEN-MFEN)/SDFEN
      ZMNN=(MNN-MMNN)/SDMNN
C     RATIO THE Z-SCORES
      R=(ZFEN-LZFEN)/(ZMNN-LZMNN)
      WRITE (11,300)N,D,R
300   FORMAT (F4.0,2X,F5.0,1X,F12.2)
      GO TO 450
500   STOP
      END
```

Appendix Xb
Program Explanation

This program standardizes elemental variable data so that these elements may be legitimately compared to one another in the form of ratios. It calculates the Z-scores (Davis, 1973) for each data point and also finds the lowest Z-score for a given variable. In order to make all elemental ratios positive, the lowest Z-score (a negative number) is subtacted from each calulated Z-score in the ratio equation. The ratio in the program above compares Fe and Mn concentrations in samples which were analyzed by the hot nitric acid digestion.

Data output is presented below for the Fe/Mn ratios for the nitric and hydrochloric acid digestion methods. In several samples, the manganese is highly depleted relative to the iron. When the Z-score of manganese approaches a number as small as the lowest Z-score for manganese, the denominator of the ratio will approach zero. This tendency produces a calculated ratio which is very large. The format statement in this program does not accommodate such large numbers. The relative magnitudes of these large numbers is not important when the values of the other numbers in the output sets are considered. A small positive number can be added to the denominator, but this is not a valid solution. The addition of different constants in the denominator produces ratios which have variable proportions, relative to each other.

In any case, this point is moot and it is considered most appropriate to let the computer calculate large numbers for the limited number of ratios which have very small denominators. These large numbers are printed as a series of asterisks. The inclusion of large numbers in these data sets significantly reduces the amount of useful information which can be obtained from the low magnitude values. Since this is the case, an arbitrarily chosen value of 10.0 was assigned to those ratios exceeding 10.0. These data were then run through program GRAPHM and plotted on the DP-8 plotter. The results are presented on Plate IV.

Appendix Xc
Fe/Mn Ratio Data for Hot Nitric Acid Digestion and Cold HCl Digestion Methods

Hot Nitric Acid Digestion R=(ZFEN-LZFEN)/(ZMNN-LZMNN)			Cold HCl Digestion R=(ZFE-LZFE)/(ZMN-LZMN)		
#	D	RATIO(R)	#	D	RATIO(R)
1	0	17.01	1	0	6.90
2	25	2.10	2	25	1.35
3	50	0.33	3	50	0.47
4	75	2.27	4	75	3.52
5	85	9.46	5	85	5.03
6	95	6.46	6	95	2.58
7	105	0.96	7	105	0.98
8	115	3.85	8	115	3.36
9	125	137.90	9	125	9.79
10	135	4.85	10	135	3.59
11	145	9.00	11	145	3.84
12	155	3.70	12	155	2.18
13	165	8.11	13	165	3.33
14	175	4.64	14	175	2.03
15	200	0.00	15	200	0.63
16	225	4.36	16	225	1.67
17	250	4.18	17	250	1.61
18	275	6.35	18	275	6.40
19	300	1.97	19	300	0.89
20	310	6.36	20	310	2.73
21	320	5.52	21	320	2.46
22	330	1.37	22	330	1.00
23	340	2.42	23	340	1.59
24	350	2.00	24	350	1.83
25	360	9.49	25	360	3.51
26	370	0.84	26	370	0.81
27	380	0.68	27	380	0.62
28	390	0.43	28	390	0.72
29	400	0.52	29	400	0.74
30	425	0.46	30	425	0.51
31	450	0.56	31	450	0.64
32	475	0.38	32	475	0.44
33	500	0.47	33	500	0.50
34	525	1.27	34	525	0.72
35	550	0.92	35	550	1.01
36	575	0.55	36	575	0.72
37	600	0.77	37	600	0.82
38	610	0.64	38	610	0.77
39	620	1.27	39	620	2.54
40	630	2.02	40	630	3.20

Hot Nitric Acid Digestion
R=(ZFEN-LZFEN)/(ZMNN-LZMNN)

#	D	RATIO(R)
41	640	1.04
42	650	0.95
43	660	0.57
44	670	0.53
45	680	0.47
46	690	0.66
47	700	0.57
48	725	0.54
49	750	0.71
50	775	0.53
51	800	0.74
52	815	0.71
53	850	0.68
54	875	0.89
55	900	0.75
56	910	0.65
57	920	0.75
58	930	0.85
59	940	0.66
60	950	0.68
61	960	0.76
62	970	0.99
63	980	1.18
64	990	0.67
65	1000	0.55
66	1025	0.59
67	1050	0.58
68	0	4.05
69	25	9.59
70	50	2.07
71	75	17.68
72	100	112.71
73	110	39.91
74	120	5.46
75	130	7.91
76	140	1.95
77	150	4.44
78	160	****
79	170	328.82
80	180	12.48
81	190	12.20
82	200	17.48
83	225	11.53
84	250	6.81

Cold HCl Digestion
R=(ZFE-LZFE)/(ZMN-LZMN)

#	D	RATIO(R)
41	640	1.65
42	650	1.02
43	660	1.05
44	670	0.66
45	680	0.53
46	690	0.48
47	700	0.56
48	725	0.55
49	750	0.55
50	775	0.50
51	800	0.50
52	815	0.68
53	850	0.56
54	875	0.56
55	900	0.41
56	910	0.51
57	920	0.48
58	930	0.55
59	940	0.53
60	950	0.48
61	960	0.66
62	970	0.62
63	980	0.83
64	990	0.46
65	1000	0.49
66	1025	0.39
67	1050	0.35
68	0	4.16
69	25	8.48
70	50	1.83
71	75	3.61
72	100	****
73	110	****
74	120	4.79
75	130	7.39
76	140	1.58
77	150	2.95
78	160	****
79	170	****
80	180	****
81	190	4.17
82	200	****
83	225	3.41
84	250	4.92

Hot Nitric Acid Digestion
R=(ZFEN-LZFEN)/(ZMNN-LZMNN)

#	D	RATIO(R)
85	275	11.86
86	300	6.49
87	325	8.46
88	350	8.56
89	375	31.79
90	400	4.62
91	425	2.18
92	435	4.87
93	445	3.08
94	455	2.17
95	465	4.31
96	475	1.91
97	485	2.43
98	495	2.80
99	505	3.59
100	515	1.82
101	525	2.03
102	550	1.86
103	575	2.60
104	600	1.53
105	625	2.28
106	650	1.35
107	675	1.26
108	700	1.26
109	725	1.22
110	750	0.96
111	775	0.93
112	800	1.00
113	825	1.57
114	850	0.95
115	875	0.91
116	885	0.87
117	895	0.76
118	905	0.89
119	915	1.06
120	925	0.81
121	935	0.64
122	945	0.78
123	955	0.69
124	965	0.68
125	975	0.72
126	1000	1.03
127	1025	0.57
128	1050	0.85

Cold HCl Digestion
R=(ZFE-LZFE)/(ZMN-LZMN)

#	D	RATIO(R)
85	275	****
86	300	6.58
87	325	4.27
88	350	1.53
89	375	11.75
90	400	2.09
91	425	1.77
92	435	3.14
93	445	5.28
94	455	2.12
95	465	2.83
96	475	1.48
97	485	1.68
98	495	0.92
99	505	0.86
100	515	0.84
101	525	1.28
102	550	1.15
103	575	1.77
104	600	0.85
105	625	0.80
106	650	0.72
107	675	0.91
108	700	0.71
109	725	0.95
110	750	0.63
111	775	0.65
112	800	0.65
113	825	0.52
114	850	0.46
115	875	0.53
116	885	0.61
117	895	0.63
118	905	0.55
119	915	0.65
120	925	0.76
121	935	0.30
122	945	0.58
123	955	0.72
124	965	0.58
125	975	0.71
126	1000	0.71
127	1025	0.58
128	1050	0.72

Hot Nitric Acid Digestion
R=(ZFEN-LZFEN)/(ZMNN-LZMNN)

#	D	RATIO(R)
129	1075	1.45
130	1100	1.29
131	1125	0.70
132	1135	0.83
133	1145	0.68
134	1155	0.57
135	1165	0.59
136	1175	0.80
137	1185	0.69
138	1195	0.82
139	1205	0.67
140	1215	0.77
141	1225	0.93
142	1250	9.22
143	1275	0.44
144	1300	0.53
145	1325	0.40
146	1350	0.51
147	1375	0.44
148	0	0.91
149	10	0.80
150	20	0.99
151	30	0.86
152	40	0.51
153	50	2.29
154	60	3.27
155	70	1.32
156	80	2.26
157	90	4.40
158	100	2.93
159	110	4.30
160	120	1.06
161	130	1.33
162	140	3.39
163	150	2.45
164	160	3.59
165	170	41.61
166	180	4.81
167	190	7.31
168	200	7.87
169	225	1.62
170	250	0.89
171	275	3.16
172	300	6.42

Cold HCl Digestion
R=(ZFE-LZFE)/(ZMN-LZMN)

#	D	RATIO(R)
129	1075	0.69
130	1100	0.78
131	1125	0.60
132	1135	0.61
133	1145	0.53
134	1155	0.43
135	1165	0.59
136	1175	0.74
137	1185	0.77
138	1195	0.60
139	1205	0.59
140	1215	0.54
141	1225	0.64
142	1250	0.12
143	1275	0.37
144	1300	0.32
145	1325	0.25
146	1350	0.33
147	1375	0.36
148	0	1.31
149	10	1.33
150	20	1.18
151	30	0.87
152	40	0.64
153	50	1.21
154	60	2.85
155	70	1.24
156	80	1.89
157	90	2.55
158	100	2.67
159	110	7.25
160	120	0.70
161	130	0.77
162	140	0.59
163	150	1.22
164	160	1.46
165	170	0.00
166	180	0.26
167	190	1.96
168	200	1.26
169	225	1.43
170	250	0.81
171	275	1.61
172	300	0.61

Hot Nitric Acid Digestion R=(ZFEN-LZFEN)/(ZMNN-LZMNN)			Cold HCl Digestion R=(ZFE-LZFE)/(ZMN-LZMN)		
#	D	RATIO(R)	#	D	RATIO(R)
173	325	1.91	173	325	0.60
174	350	0.93	174	350	0.59

D - Distance (in feet) from station 1 for traverse #1, distance from station 68 for traverse #2, and distance from station 148 for traverse #3.

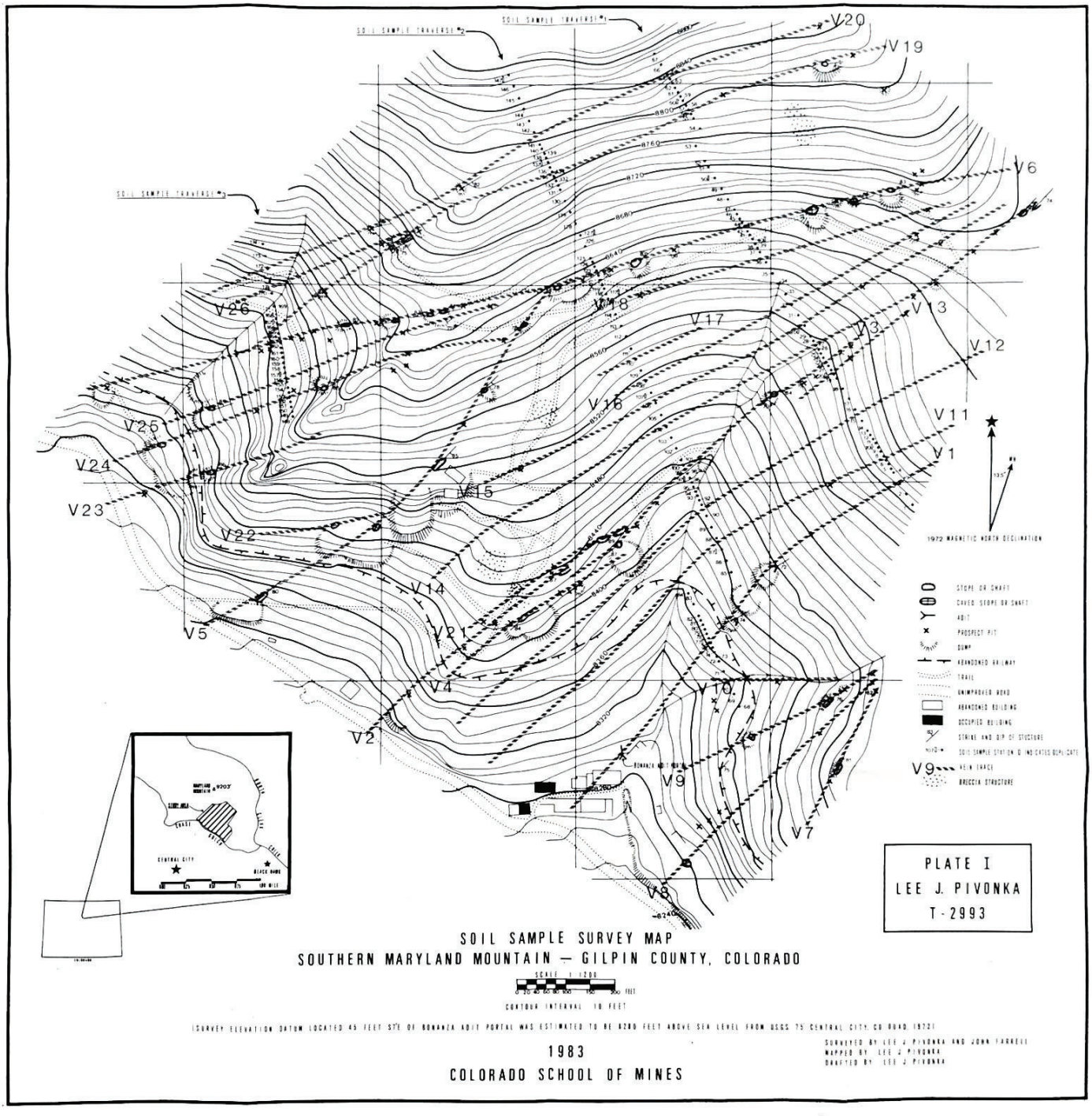

PLATE I
LEE J. PIVONKA
T-2993

SOIL SAMPLE SURVEY MAP
SOUTHERN MARYLAND MOUNTAIN — GILPIN COUNTY, COLORADO

SURVEY ELEVATION DATUM LOCATED 45 FEET SSE OF BONANZA ADIT PORTAL WAS ESTIMATED TO BE 8280 FEET ABOVE SEA LEVEL FROM USGS 7½ CENTRAL CITY, CO. QUAD. (1972)

1983

COLORADO SCHOOL OF MINES

SURVEYED BY: LEE J. PIVONKA AND JOHN TARKEY
MAPPED BY: LEE J. PIVONKA
DRAFTED BY: LEE J. PIVONKA

ELEMENTAL CONCENTRATION PROFILES - HOT NITRIC ACID DIGESTION

(1985)

COLORADO SCHOOL OF MINES

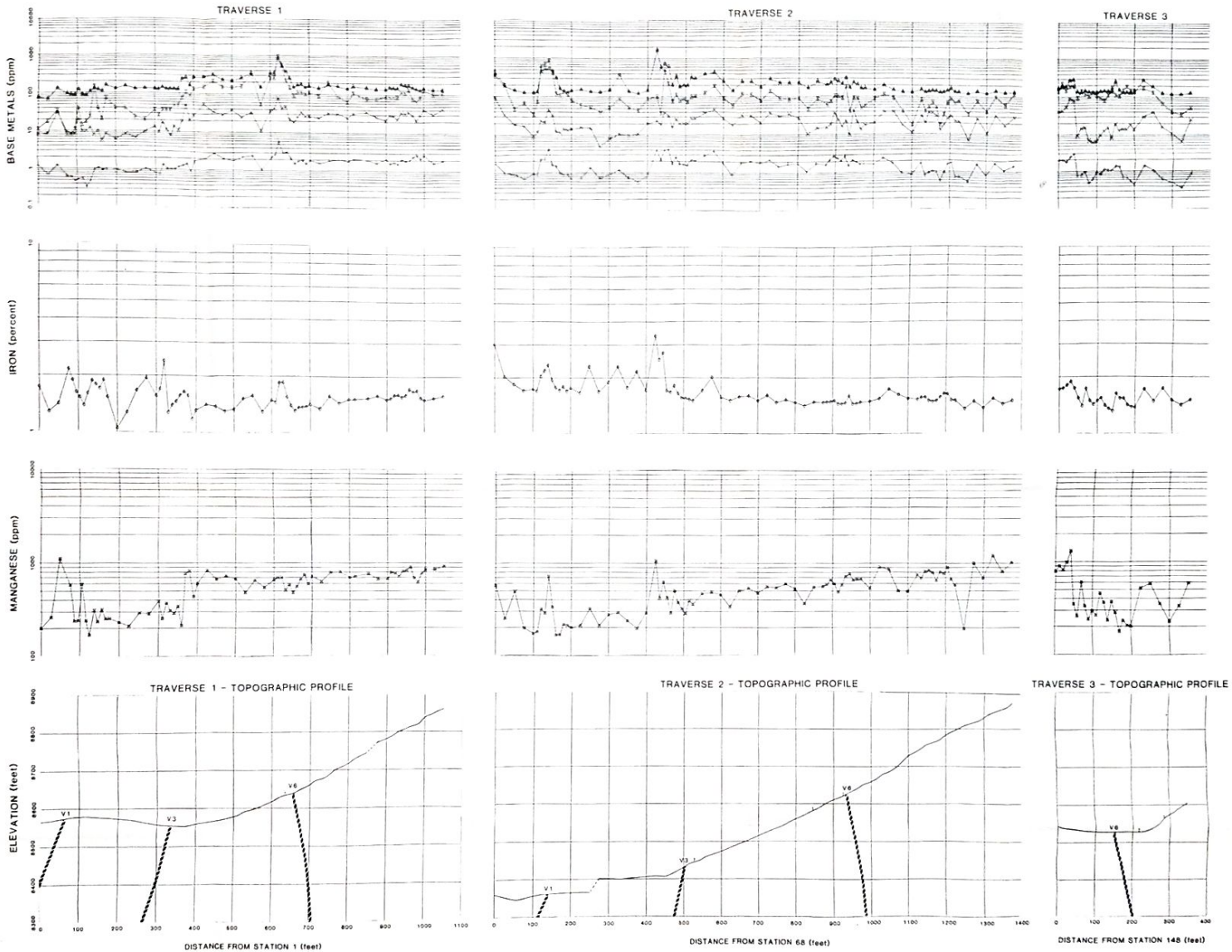

PLATE II

LEE J. PIVONKA

T-2993

ELEMENTAL CONCENTRATION PROFILES - 30 MINUTE COLD HCL DIGESTION/MAGIC EXTRACTION

(1985)

COLORADO SCHOOL OF MINES

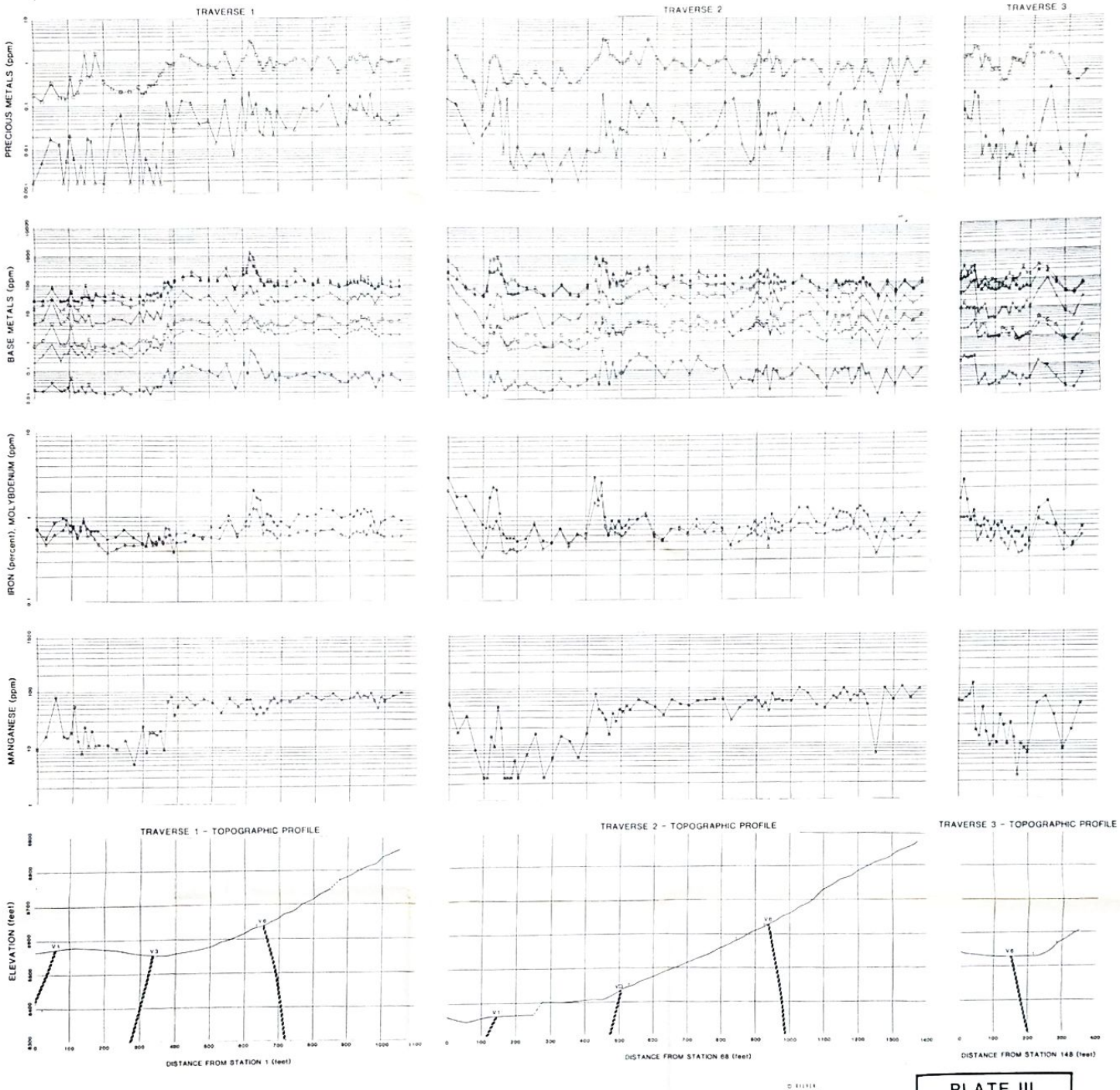

PLATE III

LEE J. PIVONKA

T-2993

IRON/MANGANESE RATIO PROFILES FOR HOT NITRIC ACID DIGESTION AND 30 MINUTE COLD HCL DIGESTION

(1985)

COLORADO SCHOOL OF MINES

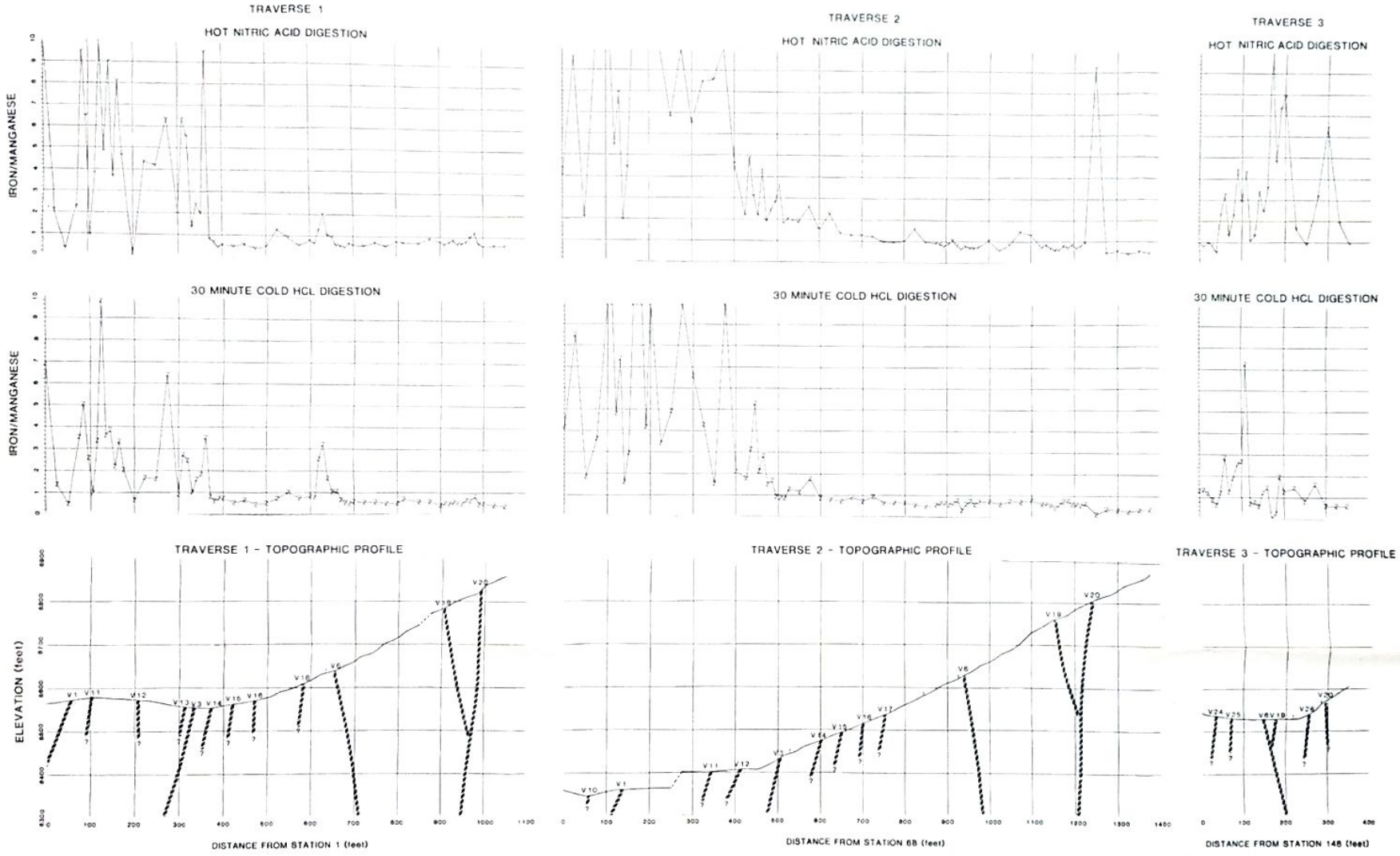

PLATE IV

LEE J. PIVONKA

T-2993